DYNAMIC LIGHT SCATTERING OF BIOPOLYMERS AND BIOCOLLOIDS

Author: **J. Michael Schurr**
Department of Chemistry
University of Washington
Seattle, Washington

Referee: Victor Bloomfield
Department of Biochemistry
University of Minnesota
St. Paul, Minnesota

INTRODUCTION

Of the physical techniques available for the study of biopolymers and other macromolecular and colloidal systems, dynamic light scattering is, perhaps, the most fascinating. The very idea of extracting useful dynamical and structural information from random fluctuations in the intensity of light scattered from otherwise unperturbed equilibrium solutions[1-3] seems, at first glance, almost too good to be true. Indeed, for fragile preparations that are prone to suffer undesirable fates at the slightest change in solution conditions, dynamic light scattering may be the perfect technique. It is nondestructive, relatively rapid, and typically requires only modest amounts of material. In routine applications, even on unfamiliar samples, the dust-removal procedure (either gravity flow Millipore® filtration or low-speed centrifugation) requires 10 to 20 min, and determination of the translational diffusion coefficient to an accuracy of a few percent, or less, requires 5 min. Verification that the dynamical motions, in fact, obey the diffusion equation requires an additional 5 to 20 min. The amounts of solution required are typically a few milliliters, although similar experiments have been run on volumes as small as 15 μl.[4] The concentrations needed, which depend on salt concentration and refractive index increment, and inversely on molecular weight, generally lie in the range 0.5 to 2.0 mg/ml for polypeptides with $M_r \sim 100{,}000$.

Although the primary interests of most practitioners are presently in problems that lie beyond simple diffusion coefficient determinations, routine collaborations with scientists in the biological sciences continue to be welcome. Dynamic light scattering experiments can be defeated by excessive sample heterogeneity or dust and large aggregates, but in such cases the experimenter is immediately aware of the problem, so that the risk of unsuspected artifacts in the data is very low, probably lower than with most other biophysical methods.

Dynamic light scattering techniques have been successfully applied not only to dilute solutions of various natural and synthetic polypeptides, nucleic acids, and other macromolecules, but also to micelles,[5-8] gels,[9-14] coacervates,[15] ordered suspensions of spherical colloids,[16] cellular organelles, including ribosomes,[17-19] flagellae,[20,21] and vesicles,[22-25] viruses,[26-40] motile and nonmotile cells,[41-47] beating cilia,[48] muscle fibers,[49-51] and cytoplasmic streaming.[52-54]

Various aspects of the dynamic light scattering field have been reviewed on numerous occasions.[55-73] Moreover, two excellent books[74,75] have also appeared on this general subject. The treatise of Berne and Pecora[74] gives quite a lucid introduction to the scattering theory and develops some of the pertinent correlation functions of the scattering medium in considerable detail, while giving the experimental methods less emphasis. The book by Chu[75] provides an extensive review of the experimental techniques, including detailed theoretical analyses of various facets of the measurement process, but gives somewhat less weight to the theory of the scattering medium.

The objective here is to provide a review of those aspects of the theory, measurement techniques, and, especially, experimental results that pertain to biopolymer systems, defined in a sufficiently broad manner to include macromolecular assemblages as large as viruses and vesicles, but not living organisms. Special emphasis is placed on recent developments not covered in the earlier reviews, and particular attention is given to the physical chemistry of the macromolecules themselves.

THEORY OF THE QUASIELASTICALLY SCATTERED LIGHT

Basic Notions

The theory for monochromatic incident radiation has been discussed at length by Berne and Pecora.[74] However, recent intensity fluctuation studies of Brownian motion using an ordinary Hg source,[76] and also a cw dye-laser,[77] both with intrinsic frequency line widths very large compared to the frequency broadening associated with the scattering process, have served to emphasize the generally polychromatic nature, or finite frequency band width, of the incident light. Visual observations of intensity fluctuations in scattered light were made before the advent of lasers.[78] The effects of intensity fluctuations in the incident beam can be obtained by a very slight generalization of an earlier treatment of the zero-angle depolarized light[32] and are explicitly incorporated into the results quoted here.

A schematic view of the scattering process in the typical scattering geometry is shown in Figure 1. When the dynamical motions of the scattering elements (m), at positions $\mathbf{r}_m(t)$, are sufficiently slow that their local excess polarizabilities $\alpha_{m,\gamma}(t)$ and phase factors $\exp[i\mathbf{K}\cdot\mathbf{r}_m(t)]$ do not change significantly in the time, t = L/c (typically $\leq 10^{-11}$ sec), required for light at speed c to traverse the length L of the illuminated scattering volume, and when also the angular frequency bandwidth $\Delta\omega$ of the incident light is sufficiently small that its principal components remain in-phase while traversing the scattering volume (i.e., $\Delta\omega\ L/c << 1$), then the electric field of the scattered light at the detector position **R** is given by

$$E^S_\gamma(\mathbf{R}, t) = -F\, E_{in}(t)\, \alpha_\gamma(\mathbf{K}, t') \qquad (1)$$

where $F = \omega_0^2/c^2|\mathbf{R}|$ is an instrumental constant, and γ = {V or H}, which denotes polarization either parallel (V) or perpendicular (H) to that of the incident light. The quantity $\alpha_\gamma(\mathbf{K},t)$ is the instantaneous amplitude of a particular Fourier component, or $\exp[i\mathbf{K}\cdot\mathbf{r}]$ wave, of the three-dimensional distribution of excess polarizability density, $\alpha_\gamma(\mathbf{r},t) = \sum_m \alpha_{m,\gamma}(t)\, \delta(\mathbf{r} - \mathbf{r}_m(t))$, in the scattering volume, as indicated in exaggerated fashion in Figure 1. The quantity $\delta(\mathbf{r} - \mathbf{r}_m(t))$ denotes a three-dimensional delta-function. The scattering vector **K** is defined by $\mathbf{K} \equiv \mathbf{k}^S - \mathbf{k}^0$, and its magnitude depends on the scattering angle θ according to[74,75]

$$|\mathbf{K}| = (4\pi n/\lambda) \sin(\theta/2) \qquad (2)$$

where n is the refractive index, and $\lambda = 2\pi c/\omega_0$ is the wavelength of the incident light in vacuo. The quantity $E_{in}(t)$ actually has the time dependence of the incident beam at a distance $|\mathbf{R}|$ downstream from the scattering volume. The difference between t and t′ is the time required for light to travel from the scattering volume to the detector.

In terms of the individual scattering elements, $\alpha_\gamma(\mathbf{K},t)$ is given by[74]

$$\alpha_\gamma(\mathbf{K},t) = \sum_m \alpha_{m,\gamma}(t)\, e^{-\mathbf{K}\cdot\mathbf{r}_m(t)} \qquad (3)$$

which shows that Brownian motions affecting the $\mathbf{r}_m(t)$ will act to modulate the phase factors, thus producing fluctuations in $\alpha_\gamma(\mathbf{K},t)$, hence also in the scattered light. In the interpretation of biopolymer data, it has generally been assumed that the optical polarizabilities of the scattering elements, or segments, are cylindrically symmetric with polarizabilities $\alpha_\parallel$ in the direction of the long axis and $\alpha_\perp$ in the transverse direction, as indicated schematically in Figure 2. In that case, one has[74]

$$\alpha_{m,V}(t) \cong \alpha \qquad (4)$$

and[78]

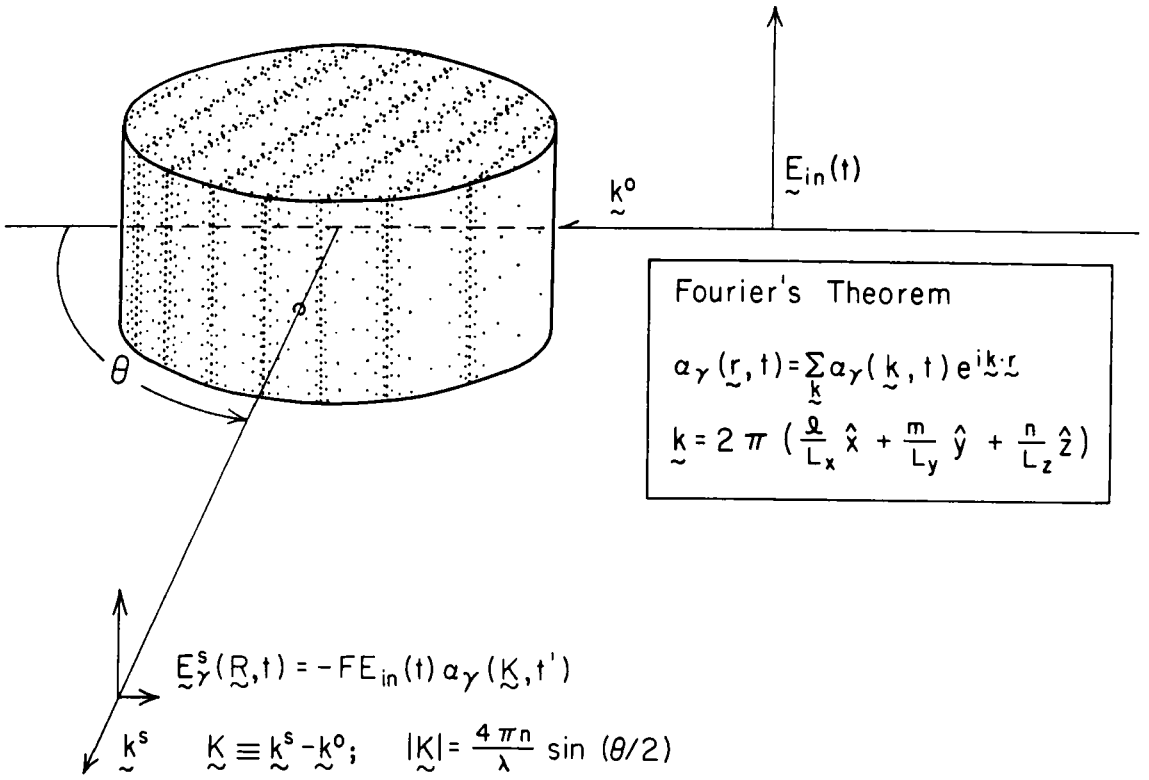

FIGURE 1. A schematic view of the scattering process. The instantaneous polarizability density, $\alpha_\gamma(r,t)$, can be written as a three-dimensional Fourier sum of complex sinusoidal waves. Only that wave with $\mathbf{K} = \mathbf{k}^s - \mathbf{k}^0$ makes a nonvanishing contribution to the scattered light in the direction $\mathbf{k}^s$. The real part of the particular $\exp(i\mathbf{K}\cdot\mathbf{r})$ wave in this instance is illustrated schematically on a greatly magnified scale. Its actual wavelength $\lambda_{eff} = 2\pi/K = \lambda_0/2n \sin(\theta/2)$ varies with scattering angle, becoming infinitely long at $\theta = 0$.

$$\alpha_{m,H}(t) = \beta \cos[\theta_m(t)] \cos[\chi_m(t)] \tag{5}$$

where $\alpha \equiv (1/3)(\alpha_{\parallel} + 2\alpha_{\perp})$ is the isotropic polarizability, and $\beta \equiv \alpha_{\parallel} - \alpha_{\perp}$ is the typically small anisotropy of the polarizability. It is apparent from Equation 5 that rotational Brownian motion of optically anisotropic elements imposes an additional modulation of the depolarized (H) scattered light.

Useful information regarding macromolecular dynamics is contained in the autocorrelation function $M_\gamma(\mathbf{K},t)$ of the randomly fluctuating Fourier amplitude,[74]

$$M_\gamma(\mathbf{K},t) \equiv \langle \alpha_\gamma(\mathbf{K},0)^* \quad \alpha_\gamma(\mathbf{K},t) \rangle \tag{6}$$

in which the angular brackets denote an appropriate ensemble average, and where the equivalence of time and ensemble averages and the invariance of the latter with respect to the origin of time have been assumed. The basic problems of dynamic light scattering have been twofold: to derive usable formulae for $M_\gamma(\mathbf{K},t)$ from appropriate models for macromolecular motions and to devise means for obtaining $M_\gamma(\mathbf{K},t)$, or at least its pertinent temporal behavior from measurements made on the scattered light.

Intensity Spectrum of the Scattered Light

The average (over a long time) intensity of the scattered light per unit angular frequency at the detector at $\mathbf{R}$ in the direction $\mathbf{k}^s$ is given by[74]

$$I_\gamma(\mathbf{k}^s,\omega) = \frac{1}{2\pi}\int_{-\infty}^{\infty} \left\langle E^s_\gamma(\mathbf{R},0)^* E^s_\gamma(\mathbf{R},t) \right\rangle e^{i\omega t}\, dt$$

$$= F^2 \int_{-\infty}^{\infty} I_0(\omega')\, M_\gamma(\mathbf{K},\omega-\omega')\, d\omega' \tag{7}$$

where the second equality is obtained using Equation 1 and the convolution theorem.[79] The quantity

$$I_0(\omega) = \frac{1}{2\pi}\int_{-\infty}^{\infty} \left\langle E_{in}(0)^* E_{in}(t) \right\rangle e^{i\omega t}\, dt \tag{8}$$

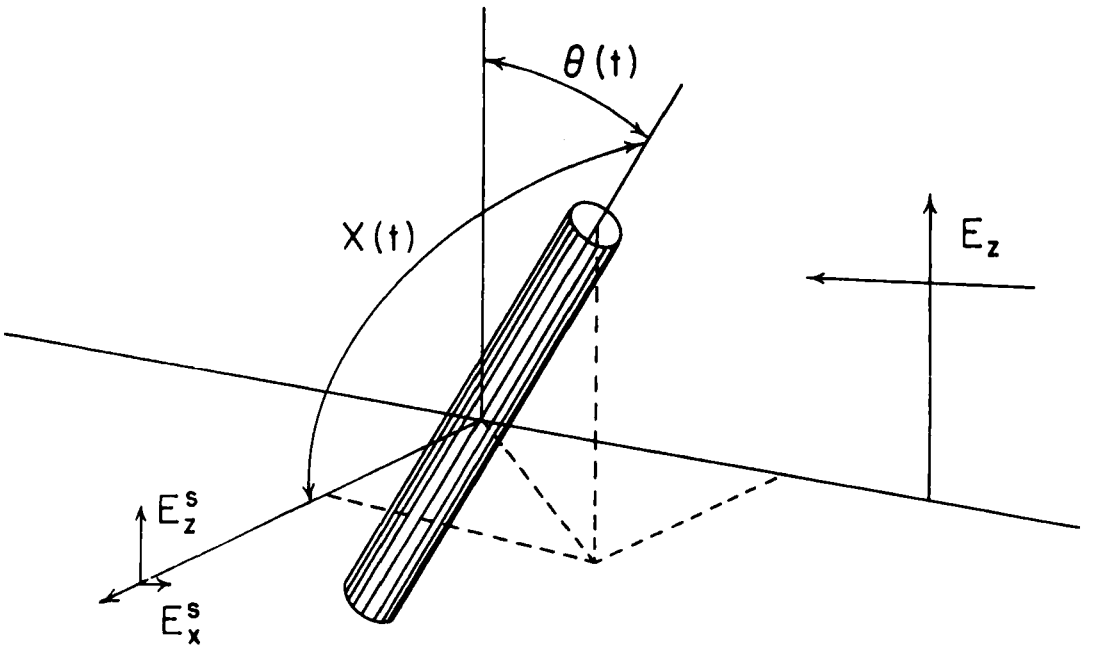

$$E_z^s = -FE_z\{\alpha_\perp + (\alpha_{||} - \alpha_\perp)\cos^2(\theta(t))\}$$

$$= -FE_z\{1/3(2\alpha_\perp + \alpha_{||}) + (\alpha_{||} - \alpha_\perp)(\cos^2(\theta(t)) - 1/3)\}$$

$$E_x^s = -FE_z(\alpha_{||} - \alpha_\perp)\cos(\theta(t))\cos(X(t))$$

FIGURE 2. Illustration of polarized and depolarized Rayleigh scattering from a single cylindrical scattering element with optical polarizability $\alpha_{||}$ in the direction of its long axis and $\alpha_\perp$ in the transverse direction. The polarized component of the scattered electric field E_z^s is proportional to a constant term, $(2\alpha_\perp + \alpha_{||})/3$, plus a small time-dependent part, $(\alpha_{||} - \alpha_\perp)\{\cos^2[\theta(t)] - 1/3\}$, that fluctuates about an average value of zero. The depolarized component of the scattered electric field E_x^s is proportional to the small time-dependent term, $(\alpha_{||} - \alpha_\perp)\cos[\theta(t)]\cos[\chi(t)]$, which monitors the indicated product of direction cosines.

is the spectral density of the incident light, and

$$M_\gamma(K,\omega) = \frac{1}{2\pi}\int_{-\infty}^{\infty} M_\gamma(K,t)\, e^{i\omega t}\, dt \qquad (9)$$

is the spectral density of the fluctuating polarizability in the K-mode examined. When the frequency width of the incident beam is very small compared to that of $M_\gamma(K,\omega)$, then the scattered intensity faithfully monitors $M_\gamma(K,\omega)$, but when the frequency width of the incident beam is large compared to $M_\gamma(K,\omega)$, then the spectral profile of the scattered light is essentially that of the incident beam. Thus, the technique of direct spectral analysis is confined to available light sources with frequency widths that are small compared to those of $M_\gamma(K,\omega)$. This obvious limitation is not shared by the intensity fluctuation techniques discussed below.[32,76,77,81]

The Homodyne Autocorrelation Function

The autocorrelation function of the fluctuating intensity of the scattered light at the detector is given by[76,81]

$$\left\langle I_\gamma^s(R,0)\, I_\gamma^s(R,t)\right\rangle = \tfrac{1}{4}\left\langle |E_\gamma^s(R,0)|^2 |E_\gamma^s(R,t)|^2\right\rangle$$

$$= F^2\left\langle I_0(o)\, I_0(t)\right\rangle \left\langle |\alpha_\gamma(K,0)^*\, \alpha_\gamma(K,t)|^2\right\rangle \qquad (10)$$

The quantity $\langle I_0(0)I_0(t)\rangle$ is the intensity autocorrelation function of the incident light and is always comprised of both a constant and a time-dependent part, the latter of which relaxes to zero at sufficiently long times.

There are two extreme situations in which fluctuations in the incident light do not interfere

with those in $\alpha(\mathbf{K},t)$. When the incident intensity fluctuates only slowly compared to the polarizability, corresponding to a very narrow spectral width of the incident light, then $\langle I_0(0)I_0(t)\rangle$ will be effectively a constant $\langle I_0(0)^2\rangle$. This circumstance is widely presumed to be the normal situation. On the other hand, when $\langle I_0(0)I_0(t)\rangle$ relaxes very rapidly compared to the fluctuations in polarizability, corresponding to a broad spectral width of the incident light, then its time-dependent part essentially vanishes in very short times, leaving only its constant term $\langle I_0 0\rangle^2$ to combine with the polarizability factor in Equation 10 at longer times. The experimental feasibility of broad-band incident light sources in dynamic light scattering experiments has already been demonstrated[76,77] and may hold great promise for the future, especially with continuous wave (cw) dye lasers operating in the ultraviolet, where the shorter wavelengths and much greater scattering powers associated with ultraviolet light offer numerous advantages.

If the fluctuating Fourier amplitude $\alpha_\gamma(\mathbf{K},t)$ of the excess polarizability density is a linear superposition of contributions from a large number of independently fluctuating sources (i.e., regions or scattering elements) with zero mean, then, according to the central limit theorem, $\alpha(\mathbf{K},t)$ must be a Gaussianly distributed (complex) random variable also of zero mean.[74] In that case, the fourth-order correlation product of the polarizability in Equation 10 may be accurately expressed[74,80,81] in terms of its second-order correlation products by

$$\left\langle |\alpha_\gamma(\mathbf{K},0)^*\,\alpha_\gamma(\mathbf{K},t)|^2 \right\rangle \cong \left\langle |\alpha_\gamma(\mathbf{K},0)|^2 \right\rangle^2 + \left| \left\langle \alpha_\gamma(\mathbf{K},0)^*\alpha_\gamma(\mathbf{K},t) \right\rangle \right|^2 \qquad (11)$$

If significant correlation among the different scattering elements prevails over a distance comparable to, or larger than, the dimensions of the scattering volume or if the number of independent scatterers is not large compared to 1.0, then this approximation is no longer valid. In all studies discussed in this review, except for those dealing with ordered suspensions of highly charged polyelectrolytes,[16,82] the correlation range is certainly very small compared to the dimensions of the scattering volume. Likewise, in the studies discussed below, the number of independent scattering regions or elements has generally been very large compared to 1.0, except in one instance.[83] In the studies reviewed here, then, except where explicitly noted, the autocorrelation function of the scattered intensity is given satisfactorily by[76]

$$\left\langle I_\gamma^s(\mathbf{R},0)\, I_\gamma^s(\mathbf{R},t) \right\rangle = W(\mathbf{K},0)\,(1 + |g_\gamma^{(1)}(\mathbf{K},t)|^2) \qquad (12)$$

in which the normalized correlation function

$$g_\gamma^{(1)}(\mathbf{K},t) \equiv M_\gamma(\mathbf{K},t)/M_\gamma(\mathbf{K},0) \qquad (13)$$

has been introduced. The quantity $W(\mathbf{K},0) = F^4\langle I_0(0)^2\rangle \cdot \langle|\alpha_\gamma(\mathbf{K},0)|^2\rangle^2$ applies for narrow band incident light. For broad band incident light, the quantity $I_0(0)^2$ should be replaced by $\langle I_0(0)\rangle^2$. The intensity autocorrelation function of the pure scattered light in Equation 12 is called the homodyne, or self-beat,[1,3] correlation function.[74,75] Its determination effectively determines the square of the normalized autocorrelation function of the fluctuating Fourier amplitude $\alpha_\gamma(\mathbf{K},t)$ of the polarizability density.

The Heterodyne Autocorrelation Function

A related technique leading directly to the real part of $g_\gamma^{(1)}(\mathbf{K},t)$ involves superposing, or mixing, an excess of unscattered (but reflected) primary or incident light with the scattered light at the detector.[2] In general there will be a time delay (Δt) between the scattered and primary light rays due to the difference in their paths. Provided that the frequency width ($\Delta\omega$) of the primary light is sufficiently narrow that $\Delta\omega\Delta t \ll 1$, the electric field of the primary light, often called the local oscillator, may be written as

$$E_{LO}(t) = AE_{in}(t) \qquad (14)$$

where A is a complex instrumental constant. The total electric field at the detector is then $E_{tot}(t) = [AE_{in}(t) - FE_{in}(t)\alpha_\gamma(\mathbf{K},t)]$, and the autocorrelation function of the total intensity is given approximately by[74,75]

$$\left\langle I_{tot}(0)\, I_{tot}(t) \right\rangle \cong \left\langle I_0(0)\, I_0(t) \right\rangle |A|^4 \left\{ 1 + 2\frac{\langle I_\gamma^s \rangle}{\langle I_{LO} \rangle} \left(1 + Re\, g_\gamma^{(1)}(\mathbf{K},t) \right) \right\} \qquad (15)$$

where $\langle I_\gamma^s\rangle \equiv \langle I_\gamma^s(\mathbf{R},0)\rangle = (F^2/2)\,\langle|E_{in}(0)|^2\rangle\,\langle|\alpha_\gamma(\mathbf{K},0)|^2\rangle$ is the mean scattered intensity, and $\langle I_{LO}\rangle = (|A|^2/2)\,\langle|E_{in}(0)|^2\rangle$ is the mean intensity of the primary, or local oscillator, light. In the

limit of narrow frequency-width incident light, $\langle I_0(0)I_0(t)\rangle$ is replaced by $\langle I_0(0)^2\rangle$, and for broad-band incident light, it should be replaced by $\langle I_0(0)\rangle^2$. The quantity $\langle I_{tot}(0)I_{tot}(t)\rangle$ is called the heterodyne[2] autocorrelation function.[74,75]

The distinctive feature of heterodyning stems from the fact[84] that uniform translational motion of the scattering centers is manifested in *Re* $g_\gamma^{(1)}(K,t)$, although it is not manifested in $|g_\gamma^{(1)}(K,t)|^2$, as discussed further below. Thus, heterodyning can be employed for electrophoresis[59,60,85,86] and motility studies.[41-44] Moreover, slow fluctuations in the number of scattering centers in the illuminated volume are not manifested in the heterodyne correlation function, although they do appear in the homodyne correlation function,[74] as discussed also in greater detail below.

Expressions for $M_V(K,t)$

For the polarized (V) component of the scattered light, the quantity $\alpha_{m,V}(t) \cong \alpha$ is essentially a constant;[74] thus, $M_V(K,t)$ can be written in either of the two forms:

$$M_V(K,t) = \alpha^2 \left\langle c(K,0)^* \, c(K,t) \right\rangle = \alpha^2 \langle N \rangle G(K,t) \qquad (16)$$

where

$$c(K,t) = \int_V e^{-iK\cdot r} \, c(r,t) d^3 r \qquad (17)$$

is the Fourier amplitude, or transform, of the instantaneous concentration of scattering elements, whether in the same or different macromolecules, and

$$G(K,t) \equiv \left\langle N^{-1} \sum_{l=1}^{N} \sum_{m=1}^{N} e^{iK\cdot[r_l(0) - r_m(t)]} \right\rangle \qquad (18)$$

is called the dynamic structure factor, which differs from the dynamic form factor of Berne and Pecora[74] by a factor of $\langle N \rangle$. The concentration formulation has been the more useful in developing theories for coupled diffusion and flow in chemically reacting systems,[74,75,87-101] and also for electrostatically coupled ionic systems,[74,89,102-109] while the structure factor approach has enjoyed particular advantage in treating flexible polymers[74,110-118] and in developing very general results for interacting spherical macromolecules in an inert solvent.[119,120] A number of problems are treated equally well by either method. It follows directly from Equation 1 that the static structure factor $G(K,0)$ is proportional to the mean scattered intensity, which is given by $\langle I_\gamma^S \rangle = F^2 \langle I_0 \rangle \alpha^2 \langle N \rangle G(K,0)$.

It will often be convenient to employ the symbol $\alpha_M = h\alpha$ for the total polarizability of a macromolecule consisting of h scattering elements.

Expressions for $M_V(K,t)$ that have been derived for a number of the most pertinent systems are listed below.

Macromolecules of Small Dimension

For macromolecules of dimension small compared to the fluctuation wavelength, $\lambda_{eff} \equiv 2\pi/K$, undergoing translational diffusion according to

$$\frac{\partial c}{\partial r}(r,t) = D\nabla^2 \, c(r,t) \qquad (19)$$

where D is the translational diffusional coefficient:[74,75,121]

$$M_V(K,t) = \langle N \rangle \alpha_M^2 e^{-K^2 Dt} \qquad (20)$$

With the inclusion of the factor $[3/(Ka)^3]$ $[\sin(Ka) - Ka\cos(Ka)]^2$ on the right-hand side, this equation holds also for spherical particles of arbitrary radius a.[74]

Rigid, Rod-like Macromolecules

For rigid, rod-like macromolecules undergoing uncoupled translational and rotational diffusion according to

$$\frac{\partial c}{\partial r}(R,\theta,t) = D\nabla^2 \, c(R,\theta,t) + D_R \nabla_\Omega^2 \, c(R,\theta,t) \qquad (21)$$

where D_R and ∇_Ω^2 are the rotational diffusion coefficient and Laplacian on the unit sphere, respectively:

$$M_V(K,t) = \langle N \rangle \alpha_M^2 e^{-K^2 Dt} \left[S_0(KL) + S_1(KL) e^{-6D_R t} + \ldots + S_{l/2}(KL) e^{-l(l+1)D_R t} + \ldots \right] \qquad (22)$$

where L is the rod length.[74,121,122] Expressions for $S_0(KL)$ and $S_1(KL)$, as well as computed amplitudes of these terms, and of the total, are given by Pecora[122] and Berne and Pecora.[74] The higher order terms exist only for even l, and relax with rates $l(l+1)D_R$.

At small K values, or scattering angles, the

coefficient $S_1(KL)$ and those of all higher order terms vanish because the molecular size is inevitably small compared to the fluctuation wavelength in that limit. Moreover, at any scattering angle the relaxation rate of the slowest relaxing-term is always K^2D. These last two properties are generally characteristic of light scattered from large noninteracting macromolecules, when translational and internal motions are uncorrelated.[123]

Treatments of coupled anisotropic translational and rotational diffusion of noninteracting species have been given by Maeda and Saito[124] and Schaefer et al.[30] Even for very long rod-like particles, such as Tobacco Mosaic Virus, the predicted effect of the modest intrinsic anisotropy of D is rather small.[30] However, in congested solutions the induced anisotropy of translational diffusion of nonspherical macromolecules may be quite large, resulting in a strong coupling of translational and orientational motions.[123] Such a phenomenon may account for the prominent slow relaxations, or long tails, observed in the correlation functions of high molecular weight DNAs under certain conditions[3,73,125-129] and more recently for filamentous F-actin.[130] This phenomenon will be discussed in further detail below.

The Rouse-Zimm Model

For the Rouse-Zimm model[131] of a flexible polymer, the h + 1 beads which obey Langevin equations of the form[74,132,133]

$$m_0\frac{d^2\mathbf{r}_n}{dt^2} + f\frac{d\mathbf{r}_n}{dt} + g\sum_{m=1}^{h+1}\sum_{p=1}^{h+1} H_{np}A_{pm}\mathbf{r}_m = \mathbf{F}_n(t) \qquad (23)$$

where $H_{np} \equiv \delta_{n,p} + f[(6\pi^3)^{1/2}\eta b|n-p|^{1/2}]^{-1}$ and $A_{mp} \equiv +2\delta_{m,p} - \delta_{p,m\pm1}$ are the hydrodynamic interaction and force constant matrices, respectively, of Zimm; $\mathbf{F}_n(t)$ is the (Gaussian) fluctuating force on the nth bead; and f, g, and $b^2 = 3k_BT/g$ are the bead friction factor, spring constant, and mean squared spring extension, respectively:[74,110,111,114,132,133]

$$M_V(K,t) = \langle N\rangle\alpha^2 e^{-K^2Dt}\sum_{m=1}^{h+1}\sum_{n=1}^{h+1} e^{-\frac{K^2}{2}\sum_{l=2}^{h+1} d_l^2}$$

$$\left(Q_{nl}^2 + Q_{ml}^2 - 2Q_{nl}Q_{ml}e^{-t/\tau_l}\right) \qquad (24)$$

where $D \equiv (h+1)^{-1}(k_BT/f)\sum_{p=1}^{h+1}\sum_{q=1}^{h+1}(Q^{-1})_{1p}H_{pq}(Q^{-1})_{1q}$ is the translational diffusion coefficient for the entire macromolecule,[131,133] and d_l^2 is the mean-squared extension of the lth normal coordinate. The normal coordinates are defined by

$$\rho_l(t) \equiv \sum_{n=1}^{h+1}(Q^{-1})_{ln}\mathbf{r}_n(t) \qquad (25)$$

where Q is the similarity transformation matrix that diagonalizes HA (i.e., $(Q^{-1}HAQ)_{ll'} = \Lambda_l\delta_{l,l'}$), and, except for the uniform ($l = 1$) mode, they obey Langevin equations identical to that of a simple overdamped harmonic oscillator,[132-135]

$$\frac{d\rho_l}{dt} + \frac{g}{f}\Lambda_l\rho_l = G_l(t) \quad l = 2,3,\ldots \qquad (26)$$

where $G_l(t) \equiv \sum_{n=1}^{h+1}(Q^{-1})_{ln}\mathbf{F}_n(t)$. The relaxation times for decay of the mean normal mode extensions, $\tau_l \equiv [(g/f)\Lambda_l]^{-1}$, are called the Langevin relaxation times[132,133] and are precisely twice the relaxation times manifested in the dynamic viscosity and birefringence, or dichroism, experiments. Historical precedence has established these latter relaxation times, which characterize the decay of the mean squared extension, as the "internal mode" relaxation times.[136] The dynamic viscosity times are related to the intrinsic viscosity and molecular weight by the famous Equation 79 of Zimm for free-draining polymers.[131] This important difference of a factor of two between the Langevin times, appearing in Equation 24 above, and the dynamic viscosity relaxation times has been a source of some confusion as noted by Jolly and Eisenberg.[137] Perico et al.[138] appear to have inadvertently equated τ_l with the dynamic viscosity relaxation times; fortunately, that error can be easily rectified when using their results. The more complicated situation for the depolarized component of the scattered light[132] is discussed in the next section.

Equation 24 is a purely formal result that, in fact, is valid for any model with a linear, separable (in the space coordinates) Langevin equation.[133] Apart from the prediction of a single relaxation time $\tau = (K^2D)^{-1}$ at sufficiently small values of K^2, Equation 24 is not of direct utility.

Pecora[74,110,111] has expanded the base ex-

ponential of the superexponential factor in Equation 24 for small values of the parameter $x = K^2 l_e^2/6 = K^2 R_G^2$, where $l_e^2 = hb^2 = h(3k_BT/g)$ is the mean squared end-to-end distance of the chain and R_G^2 the mean-squared radius of gyration. He explicitly evaluated the amplitudes of some of the leading terms, and also the total relaxing amplitude, for the special case of free-draining (i.e., $H_{nm} = \delta_{nm}$) linear chains in the limit of very large numbers (h + 1) of segments. Although the resulting expression is simple,

$$M_V(K,t) = \langle N \rangle (h+1)^2 \alpha^2 e^{-K^2 Dt} \left\{ S_0(x) + S_2(x) e^{-2t/\tau_1'} + \ldots \right\} \quad (27)$$

where $\tau_1' = \tau_2$ is the longest internal mode relaxation time, the amplitude $S_2(x)$ never exceeds 11% of the total in the region $1 \leqslant x \leqslant 3$, where that term dominates the intramolecular relaxation. Moreover, for smaller finite values of h + 1, the situation is likely to be even less favorable for observing the $S_2(x)$ term. Perico et al.[138] have extended the series by several terms and have obtained numerical values of the relaxation times and amplitudes for linear chains in both the presence and absence of hydrodynamic interactions for finite, but large, values of h + 1. Saleh and Hendrix[139] argue that the full time course of $M_V(K,t)$ should be the appropriate objective and have computed a set of "universal" curves for the correlation function, which they expressed entirely in terms of x and $t' = t/K^2D$. Their curves apply only to free-draining polymers in the limit of very large h + 1 and are predicated upon the validity of the theoretical relation between τ_l and D for the free-draining case. Few, if any, polymers of dimensions large enough to permit observation of the intramolecular motions exhibit the $D \propto M^{-1}$ dependence on molecular weight that is predicted by the free-draining model.

The limit of large $K^2R_G^2 >> 1$ has also received attention.[112,113,115] The effective width (Γ) of the Fourier (frequency) transform of $M_V(K,t)$, as estimated from its curvature at $\omega = 0$, was found to vary as $\Gamma \propto K^3, K^4$, in the presence, or absence, respectively, of hydrodynamic interactions, when $K^2R_G^2 >> 1.0$. This width is equivalent to the reciprocal relaxation time (τ^{-1}) for the very slowest relaxations that occur, and the result applies strictly in the limit of very large numbers of segments.

Motivated by direct observations of reciprocal relaxation times $\tau^{-1} \propto K^2$ for calf-thymus DNA at large scattering angles and by the similar $\tau^{-1} \propto K^2$ relation predicted[140] exactly for the independent-segment, mean-force model at large K^2, Lin and Schurr[133] have reexamined this problem for relatively modest values of h + 1 from 5 to 30 in the presence and absence of hydrodynamic interactions. Correlation functions $M_V(K,t)$ were computed numerically and then least-squares fitted to the expression $M_V(K,t) = A \exp[-t/\tau_A] + B$ to determine τ_A. The single-exponential fits obtained were surprisingly good, especially at small and large values of K^2b^2. In all cases it was observed that the apparent diffusion coefficient, defined by $D_{app} \equiv \tau_A^{-1}/K^2$, rose steadily from its limiting value D at small K^2b^2 to a plateau value D_{plat} at large $K^2b^2 \gtrsim 16$, as indicated in Figure 3. Moreover, analytic expressions valid at short times $t << \tau_l, l = 2,3,\ldots h+1$, for arbitrary K^2b^2 were obtained for free-draining linear chains,

$$M_V(K,t) = \langle N \rangle \alpha^2 (h+1) \left\{ e^{\frac{-k^2 k_B T t}{f}} + \sum_{n=1}^{h+1} \sum_{\substack{p=1 \\ p \neq n}}^{h+1} e^{\frac{-K^2 b^2 |n-p|}{3} \frac{}{h+1}} \right\} \quad (28)$$

and also for circular chains with and without hydrodynamic interaction.[133] It is immediately apparent that, when $K^2b^2/3$ is sufficiently large, the double-sum is negligible, and the entire relaxation is indeed a single-exponential decay with $\tau^{-1} \propto K^2$, and with an effective plateau diffusion coefficient k_BT/f equal to that of the independent segments. The same conclusion also holds for circular chains, even in the presence of hydrodynamic interactions. The condition $K^2b^2/3 > 4.0$ insures that the inequality $(K^2k_BT/f)^{-1} < \tau_l$, $l = 2,\ldots h+1$ holds for the plateau diffusion relaxation times, indicating that such relaxation indeed occurs in a time range where the short time approximation is valid. Although the constant term in Equation 28 does relax on a longer time scale, where the short time approximation is no longer valid, it comprises a miniscule fraction of the total relaxing amplitude when $K^2b^2 \geqslant 16$. That term is the one surviving at long times, after the great bulk of amplitude has decayed away, and to which the earlier[112,113,115] half-width predictions $\Gamma \propto K^3, K^4$ presumably apply.

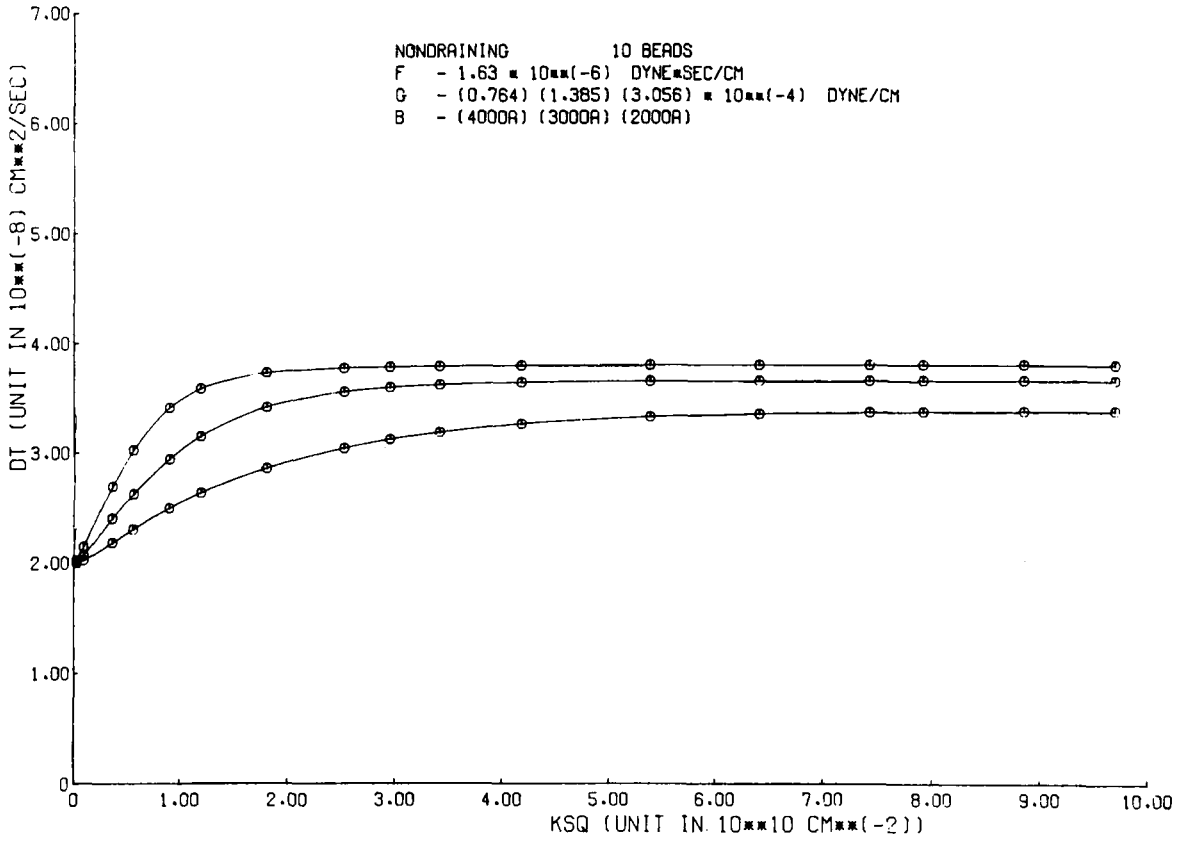

FIGURE 3. Apparent translational diffusion coefficient $D_T \equiv D_{app}(K) \equiv (\tau_A K^2)^{-1}$ vs. KSQ $\equiv K^2$ for a linear Rouse-Zimm chain in the presence of hydrodynamic interaction. Values of τ_A were obtained by fitting numerically computed correlation functions $M_V(K,t)$ to a single exponential decay, as described in the text. Pertinent parameters of the model are h + 1 = 10 beads, f ≡ F = 1.63 × 10^{-6} dyn-sec/cm, and b ≡ B = 4000, 3000, and 2000 A, respectively, for the upper, middle, and lower curves. Corresponding values of g ≡ G are 0.764, 1.385, and 3.056 × 10^{-4} dyn/cm, respectively. The center-of-mass diffusion coefficient was assigned the value D = 2.0 × 10^{-8} cm^2/sec. (From Lin, S.-C. and Schurr, J. M., *Biopolymers*, submitted. With permission.)

Based on a comparison of numerical results for the linear chain with the analytic expression for the circular chain in the presence of hydrodynamic interactions, a procedure for estimating the three parameters f, b, and h + 1 of the Rouse-Zimm model has been proposed and applied to data from calf-thymus DNA under different solution conditions.[133] The results are discussed in detail in the section on nucleic acids. Recent data of Hendrix et al.[141] on high molecular weight ($M_r \sim 9 \times 10^6$) polystyrene in toluene also appear to exhibit plateau behavior of D_{app} as a function of K^2 and should be susceptible to the same analysis. Although applicable only to flexible macromolecules with radii of gyration of several hundred nanometers, or more, this procedure allows one to examine changes in the model parameters as conditions in solution are varied, thereby providing new insights into the dynamics of intramolecular motions.

More elaborate methods for studying internal modes of flexible polymers have been suggested by Bloomfield[141a] and Schmitz.[141b] Bloomfield proposed labeling the chain ends with strongly scattering markers and nullifying scattering from the chain itself by refractive index matching, as a means of enhancing the relative contribution of internal modes at small $K^2 R_G^2$. Schmitz proposed the use of oscillatory perturbing fields in conjunction with dynamic light scattering in the study of internal mode relaxation. Because fluctuating Brownian forces were neglected, the formula of Schmitz is critically oversimplified in the sense that it fails to reduce to the correct result[141c] in any physical limit. Nonetheless, the amplitude of the purely oscillatory part of the correct result

undergoes dispersions at characteristic frequencies, corresponding to the normal mode relaxation times, as noted by Schmitz. Neither of these novel approaches has been experimentally attempted yet.

The Harris-Hearst Model

For the Harris-Hearst[142] model of a linear polymer of variable flexibility, as represented by a continuum space curve $\mathbf{r}(s,t)$ obeying the Langevin equation[118]

$$\rho \frac{\partial^2 \mathbf{r}}{\partial t^2} + \zeta \frac{\partial \mathbf{r}}{\partial t} + \epsilon \frac{\partial^4 \mathbf{r}}{\partial s^4} - K \frac{\partial^2 \mathbf{r}}{\partial s^2} = \mathbf{F}(s,t) \tag{29}$$

where s is the contour position along the chain ($0 \leqslant s \leqslant L$), ρ is the linear mass density, ζ the friction factor density, and ϵ and K are the appropriately chosen elastic constants:

$$M_V(K,t) = e^{-K^2 Dt} \langle N \rangle \alpha_M^2 \frac{1}{L^2} \int\int ds ds' e^{\frac{-K^2}{2} \sum_{l=2}^{\infty} d_l^2 \left(Q(l,s)^2 + Q(l,s')^2 - 2Q(l,s)Q(l,s') e^{-t/\tau_t} \right)} \tag{30}$$

which is simply an adaptation of Equation 24 to the present continuum model with its linear separable Langevin equation. The quantities $\tau_l \equiv (\lambda_l/\zeta)^{-1}$ and $d_l^2 = 3k_B T/\lambda_l$, as well as the complete orthonormal eigenfunctions $Q(l,s)$ and eigenvalues λ_l, can be expressed in terms of the roots α_l and $i\beta_l$ of a transcendental equation.[118] However, further simplification has yet to be achieved in the general case. A series expansion for small $K^2 d_l^2$ has been presented,[118] and the amplitudes of the leading terms and the total have been examined numerically in the limits of very large and very small persistence lengths (compared to the contour length, L). These results coincide with those of Pecora, given in Equation 27 above, for the case of very small persistence lengths. For very large persistence lengths, it is demonstrated that bending motions of the flexible rod-like chain may contribute significantly to the correlation function, although the leading internal mode term can never exceed about 25% of the total relaxing amplitude. It is notable that in the stiff-chain limit the two eigenvalues $\lambda_0 = 0$ and $\lambda_1 = 0$ are degenerate, the former corresponding to uniform translation, the latter to uniform rotation of the rod-like chain, which was neglected in the calculations just described.[118] Only if the rotation were much slower than the bending motions would those results for rod-like chains be expected to apply, as noted by Fujime and Maruyama.[118]

Numerical evaluation of $M_V(K,t)$ in Equation 30 for the various extreme and intermediate cases over a wide range of KL values would be most valuable. It is very important to know under which, if any, conditions this model exhibits plateau behavior of the apparent diffusion coefficient, as found for the finite Rouse-Zimm model above. Incorporation of hydrodynamic interactions into the light scattering development would also be a worthy objective.

The Independent-segment, Mean-force Model

For the independent-segment, mean-force model of a flexible polymer, the h + 1 beads which obey the linear separable Langevin equation[133]

$$\frac{m_0 d^2 \mathbf{r}_n}{dt^2} + f \frac{d\mathbf{r}_n}{dt} + g \sum_{m=1}^{h+1} B_{nm} \mathbf{r}_m = \mathbf{F}_n(t) \tag{31}$$

where m_0, $\mathbf{r}_n$, f, g, and $\mathbf{F}_n(t)$ are as defined for the Rouse-Zimm model (cf., Equation 23), and $B_{nm} \equiv \delta_{n,m} - 1/(h+1)$ is defined[133] to yield the displacement of $\mathbf{r}_n$ from the instantaneous center-of-mass:

$$M_V(K,t) = \langle N \rangle \alpha^2 (h+1) e^{-K^2 Dt} e^{\frac{K^2 R_G^2 \cdot (1 - e^{-t/\tau_0})}{3(h+1)}} e^{-\frac{K^2 R_G^2}{3}} \left\{ e^{\frac{K^2 R_G^2 e^{-t/\tau_0}}{3}} + h \right\} \tag{32}$$

wherein $R_G^2 = 3k_B T \cdot g$ and $\tau_0 = f/g$. A somewhat different treatment of the same problem, but neglecting the contribution of bead dynamics to the center of mass motion, has also been given.[140] In the limit of short times $t \ll \tau_0$, the preceding equation becomes

$$M_V(K,t) \cong \langle N \rangle \alpha^2 (h+1) \left\{ e^{\frac{-K^2 k_B T t}{f}} + h e^{\frac{-K^2 R_G^2}{3}} \right\} \tag{33}$$

which is quite similar to Equation 28 for the linear free-draining Rouse-Zimm chain. That feature may account for the apparent success of this model, which has also been called the "harmonically bound particle" model, in interpreting the $\tau^{-1} \propto K^2$ behavior commonly observed in gels.[9-14] It should be noted that the result of Carlson and Fraser[143] and Wun and Carlson[12] differs somewhat from Equation 32 because the average over the initial distribution P(r(0)) was omitted, as noted subsequently by Carlson.[143a] Moreover, McAdam et al.[13] also did not obtain a complete evaluation of the correlation function. The issue of whether this model or the Rouse-Zimm model better fits the data for gels and high polymers has just recently been raised[133] and is far from settled.

Chemically Reacting Systems

For a chemically reacting system in which the macromolecules undergo transformations $A \rightleftharpoons B$ between two forms with polarizabilities α_A and α_B with no change in diffusion coefficient:[88]

$$M_V(K,t) = \langle N \rangle e^{-K^2 Dt} \left[\langle \alpha \rangle^2 + (\alpha_A - \alpha_B)^2 f_A^0 f_B^0 e^{-t/\tau_R} \right] \quad (34)$$

where f_A^0 and f_B^0 are the equilibrium fractions of species A and B, the mean polarizability is $\langle \alpha \rangle \equiv f_A^0 \alpha_A + f_B^0 \alpha_B$, and $\tau_R \equiv (k_f + k_b)^{-1}$ is the chemical relaxation time. In this simple case, the chemical transformation may be viewed as an independently fluctuating internal mode of the polarizability with just two possible values $\{\alpha_A, \alpha_B\}$. The time-dependent fluctuating fraction $\Delta f_A(t) = f_A(t) - f_A^0$ obeys the relaxation equation $\partial \Delta f_A / \partial t = -k_f \Delta f_A + k_b \Delta f_b = -(k_f + k_b)\Delta f_A$, and $\langle \Delta f_A(0)^2 \rangle = f_A^0(1 - f_A^0)$. The important point is that, when the chemical relaxation time is appreciably faster than the diffusional relaxation time, there will appear in the correlation function a fast component independent of the scattering angle, provided that a significant change in polarizability is associated with the chemical transformation.[88] This conclusion holds for more complex reaction schemes as well.[74,89] Unfortunately, sufficiently large polarizability changes are seldom, if ever, the case. When the diffusion coefficients of reactant and product species differ significantly, there is afforded an additional opportunity to determine the chemical relaxation time, even if there is no change in polarizability.[95,96] Unfortunately, in that case a rather large change in diffusion coefficient is required to produce a significant amplitude of the term exhibiting chemical relaxation. Such examples have yet to be unequivocally demonstrated in practice and are likely to occur only rarely. Benbasat and Bloomfield[96] have investigated the conditions under which the chemical relaxation rate might be observed.

When the exciting light is near an absorption band, the scattered light will be phase-shifted by an amount differing from the usual 180°, corresponding to the introduction of a complex polarizability $\alpha = \alpha_R + i\alpha_I$ with both real (in-phase) and imaginary (out-of-phase) parts. In such a case, the result[144] is exactly that of Equation 34 with $|\langle \alpha \rangle|^2$ in place of $\langle \alpha \rangle^2$ and $|\alpha_A - \alpha_B|^2$ in place of $(\alpha_A - \alpha_B)^2$. A large change in the out-of-phase component of the polarizability, α_I, is known to occur in some reactions (e.g., oxygenation of hemoglobin) and could conceivably produce a significant amplitude of the chemically relaxing term. However, it is doubtful whether more than 50% of the total relaxing amplitude could occur in the chemically relaxed term for typical broad-band chromophores, although it is in principle possible for single damped harmonic oscillators, when the resonance frequencies of A and B lie on opposite sides of the incident light frequency. In that case, α_R changes sign when A converts to B.[144] The apparent observation[145] of a chemically relaxed term comprising $\geqslant$50% of the total relaxing amplitude at low angles in the (O_2 + hemoglobin) system could, perhaps, be rationalized by the observed change in the absorption cross section, which is proportional to the imaginary part, α_I, coupled with a change in the sign of α_R. However, such an interpretation is especially doubtful in view of the fact that Haas et al. did not observe any "chemical" relaxation in a similar experiment.[146] The fact that α_R is the excess (real) polarizability with respect to that of the displaced solvent might make a change in its sign a more common occurrence than suspected at first glance.

At the moment, the considerable body of theory relating to dynamic light scattering from chemically reactive fluids[87-101] stands without any unequivocal experimental realization. The promising approach of electrophoretic light scattering[99] to chemically reacting systems is still

untried. With the availability of tunable dye lasers it may be possible to examine systems at frequencies near electronic resonances, where both real and imaginary parts are large.[147] Merocyanine dyes that exhibit large changes in their absorption spectra upon changing environment also provide promising systems for the study of chemical kinetics by dynamic light scattering techniques. However, substantial laser heating effects must also be expected when studying strongly absorbing molecules.

Interacting Spherical Macromolecules

For a system of interacting spherical macromolecules obeying the generalized N-particle Smoluchowski-Einstein equation[120] without hydrodynamic interactions:

$$D_{app}(K) \equiv \lim_{t\to 0} \frac{\partial \ln g^{(1)}(K,t)}{\partial t} = \frac{D_o}{G(K,0)} \tag{35}$$

where $D_0 = k_B T/6\pi\eta a$ is the Stokes-Einstein diffusion coefficient for the macromolecules of radius a in the solvent of viscosity η.[119,120] The first rigorous derivation of this result was provided by Ackerson,[120] who also derived the correction term for incorporation of hydrodynamic forces in the Oseen tensor approximation. The following is an alternative form of the result when hydrodynamic interactions have been included.[144]

$$D_{app}(K) = D_o \left\{ 1 - G(K,0)^{-1}\, c\, 4\pi \int dr\, r^3 \left(1 - \frac{3a}{2r}\right) \frac{\partial g}{\partial r} \left[\frac{\cos(Kr)}{(Kr)^2} - \frac{\sin(Kr)}{(Kr)^3} \right] \right\} \tag{36}$$

where c is the particle concentration, and g(r) is the equilibrium radial distribution function. The entire effect of hydrodynamic interactions in the Oseen tensor approximation is manifested in the term $-3a/2r$. Because g(r) and $\partial g/\partial r$ both vanish for all $r < 2a$, the integrand is nonvanishing only when $3a/2r < 1.0$, so that hydrodynamic interactions act always to oppose the direct forces, but never to reverse the sign of the correction term in Equation 36. The sign of the correction term can always be determined from Equation 35, from which it is predicted that $D_{app} > D_0$ when $G(K,0) < 1.0$, and vice versa. The static structure factor can be expressed in terms of the radial distribution function by[120]

$$G(K,0) = 1 + c\, 4\pi \int dr\, r^2\, [g(r)-1] \frac{\sin(Kr)}{Kr} \tag{37}$$

In the $K \to 0$ limit the integral will be negative when repulsive forces predominate, giving $G(0,0) < 1.0$ and $D_{app}(0) > D_0$. Likewise, when attractive forces predominate, $G(0,0) > 1.0$ and $D_{app}(0) < D_0$. Thus, for long-wavelength motions, traditional intuition,[148] based on the osmotic pressure, or activity coefficient, remains qualitatively valid, even after incorporation of hydrodynamic interactions. At sufficiently large K, the integral in Equation 37 becomes negligible; thus, $D_{app}(\infty) = D_0$.

The apparent diffusion coefficient is defined in Equation 35 as the first cumulant of the normalized correlation function $g^{(1)}(K,t)$. Ackerson[120] has also derived expressions for the second cumulant for the same system in the presence and absence of hydrodynamic interaction.

Highly Charged Polyelectrolytes

For a system of highly charged positive polyions (P), together with both negatively charged counterions (−) and positively charged coions (+) of the added salt, all obeying the linearized coupled diffusion equation equations,[104]

$$\frac{\partial \Delta C_p}{\partial t} = D_p \nabla^2 \Delta C_p + \bar{C}_p u_p q_p \nabla^2 \psi \tag{38a}$$

$$\frac{\partial \Delta C_-}{\partial t} = D \nabla^2 \Delta C_- - (\bar{C}_c + \bar{C}_s) u q \nabla^2 \psi \tag{38b}$$

$$\frac{\partial \Delta C_+}{\partial t} = D \nabla^2 \Delta C_+ + \bar{C}_s\, u q \nabla^2 \psi \tag{38c}$$

together with Poisson's equation for the common electrostatic potential

$$\nabla^2 \psi = -\frac{4\pi}{\epsilon} [q_p \Delta C_p - q\, \Delta C_- + q\, \Delta C_+] \tag{38d}$$

wherein D_p, u_p, and $q_p = eZ$ are, respectively, the friction coefficient, mechanical mobility, and electric charge on the polyion; D, u, and ±q are the corresponding quantities for the counterions and coions; and $\bar{C}_p$, $\bar{C}_s$, and $\bar{C}_c = Z\bar{C}_p + \bar{C}_s$ are the mean concentrations of polyions, added salt, and counterions, respectively:

$$M_V(K,t) \cong A e^{-K^2 D_{app} t} \tag{39}$$

where[104,109]

$$D_{app} = \tfrac{1}{2} [D_p (1-\Omega) + D(1+\Omega)] \tag{40}$$

and

$$\Omega = \frac{D_p - D[1 + (2\bar{C}_s/\bar{C}_p)\,Z^{-1}]\,Z^{-1}}{D_p + D[1 + (2\bar{C}_s/\bar{C}_p)\,Z^{-1}]\,Z^{-1}} \tag{41}$$

The coefficient A is an undetermined constant. Within the domain of the linearization approximation, Equation 39 is valid whenever the inequality $[D_pK_p^2 + D(K_c^2 + 2K_s^2)] \gg (D_p + D)K^2$ holds,[104,109] which should be the case for any highly charged polyelectrolyte under virtually all accessible experimental conditions. The quantity K_p is defined by the usual relation $K_p^2 \equiv 4\pi C_p q_p^2/\epsilon k_B T$, with analogous definitions for K_c and K_s.[104,109]

Not surprisingly, two other fluctuating K-modes are also present. One is a pure salt diffusion mode that is completely uncoupled from the polyion motions at this level of approximation.[104,109] At the extremes of high and low salt concentration, the third K-mode can be shown[109] to be a pure charge fluctuation that is very rapidly relaxed by ohmic conduction[89] in its own self-electric field. Moreover, owing to the large electrostatic self-energy, the mean squared amplitudes of such charge fluctuations are generally negligible under ordinary circumstances.[89,149,149a] Thus, the neutral K-mode, the amplitude of which is essentially proportional to the fluctuating polyion concentration, is the only one associated with a significant intensity of scattered light.[104,109]

In the limit of high salt concentration, or low polyion concentration, or small polyion charge, D_{app} in Equation 40 can be expanded in powers of $Z^2\bar{C}_p/\bar{C}_s$ to give[109]

$$D_{app} \cong D_p + \frac{D_p}{2}\left(1 - \frac{D_p}{D}\right) Z^2\,\bar{C}_p/\bar{C}_s + \ldots \tag{42}$$

which is quite similar to the expression derived for macroscopic diffusion by Alexandrowicz and Daniel,[150] using relations analogous to Equations 38a, b, and c together with a zero-current condition. Olson et al.[151] have obtained a similar expression using the traditional formula[148] for D together with Tanford's estimate[152] (from Debye-Hückel theory) of the electrostatic contribution to the second virial coefficient of the osmotic pressure.

It should be noted that Equations 39 and 40 apply even for the case of zero added salt, $\bar{C}_s = 0$, provided that $(D_pK_p^2 + DK_c^2) \gg (D_p + D)K^2$, which, as noted above, should hold for nearly all presently accessible experimental conditions, even for weakly charged polyelectrolytes. These results are valid strictly for fluctuations of wavelength long compared to the sum of the polyion radius and the small-ion Debye length, $(K_c + 2K_s)^{-1}$.

Stephen[102] has given a similar linearized treatment, but has neglected counterion dynamics in the sense that the counterion concentration was assumed to adjust instantaneously to any changes in the electrostatic potential. The result of Stephen can be obtained from the general eigenvalues of Lee and Schurr[104] by expanding under the assumption that $D(K^2 + \kappa_c^2 + 2\kappa_s^2) \gg D_pK_p^2$. In the absence of salt, this inequality is not generally satisfied for light of visible wavelengths, unless the polyion has only a rather modest total charge $Z \ll (D/D_p)^{1/2}$ or unless the concentration of polyion is extraordinarily low. The result of Stephen,[102] and also of Doherty and Benedek,[103]

$$D_{app} = D_p + \frac{D_pK_p^2}{K^2 + \kappa_c^2 + 2K_s^2} \tag{43}$$

is equivalent at high salt concentration to Equation 42, except for the factor $(1 - D_p/D)$ that arises from incorporation of small-ion dynamics. Prospects for observing the $K^2 \gg K_c^2$ limit, in which case the correction term in Equation 43 would appear (in Equation 39) as a fast angle-independent component,[74,89,102,104] are not promising. The maximum available K^2 with visible incident light is about 10^9 cm^{-2}. Even for Z = 5 charges, the concentration of polyion would have to be about 4×10^{-8} *M*, or lower, to have $K_c^2 \lesssim K^2$. With ordinary scattering cross sections, then, molecular weights of $M_r \gtrsim 5 \times 10^6$ would be required to provide a tolerable detection efficiency at such a low concentration. Neutral, or very weakly charged, species of such high molecular weight are prone to undergo extensive aggregation in water. Even those which remain stable at their isoionic points with no net charge would exhibit very large electric moments, and also nontrivial hard-core repulsions, that would be expected to dominate the diffusion in any case.

In the absence of salt, Equation 40 gives

$$D_{app} = D_p\,\frac{(D + D/Z)}{(D_p + D/Z)} \tag{44}$$

which is independent of polyion concentration, in agreement with the free-boundary diffusion studies of Kedem and Katchalski[153] and Daniel

and Alexandrowicz.[154] In the limit of very large charge Z, one obtains $D_{app} \cong D(1 + Z^{-1})$, which predicts that sufficiently highly charged polyions should diffuse with essentially the same diffusion coefficient as that of the salt. In the opposite limit $D/Z >> D_p$, one finds $D_{app} \cong D_p(Z + 1)$, in approximate agreement with the result of Stephen when $K_c^2 >> K^2$. Equation 44 predicts always that $D_{app} > D_p$ at zero salt for charged macromolecules. The predicted enhancements are expected to be manyfold, in agreement with the free-boundary diffusion results.[153,154] The results of the light scattering experiments are more complex and will be discussed further in the experimental sections on poly(L-lysine) and long-range electrical forces.

Other theoretical developments for the polyelectrolyte problem have been given by Phillies,[105-108] and Berne and Pecora.[74] An interesting computational approach, which may ultimately be the only way of dealing quantitatively with this problem in situations where the linearized theory fails, has been proposed by Ermak and Yeh[155] and tested by Ermak.[156,157] Varoqui and Schmitt[158] have considered polyelectrolyte diffusion from the point of view of linear irreversible thermodynamics, and note the existence of a significant charge effect (i.e., enhanced friction factor), even in the presence of moderately high concentrations of added salt.

Uniformly Translating Macromolecules

For noninteracting macromolecules undergoing simultaneous diffusion and uniform translation with velocity **u**:

$$M_V(K,t) = \langle N \rangle \alpha_M^2 e^{-K^2 Dt} e^{-iK \cdot ut} \tag{45}$$

as first employed for macromolecules by Ware and Flygare.[85] Because the velocity is manifested only as a complex phase factor, it will not appear in $|g_V^{(1)}(K,t)|^2$ in the homodyne correlation function of Equation 12, but can be observed as *Re* $g_V^{(1)}(K,t) = \exp[-K^2 Dt] \cos(\mathbf{K} \cdot \mathbf{u}\, t)$ in the heterodyne correlation function of Equation 15, where the Doppler shift frequency $\mathbf{K} \cdot \mathbf{u}$ is explicitly manifested as a (damped) cosinusoidal oscillation in time.[74,75,85,86]

Expressions for $M_H(K,t)$

For a suspension of N macromolecules, each composed of h optically anisotropic segments with effective polarizabilities given by Equation 5, the correlation function $M_H(K,t)$ takes the form

$$M_H(K,t) = \langle N \rangle \beta^2 \frac{8\pi}{60} \left\langle \frac{1}{N} \sum_{m=1}^{N} \sum_{n=1}^{N} e^{iK \cdot [R_m(0) - R_n(t)]} \right.$$

$$\sum_{\beta=1}^{h} \sum_{\delta=1}^{h} e^{iK \cdot [b_\beta^m(0) - b_\delta^n(t)]}$$

$$\left(Y_{2,1}^* [\Omega_\beta^m(0)]\, Y_{2,1} [\Omega_\delta^n(t)] + Y_{2,-1}^* [\Omega_\beta^m(0)]\, Y_{2,-1} [\Omega_\delta^n(t)] \right.$$

$$\left. \left. - Y_{2,1}^* [\Omega_\beta^m(0)]\, Y_{2,-1} [\Omega_\delta^n(t)] - Y_{2,-1}^* [\Omega_\beta^m(0)]\, Y_{2,-1} [\Omega_\delta^n(t)] \right) \right\rangle \tag{46}$$

where the solid-angle notation $[(\Omega(t)] = [\theta(t),\phi(t)]$ has been employed in the arguments of the spherical harmonics. The vector $\mathbf{b}_\beta^m$ is that from the center-of-mass of the macromolecule at $\mathbf{R}_m$ to its βth segment. Equation 46 follows from Equations 3, 5, and 6 after expressing the product $\cos[\theta(t)]\ \cos[\chi(t)]$ in terms of spherical harmonics with the aid of the Addition Theorem. This formidable expression can be simplified appreciably by the following three assumptions:

1. The macromolecules are noninteracting.

2. The fluctuation wavelength is large compared to the macromolecular diameter, so that the internal interference phase factors $\exp[iK \cdot b]$ may all be replaced by 1.0.

3. The center-of-mass and internal motions are uncorrelated, under which conditions the average of the product in Equation 46 factors to the product of separate center-of-mass and angular averages.

The instantaneous fraction per unit solid angle $f(\theta,\phi,t)$ of the h segments of a macromolecule with

cylinder axes pointing in the direction specified by θ and ϕ may be expressed in terms of spherical harmonics as[32]

$$f(\theta,\phi,t) = \sum_{l,m} f_{lm}(t) Y_{lm}(\theta,\phi) \quad (47)$$

where the $f_{lm}(t)$ can be determined by inversion of the known distribution $f(\theta,\phi,t)$.

Correlation functions for the depolarized component of the excess polarizability density are listed below for several pertinent examples.

Polymers of Anisotropic Segments

For macromolecules comprised of h optically anisotropic cylindrically symmetric segments obeying the preceding three assumptions:

$$M_H(K,t) = \langle N\rangle \beta^2 \frac{8\pi}{60} e^{-K^2 Dt} h^2 2 \left\{ \left\langle f^*_{2,1}(0) f_{2,1}(t) \right\rangle - Re \left\langle f^*_{2,1}(0) f_{2,-1}(t) \right\rangle \right\} \quad (48)$$

where the angular average in Equation 46 has been carried out using $f(\theta,\phi,0)$ at t = 0, and $f(\theta,\phi,t)$ at time t.[32] For very long polymers, the $f^*_{2,1}(t)$ and $f_{2,-1}(t)$ modes should be negligibly correlated; hence, the first term in curly brackets should predominate in that instance. Evidently, at long wavelengths the depolarized light monitors the fluctuating amplitudes of particular spherical harmonic components of the angular distribution of segment axes.[32,74]

Anisotropic Rigid Rods

For rigid rods (h = 1) undergoing uncoupled translational and rotational diffusion, as in Equation 21,[74,159]

$$M_H(K,t) = \langle N\rangle \beta^2 \frac{1}{15} e^{-K^2 Dt} e^{-6D_R t} \quad (49)$$

which follows from Equation 48 using the relations[32]

$$\left\langle f^*_{2,1}(0) f_{2,-1}(t) \right\rangle = 0, \left\langle f^*_{2,1}(0) f_{2,1}(t) \right\rangle = \left\langle |f_{2,1}(0)|^2 \right\rangle \exp[-6D_R t]$$

and

$$\left\langle |f_{2,1}(0)|^2 \right\rangle = (4\pi h)^{-1}$$

The book by Berne and Pecora[74] should be consulted for results pertaining to more general rigid molecule situations, such as noncylindrically symmetric optical polarizability tensors and asymmetric diffusors. Maeda and Saito[124] have computed the spectrum for rigid rods of dimension comparable to the scattering wavelength. Correlation functions for the elements of tensors of different rank have been derived from the generalized Debye diffusion model by Favro.[160] As yet, those more complicated results have not been applied to the interpretation of data from macromolecules and biopolymers, although they have been very important in studies on small molecules.[74,161]

The Rouse-Zimm Model of an Anisotropic Polymer

For the Rouse-Zimm model of a flexible polymer, as defined by the Langevin Equation 23, the springs of which, upon extension, generate local excess polarizability tensor elements $\alpha_{n,xz}(t)$ proportional to $[z_{n+1}(t) - z_n(t)]\ [x_{n+1}(t) - x_n(t)]$:

$$M_H(K,t) = \text{const} \langle N\rangle e^{-K^2 Dt} (k_B T)^2 \sum_{r=2}^{h+1} e^{-2t/\tau_r} \quad (50)$$

which is valid only at very small scattering angles, such that $K^2 d_l^2 \ll 1$ for all normal modes.[116,132] The considerably more involved expression valid for finite angles has also recently been derived.[132]

Number Fluctuations

In studies of extremely dilute solutions of large macromolecules, or very small volumes, the number of macromolecules in the illuminated scattering region is not large compared to 1.0, and fluctuations in the number of scatterers become important. Because the characteristic times for relaxation of these fluctuations $\tau_c \sim 2L^2/D$ are generally quite long compared to $(K^2 D)^{-1}$, these so-called occupation number fluctuations ordinarily make no significant contribution to either the spectrum of the scattered light or the heterodyne autocorrelation function. Their contribution to the homodyne correlation function may be significant, however, due to the static term in Equation 11. For slow number fluctuations, Equation 12 takes the approximate form,[74]

$$\left\langle I_\gamma^S(R,0)I_\gamma^S(R,t)\right\rangle \cong \frac{W(K,0)}{\langle N\rangle^2}\left\{\langle N\rangle^2\,(1+|g^{(1)}(K,t)|^2 + \left\langle \delta N(0)\delta N(t)\right\rangle\right\} \quad (51)$$

Because $\langle \delta N(0)^2\rangle = \langle N\rangle$, the second term, which contributes an apparent baseline at long times, will be comparable to the rapidly decaying amplitude when $\langle N\rangle = 1.0$. By diluting their virus samples into the region where number fluctuations became significant, Salmeen et al. were able to estimate the concentrations of viruses in their suspensions.[83] This may prove to be a valuable technique in future applications.

DYNAMIC LIGHT SCATTERING TECHNIQUES

Experimental Methods

A typical dynamic light scattering experiment is indicated schematically in Figure 4. Detection and processing methods that have been employed for determining the intensity autocorrelation function of the scattered light may be divided into three basic categories: photocurrent spectral analysis,[1-3,74,75] photocurrent autocorrelation,[74,75,162] and photon correlation.[4,74,75,163]

In an ideal homodyne or heterodyne experiment, one should determine the autocorrelation function, or time-averaged product, $\langle n(t)\cdot n(t+\tau)\rangle_t$, of the number of photoelectron pulses, n(t), occurring in each of two nonoverlapping sampling intervals of duration T, short compared to the relaxation times of interest and separated by a delay time τ. Moreover, this process should be carried out simultaneously for a large number of τ-values, or delay channels, covering the time range of interest. Such is the technique of ideal photon correlation.

In general, the photon correlation function is related to the theoretical intensity autocorrelation function by[163-167]

$$\langle n(t)\, n(t+\tau)\rangle_t = \langle n\rangle^2\left\{1 + f(A)\left[\frac{\langle I_\gamma^S(R,0)\, I_\gamma^S(R,\tau)\rangle - \langle I_\gamma^S\rangle^2}{\langle I_\gamma^S\rangle^2}\right]\right\} \quad (52)$$

where f(A) is a factor depending on the number of coherence areas of the scattered light over the photoelectric surface of the detector and on the finite sampling time. Due to the finite extent of the photocathode, the light at two well-separated points on its surface does not necessarily arise from the same fluctuating K-mode of the polarizability. Hence, the light at those two points may not be coherent, but rather the respective intensities may be fluctuating independently. When the number N of coherence areas is large, $f(A) \approx N^{-1}$; thus, the relaxing part of the correlation function may be very small. The problem of maximizing simultaneously the coherence area, or solid angle, which is favored by smaller scattering volumes, and the wavevector resolution, which is favored by larger scattering volumes, has been discussed by Dubin.[67] Except at very small scattering angles the wavevector resolution does not seriously limit the precision of the experiment. The coherence solid angle has been discussed in great detail by Chu.[75] Roughly speaking, the coherence angle is $\phi \approx (1/2)\Delta k_x/|k^S| = \lambda/2L_x$, where $\Delta k_x = 2\pi/L_x$ is the spacing between adjacent K_x values in the illuminated scattering volume, and L_x is the corresponding scattering volume dimension. Focusing the laser beam down is a recommended procedure for enlarging the coherence area with no loss of scattered light.[75]

For the extreme cases of either monochromatic, or sufficiently broad-band Gaussian incident light, Equation 52 simplifies in the homodyne case to

$$\langle n(t)\, n(t+\tau)\rangle_t = \langle n\rangle^2\,(1+f(A)|g_\gamma^{(1)}(K,\tau)|^2) \quad (53)$$

giving directly the desired dynamical information. However, if the incident light fluctuates, even slowly, during the course of the experiment, then the result is somewhat different. For example, slowly fluctuating Gaussian incident light gives

$$\langle n(t)\, n(t+\tau)\rangle_t = \langle n\rangle^2\, 2\{(1+f(A))/2 + f(A)\,|g^{(1)}(K,t)|^2\} \quad (54)$$

Equation 54 shows that the baseline cannot in this case be computed from $\langle n\rangle^2$ unless the value of f(A) is known. The baseline should in general be determined from data at long time delays, as noted by Chen et al.,[166] unless it is certain that the laser does not fluctuate over the duration of the experiment. When the incident beam fluctuates during the experiment, the scattered light is not in general Gaussian.[168] If the incident light fluctuates insignificantly over a period of several decay

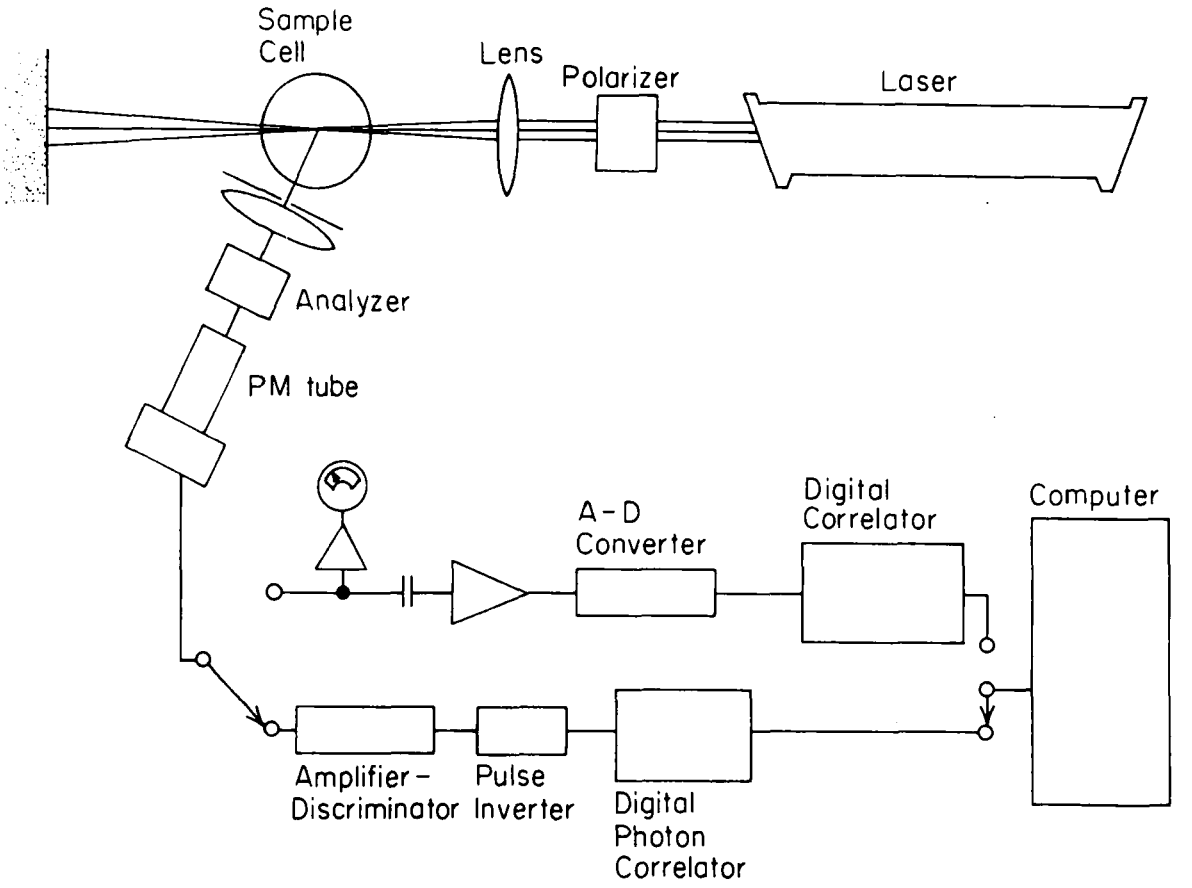

FIGURE 4. Schematic diagram of experimental apparatus for photon correlation (with switches as shown) and photocurrent correlation (with switches in alternate positions).

times of $g^{(1)}(K,t)$, then on that time scale the scattered light may, perhaps, be regarded as Gaussian, and the clipped correlation functions (described below) that have been derived for Gaussian light probably apply with minor changes, comparable to that going from Equation 53 to 54 above. When fluctuations of the incident light relax rapidly compared to the sampling time T, it seems intuitively probable that the clipped correlation results for Gaussian light also apply, but that is only a speculation. This problem certainly needs further work.

A device that operates as a nearly ideal digital correlator has been described by Asch and Ford.[169] The Massachusetts group has now had considerable experience with the construction and operation of these devices, and those contemplating the construction of such an instrument are advised to correspond directly with Professor Ford. At the shorter time scales, their original device operated effectively as a double-clipped correlator, because there was insufficient time to complete the 3 X 3 bit multiplication, which was accomplished by successive addition.[170] Their latest version completes a 4- by 4-bit multiplication in less than 100 nsec.[170]

When it is known, or believed, in advance that the scattered light is Gaussian, then the multiplication step can be avoided by employing the method of single or double clipping,[4,163-167] which is equivalent to truncating to one bit (0 or 1) either one, or both, members, respectively, of the correlation product $\langle n(t)n(t+\tau)\rangle_t$. Thus, the multiplication step is reduced to a single addition step. An excellent discussion of the principles of single-clipped correlation, illustrated schematically in Figure 5, and the details of construction of an inexpensive single-clipped digital correlator, have been given by Chen et al.[166] The interested reader is encouraged to correspond directly with Professor Chen for assistance with the circuit boards. Since multichannel clipping techniques were in-

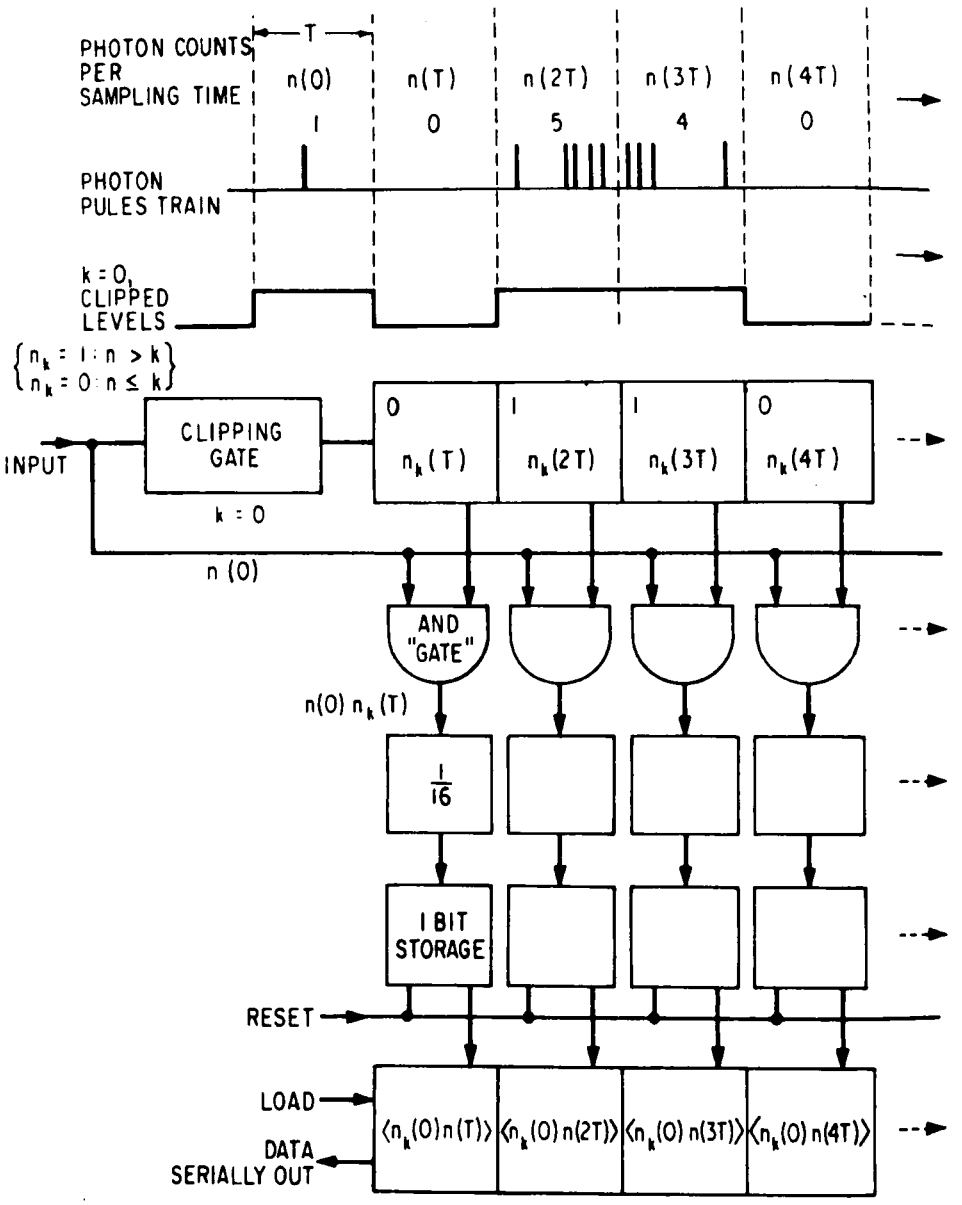

FIGURE 5. Schematic diagram of the operation of a single-clipped photon correlator. The top line indicates the various numbers of photons n(jT) arriving in the j = 0, . . . , 4 sampling intervals of duration T. The interval j = 0 corresponds to the present time, and intervals j = 1,2,3,4 denote successively earlier times. The second line shows the corresponding clipped values $n_k(jT)$ in those same intervals for the particular case when the clip level is k = 0. The output of the clipping gate is set to 1.0 when the number of photons arriving in the present interval exceeds the clip level; otherwise, it is 0. At the clock pulse initiating the next sampling interval, the output of the clipping gate enters a line of one-bit shift registers, the contents of which are likewise shifted one channel to the right on the same clock pulse, as shown on the third line. Photon pulses arriving in the present interval (j = 0) are simultaneously combined via AND gates with the clipped values for previous intervals, which reside in the j = 1, . . . , 4 shift registers, as indicated on the fourth line. The counts from the AND operation in each channel are accumulated into a four-bit register with an overflow bit that is in turn accumulated into the memory of a multichannel signal averager, which is where the developing correlation function $\langle n_k(0)n(jT)\rangle$ is stored. (From Chen, S. H., Veldkamp, W. B., and Lai, C. C., *Rev. Sci. Instrum.*, 46, 1356, 1975. With permission.)

troduced to the study of biopolymers by Foord et al.[4] in 1970, their use has become widespread.

For non-Gaussian light, the true, or full, correlation function can be obtained by either uniform sequential[171] or random[172] variation of the clip level (or truncation point). The technique of scaling, introduced by Jakeman et al.,[172] appears to be an optimum method of randomly varying the clip level to obtain an accurate approximation to the full photon correlation function. The efficiency, however, is much less than that of an ideal correlator. A comprehensive review of these techniques, including both the apparatus and the joint photocount statistics, is given by Chu.[75]

In the so-called analog or photocurrent methods, the photoelectron pulses are not shaped and used to drive digital logic devices, as in the photon correlators just described; instead, the amplified photomultiplier output is capacitively coupled to the input of an analog-digital converter. The capacitive coupling filters out the bulk of the static background. The photomultiplier output is effectively averaged over the duration of the sample-and-hold window of the A-D converter, typically 50 or 100 nsec. The resulting sequence of digital numbers may be processed by any of the procedures described above or stored in a computer[32,173] for later processing either by direct multiplication or by single clipping under software control.[174] Computer storage prior to processing offers the advantage that the same data can be evaluated on several different time scales and suffers the considerable disadvantage that the developing correlation function cannot be continuously viewed during data collection. The resulting autocorrelation function $\langle (J(t) - \langle J \rangle)(J(t+\tau) - \langle J \rangle) \rangle_t$ of the fluctuating part of the photocurrent consists principally of a dynamic part proportional to the time-dependent parts of Equations 52 to 54 and may also contain a small baseline contribution from ground-loop offset of the A-D converter or from capacitor discharge following high-intensity fluctuations (Tyndalls) due to large dust particles or aggregates traversing the scattering volume. In addition, because the $\tau = 0$ delay time is also usually processed in this mode of operation, there is an additional "shot-noise" contribution in that delay channel arising from the correlation of the photons in a given sampling interval with themselves. For the cases of either monochromatic or broad bandwidth incident light, the homodyne correlation function is[74,75]

$$C(\tau) \equiv \langle (J(t) - \langle J \rangle)(J(t+\tau) - \langle J \rangle) \rangle_t$$

$$= e\langle J \rangle \delta(\tau) + \langle J \rangle^2 f(A) |g_\gamma(1)_{(K,\tau)}|^2 + B \qquad (55)$$

where B is the baseline contribution. The first term is the shot-noise term and appears only for the $\tau = 0$ delay time.

The effect of high and low band-pass filtering on these correlation functions has been examined by King and Lee[175] and more recently by Soda et al.[176] Elimination of the filters is a prime advantage of photon correlation techniques.

Although photon correlators should have a distinct advantage in efficiency over photocurrent correlators at low light levels and short sampling times,[177] this advantage is substantially reduced at higher light levels and longer sampling times. In fact, considering the ease with which the accumulation registers of most existing photon correlators are saturated, often necessitating substantial reductions in the light flux, it is probable that the photocurrent correlators actually enjoy a slight advantage of a few percent at the higher light levels and longer time scales.

For work on complex systems, especially preparations of biological origin, the value of a large number of delay channels can hardly be overstated. By either method of correlation, the baseline must in general be determined by the correlation data. It is not uncommon to find small amplitudes of very slowly relaxing components that produce a slight tilt to the baseline, the effect of which is difficult to ascertain when only a few channels are available. In our experience, 128 channels are often too few, 256 is a reasonable compromise, and 400 or more is highly desirable for visual inspection, even when fewer points are used for the actual fitting. The correlators constructed by the Massachusetts group have the capability of expanding the scale, or time delay, between the later channels, which achieves the principal benefits of many extra channels at lower cost.[170]

Photocurrent spectral analysis was the method employed in the original homodyne[1,3] and heterodyne[2] experiments and directly yields the frequency Fourier transform of the photocurrent correlation function. The single-channel apparatus employed in the earlier experiments has given way to multichannel real-time spectrum analyzers, which are especially useful in electrophoresis and other studies of uniform translation of macro-

molecules, viruses, and cells.[59,60] The velocity of translation can be read directly from the spectrum. These real-time spectrum analyzers are fully equivalent in efficiency to photocurrent correlators.

Direct spectral analysis of the scattered light can be achieved using either pressure or piezoelectrically scanned Fabry-Perot interferometers. However, interferometry at present can be successfully applied only to spectral broadening by systems with relaxation times shorter than 10^{-6} sec.[74] Fortunately, many existing correlators operate with a minimum time delay of 10^{-7} sec, or even 5 $\times$ 10^{-8} sec, so that relaxation times in the microsecond and submicrosecond range are actually accessible by intensity fluctuation techniques. The theory and details of operation of Fabry-Perot interferometers have been thoroughly reviewed by Chu.[75]

A differential light scattering technique, in which photocurrent spectrum analysis is performed alternately with the same analyzer for light scattered from each of two adjacent cells illuminated by the same laser beam and with the same sample, but under different solution conditions, has been recently described.[178,179] Differences in diffusion coefficient between the two samples as small as 4% of D could be accurately measured for aspartate transcarbamylase in the presence and absence of succinate and carbamyl phosphate.

Dust and undesired large aggregates constitute the major difficulty in most dynamic (and static) light scattering investigations. Both centrifugation and filtration techniques are commonly employed to eliminate this problem. The novel approach of developing the correlation function through a series of moderately short data accumulation runs and interrogating each run for abnormally high light levels, indicative of dust, prior to final storage in a dedicated minicomputer has recently been demonstrated by Alon and Hochberg.[180] In the final analysis, of course, it is always better to eliminate the Tyndall problem before taking any data, but in many systems of interest that simply is not possible.

The combination of band sedimentation[181,182] and band electrophoresis[183] techniques with dynamic light scattering studies of the components of the various bands as they intersect the light beam offers a promising approach to the study of heterogeneous mixtures. The related technique of electrophoretic light scattering is now well developed and in principle offers a more rapid means for simultaneously determining the diffusion coefficient and electrophoretic mobility.[59,60] However, if charge heterogeneity on the macromolecules is significant, as cautioned by Phillies,[108] then the resulting dispersion of the electrophoretic velocity will introduce substantial error into the measured diffusion coefficient. In that case, the band electrophoresis approach suggested by Lim et al.[183] would be an attractive alternate. Electrophoretic light scattering has been reviewed by Flygare et al.[60] and by Ware.[59] A novel method for electrophoretic measurements is that proposed by Josefowicz and Hallett.[184]

Bauer et al. have recently demonstrated that the rotational relaxation time obtained from ^{13}C nuclear magnetic resonance, using the value of T_1 and the nuclear Overhauser enhancement of the α-carbons, agrees well with that obtained by interferometric measurement of the spectral broadening of light scattered by muscle calcium binding protein.[185] This is a case where the light scattering method has been used to calibrate a promising new method for studying orientational motions of rigid proteins and polypeptides and one that may be the only alternative when the anisotropy of the polarizability is too small for scattering experiments.

DATA ANALYSIS

Except for the case of uniform translational motion, all of the various correlation functions $M_\gamma(K,t)$ are monotonically decaying functions of the time, often consisting of a sum of two or more exponentially relaxing terms. The observed correlation function $C(\tau)$ in the homodyne experiment consists, then, of a baseline plus the square of the corresponding sum of exponential terms,[74,75]

$$C(\tau) = (Ae^{-t/\tau_A} + Be^{-t/\tau_B} + \ldots)^2 + C_\infty \qquad (56)$$

This expression provides all of the well-known difficulties associated with the estimation of time constants and amplitudes of multiple exponential decays from noisy data.[186] In addition, the possibility exists that macromolecules in the solution are not all identical; they may differ in molecular weight, diffusion coefficient, and relaxation times of internal motions. In such polydisperse solutions of noninteracting macromolecules, the observed correlation function has the form

$$C(\tau) = \left(\sum_j M_{\gamma,j}(K,t) / \sum_l M_{\gamma,l}(K,0) \right)^2 + C_\infty \qquad (57)$$

where the sums run over all classes of molecules present. There are, then, two potential sources of non-single-exponential decay: one due to the inherent dynamic properties of a (monodisperse) suspension of the macromolecules and the other caused by polypersity. In the former case, nonlinear least-squares techniques have generally been applied, using a squared sum of two exponentials, as in Equation 56, with an added baseline.[32,187] To improve the convergence properties, it is often desirable to reduce the number of adjustable parameters. In practice, this has been effected by computing the baseline from mean-count and clipped-count data.[137,188-191] This procedure is subject to possible errors, as noted above, unless independent verification of the baseline value is also available.[188,189] An alternative procedure useful for finite-angle scattering is to assume that $\tau_A^{-1} = K^2 D$, where D is determined from data at small angles for which the decay is (presumed to be) single exponential.[192] Although these techniques for reducing the number of variables do improve the convergence properties of the resulting least-squares iteration, they involve extra assumptions that might not be well obeyed in any given instance. Alternate methods that have been suggested for analysis of multiple exponential decays are the method of moments[186] and the Fourier[193] and eigenfunction[194] methods recently proposed by Provencher. An extrapolation method, called asymptotic analysis, has been successfully applied to determine the time constants of very slow relaxations observed in solutions of λ DNA.[127] An integration least-squares method has been proposed by Lee and Chu.[195]

When solutions are polydisperse, the method of data analysis employed depends to some extent on the nature of the polydispersity and the number of correlator channels available. If the distribution is bimodal, comprised principally of two species with substantially different (i.e., $D_A/D_B \gtrsim 2$) diffusion coefficients, and if the number of correlator channels is sufficiently large, then nonlinear least-squares analysis employing an expression similar to that in Equation 56 seems to work best.[191,196] This conclusion applies strictly only when internal modes make a negligible contribution and when the individual species exhibit single-exponential relaxations. For unimodal distributions, the method of cumulants[197] appears to be the method of choice.[198,199] In this method, one employs the expansion

$$\ln|g_\gamma^{(1)}(K,t)| = 1 - K_1 t + \tfrac{1}{2}K_2 t^2 - \frac{1}{3!}K_3 t^3 + \frac{1}{4!}K_4 t^4 + \ldots \qquad (58)$$

to fit the data by adjusting the constants K_i, the first two of which are given by $K_1 = K^2 \langle D \rangle_Z$ and $K_2 = K^4 \langle D^2 - \langle D \rangle_Z^2 \rangle_Z$.[69,74,75,197] The diffusion coefficient obtained from K_1 is the so-called Z-average over the distribution,

$$\langle D \rangle_Z \equiv \sum_i n_i m_i^2 D_i / \sum_i n_i m_i^2 \qquad (59)$$

where n_i and m_i are the molecular concentrations and masses of species i, respectively. Moreover, $\langle D \rangle_Z$ can be combined with the weight average sedimentation coefficient $\bar{S}_w$ in the Svedberg equation to give the weight-average molecular weight,[69,167,197]

$$\bar{M}_W = \frac{N_{Av} k_B T \bar{S}_W}{\langle D \rangle_Z (1 - \bar{v}\rho)} \qquad (60)$$

where N_{Av} is Avogadro's number, $\bar{v}$ is the partial specific volume, and ρ is the solution density. A procedure for estimating the number-average diffusion coefficient from K_1 and K_2 has also been proposed.[24] Several treatments have discussed the two-parameter Schulz distribution of molecular sizes and methods for estimating those parameters from experimental data.[70,200-203] Methods for obtaining higher moments of the size distribution of large particles using the angular dependence of the K_j have also been proposed.[204]

DIFFUSION COEFFICIENTS

The static structural information available from translational and rotational diffusion coefficients is contained in the hydrodynamic friction factors f and f_R for translational and rotational motions, respectively; that is

$$D = k_B T / f \qquad (61)$$

$$D_R = k_B T / f_R \qquad (62)$$

For large spheres of radii a, the standard Stokes law friction factors $f = 6\pi\eta a$ and $f_R = 8\pi\eta a^3$

apply, where η is the solvent viscosity. Formulae for prolate and oblate ellipsoids given originally by Perrin have been summarized in a review by Benoit et al.[205] in a form already incorporating the correction of the sign error.[206] Wright and Baxter[207] have recently discussed numerical inversion of the Perrin equations to obtain the ellipse parameters. The review by Benoit et al. also gives the formulae of Broersma[208,209] for translational and rotational friction factors of rigid cylinders, as well as the approximate formula of Kirkwood[210] for arrays of spherical beads of equal size. Exact friction factors (within the Oseen tensor approximation) are given for rigid planar polygons by Paul and Mazo.[211] The approximate formula of Kirkwood gives the same value as that of Paul and Mazo for planar hexagons,[212] but appears to give values up to 10% below the observed friction factors for various proteins, when their crystal structure dimensions are employed in the calculation.[213]

Much closer agreement with the experimental data can be obtained by using the modified interaction tensor of Rotne and Prager[214] and Yamakawa[215] and numerically solving the simultaneous force equations.[213,216,217] That approach is being actively explored at the present time,[213,216,217] and prospects for calculating translational diffusion coefficients, accurate to a few percent for macromolecules of any arbitrary shape, now appear to be quite promising.

The current status of rotational friction factors is not so clear, especially for small molecules. For small aromatics it has been shown that slip rather than stick surface boundary conditions are most appropriate.[218] For large proteins with $M_r \geq 20{,}000$, it seems clear that the standard stick boundary condition must be used, but it is not at all apparent for what sizes or shapes or degree of solvent binding the change-over from slip to stick conditions takes place.

For very large random-coil macromolecules, the elementary quantities of interest are the radius of gyration R_G, which is related to the effective Stokes law radius, $R_{St} \equiv k_B T/6\pi\eta D$, by the formula of Kirkwood and Riseman,[219]

$$R_G \cong 1.51\, R_{St} \tag{63}$$

as discussed by Flory,[220] and the power law coefficient b in the molecular weight relation $D = K_d M^{-b}$, which is generally obeyed by flexible chain macromolecules.[220] Moreover, the intrinsic viscosities $[\eta]$ of such molecules also generally obey the Mark-Houwink relation, $[\eta] = K_v M^a$.[220] A criterion for randomly coiling macromolecules is that the relation $3b = 1 + a$ be obeyed.[220]

Results for semirigid macromolecules are also given in the review of Benoit et al.[205] Porous sphere hydrodynamics in the mean-field approximation has been employed to determine the rotational diffusion coefficient of an arbitrary, spherically symmetric polymer[221] and to rationalize some anomalously low values of the Scheraga-Mandelkern β parameter.[222]

CONCENTRATION DEPENDENCE OF D

Even in the absence of long-range correlations between macromolecules, there always exist short-range interactions which also produce changes in the diffusion coefficient with increasing molar concentration C. According to the conventional wisdom[71,152] of linear irreversible thermodynamics,

$$D = \frac{C\dfrac{\partial \mu_2}{\partial C}(1-\bar{v}_2 C)}{N_{Av} f} = \frac{\left(\dfrac{\partial \pi}{\partial C}\right)_{T,P}(1-\bar{v}_2 C)}{N_{Av} f} \tag{64}$$

where N_{Av} is Avogadro's number, f is the concentration-dependent friction coefficient, μ_2 and $\bar{v}_2$ are the molar chemical potential and partial molar volume of solute, and π is the osmotic pressure. The term $1 - \bar{v}_2 C$ accounts for solvent backflow and is not significantly different from 1.0 in virtually all of the studies discussed here. For nonelectrolyte spheres, the expansion of Batchelor[221]

$$f = f^{\circ}(1 + 6.55\bar{v}_2 C + \ldots) \tag{65}$$

and the virial series

$$\left(\frac{\partial \pi}{\partial C}\right)_{T,P} = RT(1 + 2A_2 C + \ldots) \tag{66}$$

are often employed at low concentration to give

$$D = D_0 (1 + k_D C + \ldots) \tag{67}$$

where $k_D = 2A_2 - 6.55\bar{v}_2$, neglecting solvent backflow. For dilute hard spheres, $A_2 = 4\bar{v}_2$, so that $k_D = 1.45\bar{v}_2$ when solvent backflow is neglected and $k_D = 0.45\bar{v}_2$ if it is included.

For hard spheres in the absence of solvent backflow, Altenberger and Deutch[224] obtain precisely the value $k_D = 2.0\bar{v}_2$, when hydrodynamic interactions are incorporated in the Oseen tensor approximation. Anderson and Reed[225] find a

value $k_D = -1.83\bar{v}_2$ using a different averaging procedure, but a more sophisticated representation of the hydrodynamic forces. This result has been challenged by Phillies[226] and also by Mou and Chang,[227] the latter of whom obtained the value $k_D = 1.125\bar{v}_2$ after quite a rigorous calculation. The result of Anderson and Reed violates the physical notion that hydrodynamic forces should only diminish the effect of direct forces, but never invert the sign of the correction term. For this reason, their conclusion that mutual diffusion coefficients and tracer diffusion coefficients are equal is also suspect.[225] The former quantity is that determined in quasi-elastic light scattering or free-boundary diffusion experiments, while the latter is measured by tracer techniques in the complete absence of macromolecular concentration gradients. At infinite dilution, these quantities have the same value, D_0. Mou and Chang obtain $k_D' = -4.875\bar{v}_2$ for the corresponding hard-sphere tracer diffusion constant,[227] showing the disparity in these quantities as the concentration increases.

Phillies et al.[228] have studied diffusion in solutions of bovine serum albumin up to very high concentrations (334 g/*l*) over the pH range, 4.3 to 7.6 by quasi-elastic light scattering. Using osmotic pressure and tracer diffusion data from the literature, they find that Equation 64 is reasonably well obeyed, provided that the tracer diffusion coefficient is given by $D_T = k_B T/f$, as predicted from conventional linear irreversible thermodynamics. In any event, the mutual diffusion coefficient D was observed to be as much as three times larger than the observed D_T at concentrations greater than 200 g/*l*. Several other theoretical treatments of the concentration dependence of D have also appeared.[229-231]

HIGHLY CHARGED POLYSTYRENE LATEX SPHERES

Interesting model systems for solutions of charged biocolloids are suspensions of detergent-bearing polystyrene latex spheres under very low-salt conditions. At sufficiently high concentrations of spheres, a periodic ordered array is formed, the structure of which has been determined from Bragg scattering of visible light of different colors to be body-centered cubic.[82] Moreover, the melting of such a colloidal crystal has been observed near 40°C under conditions where the mean spacing between spheres was about four times the sphere diameter of 1100 Å.[16] A review of periodic ordered colloids has been provided recently by Efremov.[232]

Brown et al.[233] have performed a thorough study of both the intensities and correlation functions of light scattered from a dilute suspension of charged polystyrene latex spheres of radius 250 nm under conditions such that no periodic order was present. Nonetheless, the scattering structure factor exhibited oscillations as a function of K, which upon inversion revealed liquid-like "short-range" order in the radial distribution function of the spheres. The correlation functions were observed to be generally nonexponential. The apparent diffusion coefficient obtained from the first cumulant also exhibited oscillations as a function of K and gave surprisingly close agreement with Equation 35, as shown in Figure 6, except at small K values, where multiple scattering effects may have been important.[234] The points represent the observed $D_{eff}^{-1} \equiv D_{app}(K)^{-1}$, and the full curve is $S(K)\bar{D}_0^{-1} \equiv G(K,0)\bar{D}_0^{-1}$, where G(K,t) is defined in Equation 18, and $\bar{D}_0$ is the free-particle diffusion coefficient.

It should be noted that when the fluctuation wavelength is long compared to the range of the interparticle correlations, which occurs here only at very small K values, the observed $D_{app}(K)$ is as much as five to seven times larger than the free-particle value, showing the enormous enhancement due to the long-range repulsive forces.

The unique value of the polystyrene latex sphere suspensions is that they do permit studies on a dilution scale where the mean interparticle distances are comparable to the wavelength of the scattering light, so that full details of the particle correlations and variations in $D_{app}(K)$ can be investigated. Most ordinary biopolymer systems simply do not scatter sufficient light for study at these great dilutions, and one may expect to be operating effectively in the long-wavelength range near K = 0 for most such systems, except for high molecular weight DNAs, vesicles, viruses, and other very large particles which may be studied with mean interparticle spacings comparable to the fluctuation wavelength.

Schaefer and Ackerson[16] also found that their data followed the form predicted by Equation 35, but the value of D_0 was several times larger than the Stokes law diffusion coefficient. This peculiar disparity is an outstanding mystery.

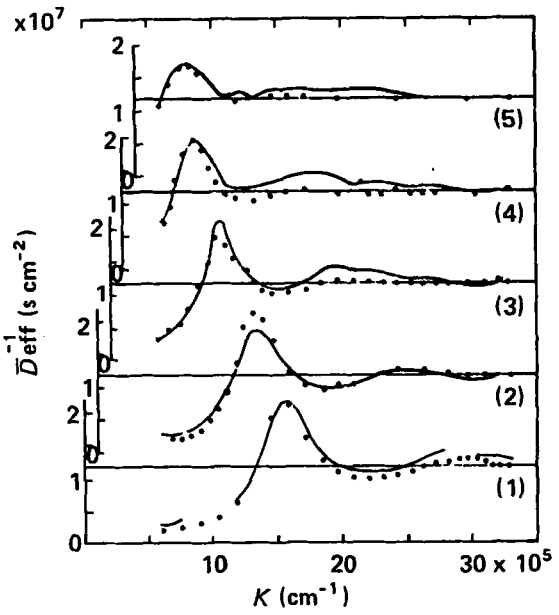

FIGURE 6. $D_{eff}^{-1} \equiv D_{app}(K)^{-1}$ vs. K for charged polystyrene latex spheres of 250-nm radius. Points are the observed data, while the solid lines are computed from $D_{app}(K)^{-1} = G(K,0)D_o^{-1}$ according to Equation 35, using observed values of the static structure factor G(K,O). The concentrations in Samples 1 to 5 are, respectively, 8.46, 5.70, 2.90, 1.67, and 1.24 × 10^{12} spheres/cm^3. (From Brown, J. C., Pusey, P. N., Goodwin, J. W., and Ottewill, R. H., *J. Phys. A Math. Nucl. Gen.*, 8, 664, 1975. With permission.)

EXPERIMENTAL RESULTS

Discussions of pertinent results for various systems are catalogued alphabetically in this section according to the kind of system studied.

Antifreeze Glycoproteins

Ahmed et al.[235] have studied antifreeze glycoproteins from the blood sera of Antarctic fish. Two major components with M_r = 10,500 and 17,500, respectively, were isolated chromatographically, and diffusion coefficients were determined over a range of temperatures in a search for conformational changes associated with antifreeze activity. Although the effective Stokes radii of both species declined slightly from T = 22°C to -0.2°C, no abrupt conformational change was observed. It was also found that $D \propto M^{-0.62}$, which indicates a somewhat larger extension than that of an ideal (i.e., no excluded volume) random coil. It was subsequently found[236] that borate ion binds to the antifreeze protein and, at the same time, eliminates its antifreeze activity without producing a significant alteration in overall conformation or shape. Borate-lectin and borate-lectin-antifreeze protein interactions were also studied by several techniques.

Blood Proteins (Albumins, Globulins, Fibrinogen, Antigen-Antibodies)

After polystyrene latex spheres, bovine serum albumin (BSA) is the substance most commonly studied by dynamic light-scattering techniques,[3,4,39,85,103,237-239] having served often as an instrument calibrator. Using electrophoretic light scattering, Ware and Flygare[85] have measured simultaneously the diffusion coefficient and electrophoretic mobility of BSA. They have also observed the dimer of BSA, which comprises 10 to 20% of their commercial sample, and have effected electrophoretic resolution of mixtures containing BSA monomers, dimers, and the more slowly migrating fibrinogen.[237]

Two important studies[103,239] concerned the effects of electric charge and, also, concentrations of salt and BSA on the diffusion coefficient. Raj and Flygare[239] found that D_{app} depended linearly on $\bar{C}_p$ with an extrapolated infinite dilution value D_p that was independent of ionic strength, as predicted by Equation 42. Moreover, the slopes $\partial D_{app}/\partial \bar{C}_p$ increased as the salt concentration declined, in qualitative agreement also with Equation 42. It was found that BSA underwent a marked expansion, independent of ionic strength, as the pH was lowered from its isoelectric point at pH 5.0 to 2.0. This was manifested by an approximately 20% decrease in D_p from its value of 5.7 × 10^{-7} cm^2/sec at the isoelectric point.

Doherty and Benedek[103] studied the dependence of the monomer diffusion coefficient on the ionic strength of added salt plus counterions for solutions with different titration charges. Their analysis was presented in terms of the relative enhancement factor $\alpha \equiv (D_{app} - D_p)/D_p$, which can also be expressed in terms of parameters of the linearized coupled-mode theory by $\alpha = (1/2)(1 + \Omega)(D - D_p)/D_p$, where D is the small-ion diffusion coefficient and Ω is given in Equation 40. A comparison of experimental and theoretical enhancement factors is shown in Table 1. Using the 1.0 *M* salt value for D_p, a charge $\bar{Z}$ = 7.2 is employed to give the observed α = 0.19 at 0.0915 *M* added salt. The remaining α are computed with no further adjustable parameters. It is clear that the experimental α falls progressively farther

TABLE I

Comparison of Theoretical and Experimental Enhancement Factors (α) for BSA at 25°C

C_s	$D_{app} \times 10^7$[a] (cm^2/sec)	α[b] (Th)	α[c] (Exp)
0	20.6	5.16	1.97
0.0005	19.6	4.51	1.82
0.0015	18.7	3.61	1.69
0.0024	18.2	3.06	1.62
0.0033	17.1	2.65	1.46
0.0061	14.6	1.88	1.11
0.0078	14.5	1.60	1.09
0.0103	12.8	1.30	0.84
0.0915	8.27	0.19	0.19
1.0	6.94	0.00	0.00

[a]Corrected to the viscosity of water at 25°C.

[b]Computed using $\alpha = (1/2)(1 + \Omega)(D - D_p)/D_p$, where Ω is given in Equation 41, $D = 1.5 \times 10^{-5}$ cm^2/sec, $D_p = 6.94 \times 10^{-7}$ cm^2/sec, $\bar{C}_p = 7.24 \times 10^{-4}$ M, and $Z = 7.2$.

[c]Data of Doherty and Benedek.[103]

below the theoretical α as the salt concentration declines. This may be an indication of an anomalous increase in the friction coefficient as the salt concentration decreases.

Although short-range excluded volume forces are also present, they are estimated to contribute less than 2% to D for BSA concentrations as high as 20 g/*l*.[239] The studies of Phillies et al.[228] on BSA at very high concentrations showed that D conforms approximately to Equation 64, as discussed previously.

Palmer and Fritz[240] have completed a homodyne study of human fibrinogen. The diffusion coefficient remained constant at $1.50 \pm 0.09 \times 10^{-7}$ cm^2/sec independent of concentration from 0.4 to 20 g/*l*. Moreover, the effective Stokes radius remained constant as the temperature was varied from 15 to 42°C, at which point aggregation associated with denaturation occurred. There was no indication of appreciable dissociation to subunits at 37°C. The diffusion coefficient of human fibrinogen was similar to that reported for bovine fibrinogen[241] ($1.53 \pm 0.05 \times 10^{-7}$ cm^2/sec), which was also determined by dynamic light scattering. However, both values were significantly lower than those obtained for human and bovine fibrinogens (1.98×10^{-7} and 2.02×10^{-7}, respectively) by earlier sedimentation techniques. The cause of this discrepancy is not known at present.

Electrophoretic studies of human blood plasma have also been reported.[60,242] In addition to the albumins, several globulin peaks have been identified.

Uzgiris[243] has employed electrophoretic light scattering in a clever antigen-antibody assay. Polystyrene latex spheres were first coated with antigen (bovine serum albumin), and the change in electrophoretic mobility was monitored as its rabbit antibody was added. Amounts of antibody as small as 5 to 10 ng/ml could be detected in one half hour.

Chromatin and DNA-Histone Complexes

Shaw and Schmitz[244] have studied the sedimentation and diffusion behavior of multimeric subunits of chicken erythrocyte chromatin. Molecular weights computed from the respective values of S_{20} and D_{20} were empirically related to the sedimentation coefficient by $S_{20} = 0.011 M^{0.554}$, while for free DNA the corresponding relation was $S_{20} = 0.163 M^{0.280}$. The difference in exponents clearly indicates a much more compact structure for the chromatin multimers. From the large observed friction factor for the dimer ($M_r = 5.3 \times 10^5$) and literature estimates of the core particle radii (50 to 55 Å), it was inferred that spacer regions between core particles exist and contribute as much as 20% to the frictional properties of the dimer. Model calculations using the approximate theory of Kirkwood[210] showed that the molecular weight dependence of the friction factors of the various multimers could be accounted for by either a helical conformation or a flexible coil with attractive interactions between chain elements, but not by either rods or planar polygons.

Wun and Prins[245] have studied complexes formed by F1 and F2A histones with low molecular weight ($M_r = 1.5 \times 10^6$) calf-thymus DNA. The reciprocal relaxation times obtained from single-exponential fits of the correlation functions showed positive curvature as a function of $\sin^2(\theta/2)$ at the higher scattering angles, indicating a significant contribution from internal modes of motion. Assuming that only a single dominant internal mode was involved, they obtained its relaxation time τ_{int}, as well as the macromolecular diffusion coefficient of the complex. Data for 1:1

TABLE 2

Translational Diffusion Coefficients and Internal Mode Relaxation Times of DNA and DNA-histone complexes[a,b]

System	$D_{20} \times 10^8$ (cm^2/sec)	$\tau_{int} \times 10^4$ (sec)
DNA[c]	1.6	5.0
Histone F1-DNA	1.0	9.5
Histone F2A-DNA	2.6	2.8

[a]Data of Wun and Prins.[245]
[b]Solvent conditions: 0.8 *M* NaCl, 2 *M* urea, 20°C.
[c]$M_r = 1.5 \times 10^6$.

(histone:DNA) weight ratios in 0.8 *M* NaCl and 2 *M* urea at pH 7 are given in Table 2 which is taken from the work of Ramsay-Shaw and Schmitz.[246] The effect of F1 histone is to decrease D and increase the internal mode relaxation time in comparison to free DNA, thus implying a more extended structure; F2A has the opposite effect, implying a more compact structure. It was argued that the observed internal mode relaxation times are too small to represent pure rotational motion and must instead represent bending and flexing motions. Wun and Prins have interpreted the effect of F2A as promotion of superhelix formation and the effect of F1 as causing unwinding of DNA.

Ramsay-Shaw and Schmitz[246] point out that the observed value of τ_{int} for free DNA is consistent with that expected for a terminal Rouse-Zimm relaxation time, which should decrease upon unwinding, presuming that the intrinsic viscosity also decreases, contrary to the Wun-Prins interpretation. These authors give an alternate explanation involving aggregation of DNA molecules to form a more extended structure under the influence of F1 histone and either partial unwinding or kink formation to produce the more compact structure in the presence of F2A histone.

Collagen and Gelatin

Diffusion in collagen solutions has been studied by French et al.,[247] Öbrink,[248] and Fletcher.[249] A very slowly diffusing large aggregate was detected by French et al. and also by Fletcher, although the amount of aggregate material was greatly reduced in the latter case by treatment with pronase. Öbrink reported no large aggregates in his lathyritic collagen.

The reported concentration dependence of D_{app} for free collagen molecules was bizarre, showing a prominent maximum value of 8.8×10^{-8} cm^2/sec at 0.4 g/l, with a rather steep decline at lower concentration.[249] An intriguing possibility is that this phenomenon is related to the labile supramolecular spatial array detected by Privalov et al.[250] in collagen solutions of still lower concentration.

Any contributions of macromolecular rotation to the correlation function were so small as to remain undetected.[247,249] Because such components should have been observed at the higher angles for rigid rods with the length of a collagen molecule (~300 nm) it could be inferred either that the molecules were not undergoing unrestricted rotational diffusion or that substantial flexing and bending was taking place to reduce the effective length.

French et al.[247] observed an enormous spike in the temperature profile of the spectral half-width (or reciprocal relaxation time) of light scattered at $\theta = 135°$ from a concentrated (70 g/*l*) gelatin solution. This large peak centered at $T \approx 31°C$ was observed on both upward and downward sequential temperature runs. It seems highly probable that this is another manifestation of the same thermal transition observed earlier in the temperature dependence of the kinetics of trypsin attack[251] and also in the reduced viscosity. The enormous rise in $1/\tau$ at the transition indicates either a more compact structure or a more fluid supramolecular arrangement, or both, and is consistent with the local minimum in the reduced viscosity found earlier.[251] At T = 31° there was also a local minimum in both the Michaelis constant and the rate constant for tryptic attack, as well as a change in activation enthalpy at that point. It was found that these gelatin solutions, even at 1 g/*l*, form large aggregates with effective Stokes radii of several thousand angstroms.[247] The cause of the structural collapse near T = 31°C is not known.

Dermatan Sulfate from Human Placenta

Jamieson et al.[252] have characterized the highly sulfated mucopolysaccharide, dermatan sulfate, from both fetal and term human placenta. The empirical relation $D = 2.70 \times 10^{-5} M_V^{-0.59}$ was established using three similar glycosaminoglycans: chondroitin-6-sulfate, heparin, and a standard dermatan sulfate. With this calibration, the molecular weights (viscosity average) of fetal and term dermatan sulfates were determined from

their diffusion coefficients to be 27,000 and 29,000, respectively. Upon treatment with hyaluronidase, the former value decreased by 50% while the latter decreased by only 30%, indicating either a different frequency or distribution of occurrence of glucuronic acid in the chains of the young fetus.

Elastin

Two dynamic light-scattering studies of elastin coacervation have been reported.[15,253] At 15°C, the tropoelastin apparently exists primarily in the form of micellar aggregates of effective radius 200 Å. As the temperature is raised, the effective radii of these micellar aggregates increase steadily until the coacervation transition temperature (33°C) is reached at a critical radius of about 420 Å. At that point, both a very fast and a very slow component appear in the correlation function.[15] The very slow component grows in amplitude as the coacervation proceeds in time, indicating the formation of large particles of the coacervate phase. The fast component is believed to arise from diffusion of the tropoelastin molecules inside the coacervate particles. Thus, the tropoelastin molecules may themselves experience a significant increase in total configurational entropy upon transfer from the micellar to the coacervate phase.

The marked temperature dependence of the rate of formation of the large coacervate particles is interpreted by Jamieson et al. in terms of a nucleation process.[15]

Enzymes (Lysozyme, Asparate Transcarbamylase, Glyceraldehyde-3-Phosphate Dehydrogenase, Bovine Glutamate Dehydrogenase, and Chymotrypsinogen)

Both translational[3,4] and rotational[254] diffusion coefficients of lysozyme have been measured, the latter by interferometric determination of the spectral broadening of depolarized scattered light. Combining these results, $D^{T}_{20,w} = 10.6 \pm 0.1 \times 10^{-7}$ cm^2/sec^{-1} and $D^{R}_{20,w} = 16.7 \pm 0.8 \times 10^{6}$ sec^{-1}, with Perrin's expressions for ellipsoids indicates that lysozyme is hydrodynamically equivalent to a prolate ellipsoid of revolution with a major axis of 55 ± 1 Å and a minor axis of 33 ± 1 Å. The hydrodynamically equivalent oblate ellipsoid was ruled out as being too far from the known crystal shape and allowing too little hydration. The former argument is not completely satisfying because, if one is to believe that the structure in solution always remains faithful to that in the crystal, then dynamic light-scattering measurements for purposes of structure determination are, in a way, superfluous. The hydration argument is specious, since the authors compare their figures with values determined by total weight loss of water from crystals in a 20 min period at 100°C.[255] It is difficult to believe that much of the crystal water is not simply filling interstitial spaces and does not represent bound water in solution. Protein crystals generally trap large amounts of solvent. In any case, four of the five crystalline forms presented by Steinrauf exhibit only 0.33 g water per gram of protein, rather than 0.50 as stated by Dubin et al.,[254] who compute values of 0.60 (gram solvent per gram protein) for the equivalent prolate ellipsoid and 0.12 (g solvent per gram protein) for the equivalent oblate ellipsoid by comparing the protein partial molar volume with the hydrodynamically equivalent prolate and oblate ellipsoid volumes. The general question of shape and bound water of lysozyme in solution is not yet resolved.

The progressive denaturation of lysozyme in guanidine hydrochloride (Gdn·HCl) was studied by Dubin et al.,[256] with particular emphasis on the possible existence of intermediate species in the transition region. Although no intermediate states could be detected, a 45% decrease in $D_{20,w}$ between the native and denatured forms was observed, and, assuming a two-state model, the relative abundance of native and denatured species could be determined at any given concentration of Gdn·HCl.

Aspartate transcarbamylase was observed to undergo a 4.1 ± 0.6% decrease in diffusion coefficient in the presence of succinate and carbamyl phosphate.[179] Combining the sedimentation and diffusion coefficients gave a molecular weight of 2.9 ± 0.1 × 10^5. Because changes in both S and D induced by succinate and carbamyl phosphate are comparable, it may be inferred that the change observed is one of shape, rather than a change in partial specific volume. The dimer of ATCase was also observed to undergo a 4% decrease in S in the presence of succinate and carbamyl phosphate.

Glyceraldehyde-3-phosphate dehydrogenase was studied over a range of temperatures in the presence and absence of ATP.[257] This enzyme was observed to dissociate with increasing temperature; approximately 15 to 23% of the original enzyme was dissociated at 22°C in the absence of

ATP. In the presence of ATP, the enzyme was observed to undergo a temperature-dependent conformation change, distinct from dissociation, over the range of 14 to 28°C. At a temperature of 28°C and above, the enzyme underwent a pronounced aggregation reaction in either the presence or absence of ATP.

The relation between degree of polymerization, allosteric control, and catalytic activity of beef liver glutamate dehydrogenase has been studied by Cohen et al. using a variety of techniques, including dynamic light scattering.[258-260] The data have been analyzed in terms of three related models, the common ideas of which are the following:

1. There is an allosteric equilibrium between active and inactive conformers of the free monomer, of which the effective equilibrium constant can be altered by effectors in the usual way.
2. Both active and inactive monomers engage in polymerization equilibria to form linear aggregates in which their conformations are locked, but their enzymatic activities remain unaltered.
3. The equilibrium constant for incorporation of active species into the polymer is much greater than that for inactive species, and both constants are independent of effector concentration.

In such models the concentration of enzyme itself, as well as the concentration of effector, serves to modulate the enzyme activity by altering the ratio of total (free plus polymerized) active to inactive monomer units. In support of the model, the authors[260] have obtained impressive evidence of the correlation between the degree of polymerization and its dispersion, as determined by quasi-elastic light-scattering and sedimentation methods, and the activity of the enzyme for a variety of concentrations of enzyme and allosteric inhibitor (guanosine triphosphate) and activator (adenosine diphosphate).

The diffusion and sedimentation coefficients, molecular weight of the monomer, and polymerization constants of the active and inactive monomers in the presence of ligands were obtained. This problem has also been studied by Jullien and Thusius.[261]

A precise determination of the translational diffusion coefficient of carefully purified α-chymotrypsinogens under a variety of conditions was made by Raj and Flygare.[262] They obtained the value $D_{20,w} = 8.40 \pm 0.2 \times 10^{-7}$ cm²/sec, somewhat higher than most previous results.

The diffusion coefficients of both urease (from jack-bean meal) and chymotrypsinogen were determined by Sellen.[238] Denaturation and aggregation of ribonuclease have been studied by Rimai et al.[263]

Flagellae

Normal (curved) and mutant (straight) flagellae from *Salmonella* have been studied by Fujime et al.,[20] who also studied short fragments of various lengths of these same types,[21] as well as flagellae produced by copolymerization of both normal and mutant flagellins. In the former study,[20] flagellar lengths ranged from 16,000 to 100,000 Å and filament diameters were about 120 Å. Although the concentrations were varied from 0.1 to 4.0 g/l with no apparent change in the observed (homodyne) spectral widths, it is difficult to see how intermolecular interactions of these highly anisometric macromolecules could not have been important at those concentrations, which (as noted by the authors) were so high that the superhelical domains, or diameters, of adjacent neighbors actually overlapped. Significant effects due to congestion of Brownian motion have been observed in solutions of much less extended macromolecules at appreciably lower concentrations.[73,123] For this reason, a completely satisfactory theoretical interpretation of the data has probably not yet been achieved.

Plots of spectral width (or $1/\tau$) vs. K^2 were surprisingly linear with slopes in the correct range to be diffusion coefficients for center-of-mass motion, but also exhibited substantial positive intercepts. Such data were interpreted using the relation $\Gamma = 2K^2D + 1/\tau_1$, where τ_1 was regarded as the characteristic relaxation time for the longest wavelength flexing motion of the filament. Fujime et al.[20,21] have argued that there is a domain of validity of such an expression for the Harris-Hearst model discussed above, but their argument is far from rigorous. An equally plausible explanation of the observations would involve the induced coupling between internal motions and translational diffusion in congested solutions of anisometric molecules, as previously suggested for DNAs.[73,123] In the case of flagellae, such internal motions surely are not end-over-end rotations,

which are too slow, but could well involve axial rotation, flexing, and superhelix deformation and propagation. In either explanation, the existence and magnitude of the intercept are related to an internal mode with a characteristic relaxation time. However, the congested solution explanation also predicts the existence of a very slow component (the lower branch), as well as an upper branch with a slope approximately equal to the translational diffusion coefficient. The slow component in this case could well be so slow as to have escaped detection.

By examining flagellae of several different kinds by both light scattering and electron microscopy, Fujime et al.[20,21] have established a firm empirical correlation between their D and τ_1, and the qualitative flexural rigidity. In any given case, assignment of a numerical value to the flexural rigidity hinges on the validity of their interpretation of the data in terms of the Harris-Hearst model. A value of 10^{11} dyn/cm was estimated in this manner for the Young's modulus of a cylindrical flagellum with inside diameter 100 Å and outside diameter 120 Å.

The investigation of shorter pieces in the length range 7000 to 9000 Å showed interesting differences between straight and curved rods and clearly show the need for theoretical work on the rotational motions of curved rigid rods.[21]

Hemoglobin

Normal hemoglobin has been studied by Uzgiris and Golibersuch[145] and by Haas et al.[146] A discussion of those results pertaining to the possible observation of tetramer ⇌ dimer kinetics (with associated changes in O_2 binding) was given in the theoretical section above.

Normal and sickle cell (S) hemoglobins in both oxygenated and deoxygenated forms have been studied by Wilson et al.[264] Over the concentration range studied, normal oxyhemoglobin, deoxyhemoglobin, and sickle cell oxyhemoglobin gave substantially identical power spectra and showed no sign of aggregation. In contrast, below a critical oxygen pressure aggregation was invariably observed for sickle cell hemoglobins, as manifested in a dramatic narrowing of the linewidth. The linear change in scattered intensity with time supports the notion of linear condensation of bifunctional polymers with each other, rather than addition of free monomers to the polymer growing ends.

Hemocyanin

The diffusion coefficient and molecular weight of hemocyanin from *Murex trunculus* were determined to be $D_{20,w} = 1.08 \pm 0.01 \times 10^{-7}$ cm^2/sec and $M_r = 9.2 \pm 0.1 \times 10^6$, respectively.[4] Dissociation in 5 *M* (Gdn·HCl) containing 0.5 *M* 2-mercaptoethanol to molecules with M_r = 210,000 ± 20,000 was also reported.

Histones

The value $D_{25,w} = 8.5 \times 10^{-7}$ cm^2/sec for the monomer of histone (lysine rich) was extracted from observed correlation functions that also manifested the presence of larger aggregates.[265] From both scattered light intensity and diffusion coefficient determinations, the value $M_W \cong 1.4 \times 10^4$ was obtained for the histone monomer under the assumption that both monomers and aggregates were globular. A standard Zimm plot gave $M_W = 1.1 \times 10^4$, where the constant relative amplitudes of fast and slow components in the correlation functions were used. The constancy of the relative amplitudes was a strong indication that the monomers were not in equilibrium with the aggregates.

Lactoglobulin

The protein β-lactoglobulin A was studied over the concentration range of 16 to 82 g/l at pH 5.6 by Chu et al.[266] The dimer diffusion coefficient was determined at the lower concentrations and extrapolated to infinite dilution to yield $D_{20,w} = 7.38 \times 10^{-7}$ cm^2/sec. Using literature data for the light-scattering second virial coefficient and molecular weight of the octamer, and assuming that only a simple dimer ⇌ octamer equilibrium was involved, it was possible to estimate the weight percent of octamer present and then to extract the octamer diffusion coefficient from the mean linewidth. The results indicated that neither the dimer nor octamer changed size significantly over the temperature range from 3.5 to 25°C or with a change in pH from 5.6 to 4.6. The octamer diffusion coefficient gave a Stokes radius of ~45 Å, which is compatible only with a rather compact structure.

Micelles

Characterization of bovine milk casein micelles has been the object of a series of investigations.[5-7,267-269] Size distributions were determined by fractionation using rate-zone centrifugation followed by dynamic light scattering to

determine the effective Stokes radii of the various fractions. About 80% of the micelles were found to have radii in the range 500 to 1000 Å, values two to three times larger than those obtained by electron microscopy on comparable micellar preparations. The advantage of the *in situ* dynamic light-scattering measurements over electron microscopy is clear in this case. Combination of the (Z-average) diffusion coefficient and intrinsic viscosity yielded[268] the (approximately) weight-average molecular weight of 5.2×10^8. Diffusion and sedimentation velocity data on two monodisperse subfractions yielded molecular weights of 2.3×10^8 and 1.8×10^9, corresponding to 800 S and 2200 S, respectively.[269] Application of this technique to all fractions of the pooled skim milk permitted determination of the entire molecular weight distribution,[7] which gave a weight average of 2.5×10^8, implying about 10^4 monomers per micelle. In addition, the empirical relation $S = 1.79 \times 10^{-3} M^{0.665}$ was established, indicating that casein micelles behave hydrodynamically like spheres. It has also been shown that removal of small amounts of Ca^{++} removes caseins, mainly β- and K-casein, from the micelles without changing significantly the micelle Stokes radius.[6] However, when the Ca^{++} concentration drops below a critical value, the micelles dissociate completely. A study of casein micelles from a cow homozygous for α_{s1}-casein, the product of a deletion mutation involving 13 amino acid residues, showed that both much larger micelles and a greater proportion of smaller micelles were present than in normal pooled skim milk.[267]

Pure bile salt micelles and bile salt-mixed lipid micellar systems were studied by Holzbach et al.[270] The Stokes radii of pure bile salts were found to depend strongly on their molecular structure, with radii extrapolated to the respective critical micelle concentrations ranking in the order sodium glycocholate < sodium glycodeoxycholate < sodium glycochenodeoxycholate and also sodium taurocholate < sodium taurodeoxycholate < sodium taurochenodeoxycholate. Addition of phosphatidyl choline causes small changes in micellar size or shape. Simultaneous addition of phosphatidyl choline and cholesterol does not appear to significantly alter micellar size. Studies of sphingomyelin micelles with the detergent Triton® X-100 have also been reported.[270a]

Mazer et al.[8] have studied sodium dodecyl sulfate micelles. Using both static and dynamic light scattering measurements, it was possible to determine the prolate ellipsoid parameters that gave the correct volumes and hydrodynamic cross sections, assuming that the micelles were spherical at the critical micelle concentration. At sufficiently high T, the micelles returned to spheres of 25 Å radius. At lower temperatures, prolate ellipses with 25 Å semiminor axes, and semimajor axes up to 675 Å were reported in 0.6 *M* NaCl.

Microsomes

Hepatic microsomes were studied by Holtzman et al.,[271] who found remarkably similar Stokes diameters (3200 Å) and surprisingly little polydispersity in several different preparations, which may indicate a characteristic property of homogenized endoplasmic reticulum. Treatment with detergents and fractionation resulted in smaller particles that were, however, still much too large to represent single molecular species of the principal membrane proteins. It was concluded that these fractions contained aggregates of membrane proteins with various amounts of lipids.

Muscle Proteins

Fujime and co-workers have performed a series of investigations of F-actin polymers[272,273] and their complexes with heavy meromyosin (HMM),[274,275] tropomyosin,[276] tropomyosin plus troponin,[277] and HMM plus actinin.[278] In addition, the effect of calcium ions on reconstituted thin filaments, which are F-actin-tropomyosin-troponin complexes, has also been examined.[279] The basic approach in all of these studies was to fit the observed photocurrent spectrum to a single Lorentzian to determine an effective Γ width. As with the flagellae discussed above, it was almost invariably found that the observed width (or $1/\tau$) depended on K^2 according to $\Gamma = 2DK^2 + 1/\tau_1$, where τ_1 was presumed to be the relaxation time of the longest wavelength flexing mode of the macromolecule. Variations in the observed D and τ_1 with changing solution conditions were observed and interpreted in terms of changes in flexibility of the F-actin complexes according to Fujime's development of the Harris-Hearst model for isolated polymers.[118]

The basic observations of Fujime et al. have been disputed by Carlson and Fraser,[143] who find for F-actin the Γ vs. K^2 relation shown in Figure 7, which appears to give a zero intercept. Moreover, the shape of the curve is quite similar to that

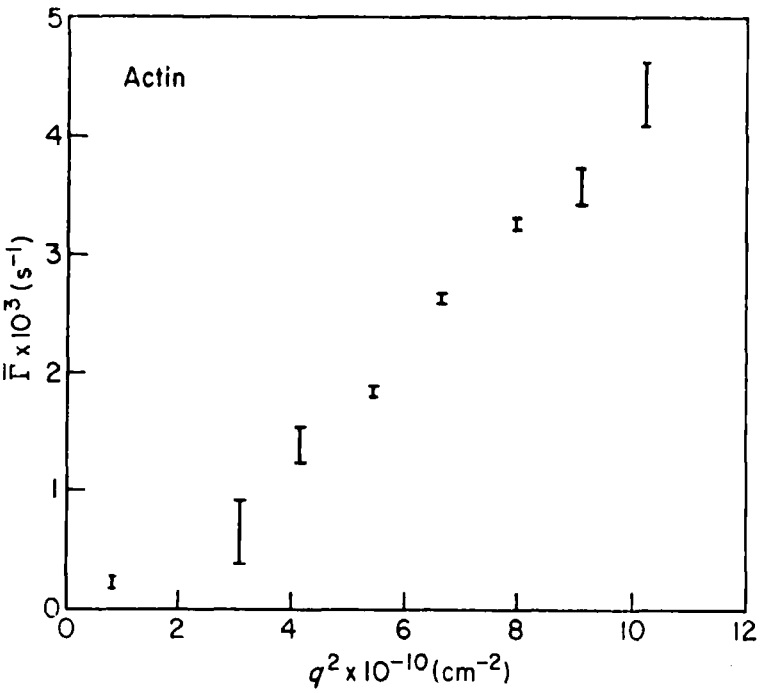

FIGURE 7. Bandwidth $\bar{\Gamma} = \tau_A^{-1}$ vs. $q^2 \equiv K^2$ for light scattered from F-actin. Conditions as in Fujime and Ishiwata,[272] pH 8.4, Tris buffer, 22°C. Similar results were obtained with all temperatures, ionic strengths, and buffer conditions tried. Each error bar represents the mean and standard deviation of the mean for three measurements. (From Carlson, F. D. and Fraser, A. B., *J. Mol. Biol.*, 89, 273, 1974. With permission.)

computed for the independent segment, mean-force model[73,140] and to that reported for calf-thymus DNA at high salt.[73] Indeed, a similar shape has also been computed rigorously for the Rouse-Zimm model of a flexible polymer.[133] Both theoretical and experimental bases exist for the shape of the curve observed by Carlson and Fraser. In addition, there is a substantial difference in the rates of the relaxation, those of Fraser and Carlson being about a factor of five faster at $K^2 = 6 \times 10^{10}$ cm^{-2}. As noted by Fraser and Carlson, the decays are highly nonexponential and in fact appear to consist of a rather faster component superposed on one that is roughly an order of magnitude slower. Such correlation functions have also been observed for DNAs with $M_r \cong 11 \times 10^6$ at ionic strengths below 0.1 *M* and for DNAs with $M_r \gtrsim 25 \times 10^6$ at ionic strengths up to 1.0 *M*. An explanation offered for the slow component in those cases, in terms of the coupling between anisotropic translational diffusion and internal modes in congested solutions,[73,123] might well apply here. Such a model predicts two components, the faster of which is more characteristic of free molecule diffusion and the slower of which exhibits an apparent nonzero intercept at large K^2.

Perhaps the apparent dilemma here could be partially resolved by the following considerations. Carlson and Fraser[143] employed a digital autocorrelator and the method of cumulants, both of which lead one to emphasize the short-time behavior of the correlation function; this should be the part that is most characteristic of freely translating and deforming F-actin polymers and which would, for sufficiently large and flexible macromolecules, be expected to yield Γ vs. K^2 data similar to those in Figure 7. On the other hand, Fujime and co-workers employed a spectrum analyzer and have fit the central peak of their low-frequency spectrum to a single Lorentizian. In so doing, they may have completely neglected the rapid relaxation that would have appeared almost as part of the shot-noise base line at higher frequencies. Thus, they may simply have been analyzing the slow component, as was done by Schmitz and Pecora,[127] for example, for DNA. Their much slower relaxation rates and apparent diffusion coefficients and the nonzero

intercepts are all in accord with such an hypothesis. Unfortunately, in this interpretation the connection between the slope and intercept values and the parameters of the Harris-Hearst model is not so clear. Still, it seems quite likely that the intercept value is a faithful monitor of some internal mode relaxation time. The interpretation, however, may vary greatly, depending upon whether the internal mode is rotational diffusion or internal deformation of a random coil, or flexing of a semirigid rod; that is, a slight stiffening of a random coil would be expected to increase all of the characteristic dimensions, resulting in larger friction coefficients and longer internal mode times, while stiffening a semirigid rod would result primarily in greater restoring forces, smaller amplitude motions, and shorter relaxation times. The latter was the interpretation of Fujime et al., although the former would be in better accord with the dynamic rigidity measurements performed on F-actin-HMM complexes in their laboratory.[274]

Recently, Fujime and Maeda[280] have reported data taken with a digital correlator that are similar to those of Carlson and Fraser. They also found an extremely slow component with a relaxation time much longer than 1 sec.

It has been pointed out[143] that the complexes of F-actin and HMM exist as gels, in which the macromolecules do not diffuse freely. Moreover, the scattered light exhibits far smaller fluctuations for a given scattered intensity than expected for Gaussian light. Such behavior is characteristic of quasi-stationary scatterers. Carlson and Fraser,[143] and later Wun and Carlson,[12] have advanced the so-called harmonically bound particle model to account for the observed dynamic behavior. Such a model is equivalent to Equation 32 for the independent-segment mean-force model[140] for $h + 1 = 1$ segments, when the center-of-mass factors $\exp[-k^2Dt]$ and $\exp[(K^2R_G^2/3(h + 1)(1 - e^{-t/\tau_0})]$ are ignored. The expressions of Carlson and Fraser[143] and Wun and Carlson[12] differ in a few places by a factor of two, as noted previously.[143a] In view of present uncertainties in interpretation of the data, further detailed discussion of the earlier F-actin results is not warranted at this time.

In a more recent study, Fraser et al.[281] have employed turbidity, viscosity, and dynamic light scattering to show that acto-HMM and acto-S-1 complexes present in the absence of ATP were almost completely dissociated under conditions of maximal actin activation of the ATPase activities of the HMM and S-1 fragments. This suggests the seemingly paradoxical conclusion that HMM and S-1 fragments exist in a refractory state unable to bind to actin when their actin-activated ATPase activity is maximal.

A careful static and dynamic light-scattering study of myosin solutions was made by Herbert and Carlson.[282] From static light-scattering Zimm plots, they were able to obtain the molecular weight and radius of gyration of the monomer and assuming the virial coefficients to be the same for both monomer and dimer, to then determine the equilibrium constant for dimer formation. Then, with the computed relative abundances of monomer and dimer, the photocurrent power spectra were resolved by 2-Lorentzian fits. The resulting diffusion coefficients were employed in Perrin's equation for prolate ellipsoids along with an assumed monomer diameter of 20 Å to determine a length of 1421 Å for the monomer and 2121 Å for the dimer.

Bauer et al.[185] determined a value $\tau \cong 12$ nsec for the rotational relaxation time of muscle calcium binding protein by both depolarized light scattering and ^{13}C NMR techniques, as discussed above, from which an effective Stokes radius of 22 Å was calculated. This figure is some 5 Å larger than that estimated from the crystal structure, implying either a different shape in solution or the presence of a layer of bound water.

Nucleic Acids (Calf-thymus, *Escherichia coli*, N1, λ, φ29, and fd DNA)

Studies of the rotational motions of calf-thymus ($M_r \cong 15 \times 10^6$) and sheared *E. coli* DNAs using the zero-angle depolarized scattered light have been reported[126] and also briefly reviewed.[32] The bulk (50 to 70% or more) of the relaxing amplitude of the observed homodyne autocorrelation function decayed rapidly with a time constant of 10 to 15 μsec. A more recent heterodyne correlation function[32] relaxed in about 10 μsec. These rough observations suggest a relaxation time of about 10 to 15 μsec in the molecular correlation function $\langle f^*_{1,2}(0)f_{1,2}(\tau)\rangle$, in approximate agreement with the electric dichroism results of Ding et al.[283] They also showed that a time of 8 μsec corresponds to the rotational diffusion time for a rigid rod with the diameter of DNA and a length equal to one persistence length

(~800 Å). In addition to this very fast component, a spectrum of slower components with molecular relaxation times in the range 0.5 to 18 msec for calf-thymus DNA ($M_r \cong 15 \times 10^6$) was also observed. These slower modes correspond to overall deformations of the DNA coil in solution. The longest rotational relaxation time (18 msec) was found to shorten by about 30% when the ionic strength was raised from 0.02 to 0.1 *M* and to lengthen by 40% when the DNA concentration was increased by 100-fold from 0.006 to 0.6 g/l. This longest relaxation time was in satisfactory agreement with that (14 msec) computed from the empirical relation of Callis and Davidson,[284] based on their stopped-flow dichroism data, especially when allowance was made for differences in solution conditions. It was also in agreement with the theoretical predictions of 16 and 23 msec for nondraining and free-draining limits, respectively, of the Rouse-Zimm model based on the intrinsic viscosity of this same DNA. These slower relaxation times may be identified[132] with the half-Langevin times ($\tau_r/2$) that appear in the formula of Ono and Okano,[116] given in Equation 50 above. Such components have also been observed in the forward depolarized scattered light from solutions of isotactic polystyrene and poly(*n*-hexyl isocyanate).[285] The temperature profile of the longest rotational relaxation time displayed a prominent spike in the course of the melting transition that, in view of the monotone decreasing viscosity, could be interpreted only as an increase in molecular weight over a narrow interval in the transition region.[126]

The polarized component of the scattered light from DNA solutions has also been studied in some detail.[125-129,137,188,189,192,245] A prominent feature in the autocorrelation functions of high molecular weight DNAs is the presence of an appreciable amplitude of a very slowly relaxing component that is much too slow to represent unimpeded translational diffusion of the macromolecular center-of-mass. Such long tails have been observed for N1 DNA ($M_r \cong 31.6 \times 10^6$) in both 1.0 and 0.01 *M* sodium ion,[125,128] for λ DNA ($M_r \cong 31 \times 10^6$) at 0.02 *M* ionic strength,[127] for calf-thymus DNA ($M_r = 11-15 \times 10^6$) at 0.02 *M* ionic strength,[3,126,192] and for ϕ29 DNA ($M_r = 11 \times 10^6$) in 0.01 *M* sodium ion.[129] For the calf-thymus DNA, it was found[123] that the amplitude of the long tail could be substantially diminished by reducing the DNA concentration or by adding salt, with total suppression of the tail in 1.0 *M* NaCl. Chen et al.[189] have recently performed extensive studies to show that the long tail is absent from solutions of sheared calf-thymus DNA ($M_w = 1.5 \times 10^6$) at 0.14 *M* ionic strength. On the basis of considerably less data, they also infer that tails are totally absent for unsheared calf-thymus DNA ($M_r \cong 12 \times 10^6$) in 0.14 *M* NaCl. However, the data in their Table XI rather strongly suggest the presence of a sloping base line, which could be interpreted as a small amplitude of slow component in that case. Such slow components were not observed in studies of circular fd DNA ($M_r = 1.86 \times 10^6$) at 0.17 and 1.8 *M* sodium ion[188] or in studies of sheared calf-thymus DNA ($M_w = 3.7 \times 10^6$) in 0.2 *M* sodium ion.[137] It is evident that higher molecular weights and DNA concentrations and lower ionic strengths enhance the amplitude of the long tail.

A simple model for the long tails has been proposed, based on the idea that a large induced anisotropy of translational diffusion in congested solutions of nonspherical macromolecules should result in a substantial coupling between internal reorienting modes and center-of-mass translation.[73,123] The instantaneous DNA coil envelope is modeled as a prolate ellipsoid, or cucumber, which diffuses through the congested solution with a coefficient $D_\parallel$ in the direction of its long axis and a coefficient zero in any direction perpendicular to that axis. The equation of motion is

$$\frac{\partial c}{\partial r}(z,\theta,t) = D_\parallel \cos^2\theta \frac{\partial^2 c}{\partial z^2}(z,\theta,t) + D_\Omega \nabla_\Omega{}^2 c)z,\theta,t) \quad (68)$$

where the polar axis z has been taken to lie along the scattering vector, and $c(z,\theta,t)/4\pi$ is the number of ellipsoids per unit z per unit solid angle, making an angle θ with respect to z. By keeping only the two most strongly coupled ($l = 0,2$) $P_l(\cos\theta)$ modes of the angular distribution, the problem reduces to one of finding the relaxation times and amplitudes of a pair of coupled diffusion equations. Computed values of the two reciprocal relaxation times as a function of $\sin^2(\theta/2)$ are given in Figure 8 along with data of Schmidt for N1 DNA.[125] The adjustable parameters are $D_\parallel = 1.06 \times 10^{-8}$ cm^2/sec, chosen to fit the slope of the faster component, and $D_\Omega = 12.75$ sec^{-1}, chosen to provide the correct intercept of the slow component, or long tail. The computed relative ampli-

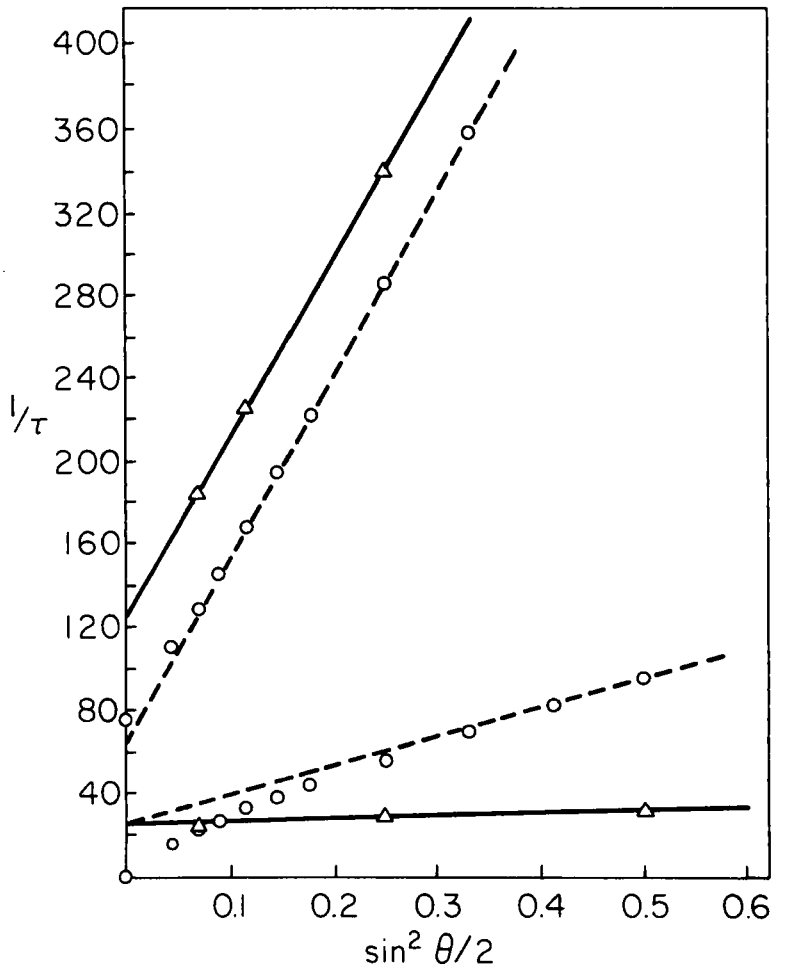

FIGURE 8. Reciprocal relaxation time vs. K^2 for both fast and slow components in the autocorrelation functions of N1 DNA. The triangles (Δ) are data of Schmidt[125] for N1 DNA. The circles (○) are computed from the coupled rotation-anisotropic translational diffusion model,[73,123] as described in the text. The parameters are $D_{\parallel} = 1.06 \times 10^{-8}$ cm²/sec, chosen to fit the observed slope of the upper branch, and $D_R = 12.75$ sec^{-1}, chosen to give the observed apparent intercept of the lower branch.

tudes are also in rough agreement with the observed values. Although this rather crude model is incapable of providing a better quantitative fit, the striking qualitative agreement suggests that in these congested solutions there exists a significant coupling between some internal mode of motion and translational diffusion. Besides reorientation, unraveling of entanglements is also a possibility. It is notable that for very long wavelength motions essentially the entire relaxing amplitude shifts into the slower component, which then has the average diffusion coefficient $D_{\parallel}/3$. This is a situation where distinctly different phenomena are observed in the dynamic light-scattering and macroscopic diffusion experiments, because of the different distance scales examined.

Schmitz has observed a peak in the temperature profile of the long-tail relaxation time of λ DNA in the region of its thermal denaturation transition, as illustrated in Reference 73.

Schmidt et al.[128] have analyzed their small-angle correlation functions for N1 DNA using a single exponential plus a baseline to account for the long tail. In a very careful study of the variation of the $\theta = 25°$ relaxation rate with temperature, they were able to resolve fine-structure changes in the thermal transition region corresponding to those in the temperature derivative

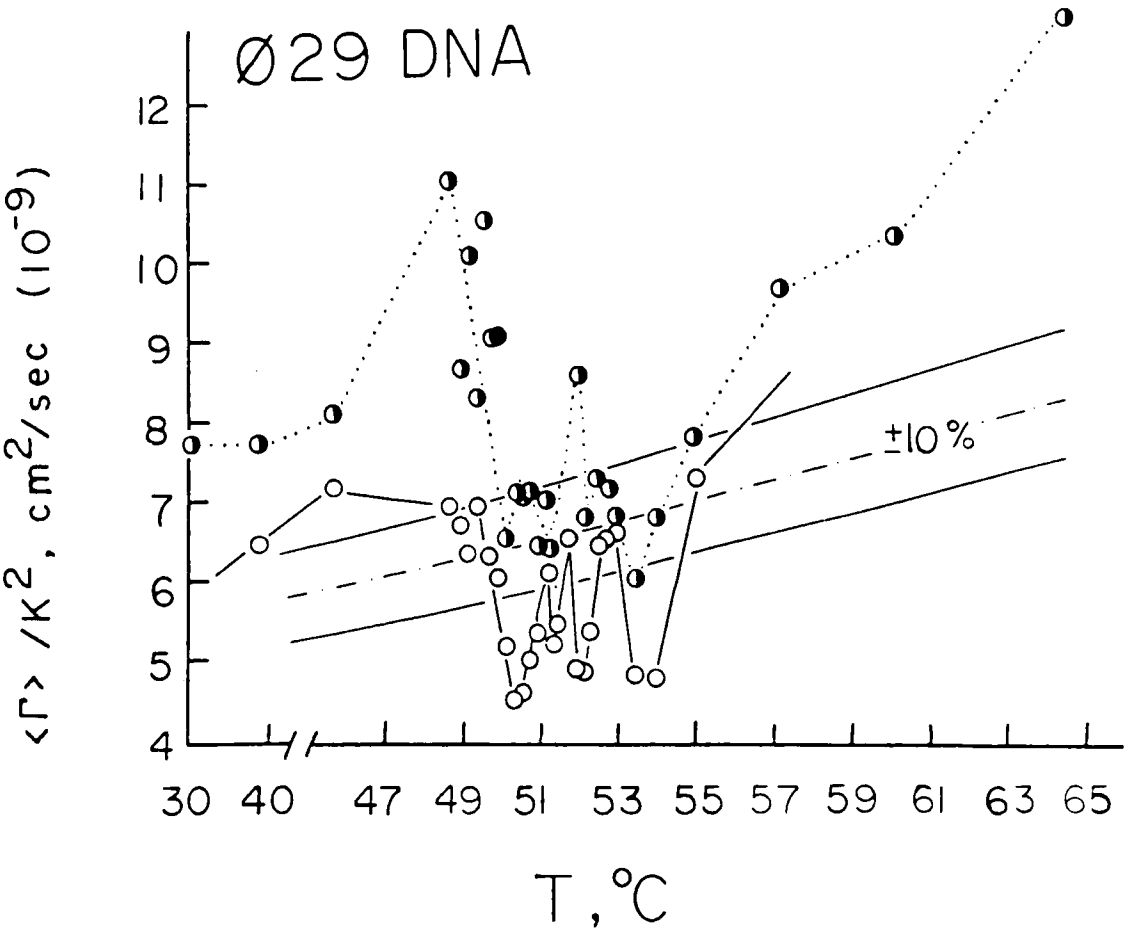

FIGURE 9. Apparent diffusion coefficient $\langle\Gamma\rangle/K^2 = (\tau_A K^2)^{-1}$ vs. temperature for ϕ29 DNA ($M_r \cong 11 \times 10^6$). The DNA concentration is 0.06 g/l and solution conditions are pH 6.8 phosphate buffer containing 0.012 *M* free sodium ion. The empty circles (○) represent low-angle data $\theta \leq 20°$, while the half-filled circles (◑) represent data in the range $20° \leq \theta \leq 30°$. The dashed line represents the temperature dependence expected for a Stokes-Einstein diffusion coefficient, and ±10% lines have also been drawn in for purposes of comparison. (From Schmidt, R. L., Whitehorn, M. A., and Mayo, J. A., *Biopolymers*, submitted. With permission.)

of the optical absorbance. In addition, a substantial decline in relaxation rate associated with the onset of the thermal transition was also observed. In this instance, the decrease in relaxation rate and the remarkable thermal fine structure were both associated primarily with changes in the translational diffusion coefficient.

In a related study of ϕ29 DNA, Schmidt et al.[129] also observed definite fine structure in the thermal profile of the translational diffusion coefficient, as well as an overall decrease in the transition region, as shown in Figure 9. Moreover, data at higher angles, where internal modes contribute appreciably, also manifested essentially similar fine structure, as illustrated in Figure 9.

The apparent overall decrease in translational diffusion coefficient in the thermal transition region is in harmony with the spike in the longest rotational relaxation time observed by Schmitz and Schurr[126] and with the peak in the long-tail relaxation time observed by Schmitz. These diverse observations, taken together with the monotone decrease in viscosity, imply that DNA actually aggregates over a narrow interval in the transition region. A counterion-escape driving mechanism for such an aggregation has been proposed.[126] It is time to seriously reevaluate the notion that DNAs in the thermal denaturation zone can only bind to one another when completely in register. An allowed binding degeneracy in the melting region would not only help explain these data, but could well account for the failure to observe transitions as sharp as those predicted by the melting theory (i.e., $\Delta T \sim 0.02°C$).[286]

The earliest attempt to extract the longest

internal mode relaxation time of a DNA from its polarized scattered light was made by Wun and Prins,[245] who also studied DNA-histone complexes, as noted above. They obtained the values D = 1.6×10^{-8} cm^2/sec and $\tau_1'/2 = 5 \times 10^{-4}$ sec for a sheared calf-thymus DNA ($M_r = 1.5 \times 10^6$), where τ_1' is the Langevin relaxation time in Equation 27. In a recent study of essentially identical DNA, but under quite different solvent conditions, Chen et al.[189] obtained D = 5.3×10^{-8} cm^2/sec and $\tau_1'/2 = 5 \times 10^{-4}$ sec. Both values of $\tau_1'/2$ are in excellent agreement with that ($\tau_1'/2$) observed in the relaxation of the electric dichroism by Ding et al.[283] for a DNA of similar weight.

Jolly and Eisenberg[137] have attempted a similar analysis of a sheared calf-thymus DNA ($M_r \cong 3.7 \times 10^6$) of somewhat higher molecular weight with the results, D = 2.23×10^{-8} cm^2/sec and $\tau_1'/2$ = 9 msec. From the unknown approximate molecular weight dependences, $D \propto M^{-0.5}$ and $\tau_1' \propto M^{1.6}$, one would have expected for such a DNA the values D $\cong 3.4 \times 10^{-8}$ cm^2/sec and $\tau_1'/2 \cong 2.1$ msec from the results of Chen et al.[189] and the value $\tau_1'/2$ = 1.9 msec from the results of Schmitz and Schurr (without correcting for ionic strength).[126] Neither the D value nor the $\tau_1'/2$ value of Jolly and Eisenberg fits into the pattern of the other data. The origin of this discrepancy is not known.

The difficulties associated with attempts to determine τ_1' values for higher molecular weight DNAs have been noted by Chen et al.[189] and Schmidt et al.[129] Briefly, the problem is that higher internal modes already contribute significantly at very small angles, because of the very large radii of gyration (≥4000 Å) of such molecules. Thus, applications of Equation 27 to determine τ_1' for DNAs with molecular weights of 10^7 or more have been fruitless.

A novel approach is that of Caloin et al.[192] who have simply force-fit their photocurrent spectra for calf-thymus DNA ($M_r = 11 \times 10^6$) to the Fourier transform of Equation 56 with $1/\tau_A = DK^2$ and $1/\tau_B = DK^2 + 1/\tau_{int}$. The value D was first determined by extrapolating single Lorentzian line widths to the K = 0 limit. The quite interesting result emerging was that $1/\tau_{int}$ was itself proportional to K^2 with a slope that depended only slightly, if at all, on ionic strength. Moreover, the fractional amplitude A/(A + B) of the $1/\tau_A$ term essentially vanished at large values of K^2, while the fractional amplitude B/(A + B) of the $1/\tau_B$ term was found to be a universal function of KR_G. All of this behavior, apart from the ionic strength dependence, is predicted by Equation 28 above for the linear free-draining Rouse-Zimm model. However, it is not understood just why that equation should be valid for values of $K^2b^2 < 1.0$. It should be mentioned here that Büldt[287] has obtained what amounts to the first cumulant of Equation 28, which predicts $1/\tau \propto (k_BT/f)K^2$ irrespective of K^2, but that clearly ignores the dominant slower component at small K^2.

Lin and Schurr[133] have studied calf-thymus DNA ($M_r = 11 \times 10^6$) at 1.0 *M* salt where the long tails were effectively suppressed. Their data were force-fit to single exponential curves, with especially good results at both low and high scattering angles. The apparent diffusion coefficient defined by $D_{app}(K) = 1/\tau_A K^2$ was determined as a function of K^2 and invariably gave a curve qualitatively similar to that in Figure 10. The solid line represents a fit to the simple independent-segment mean-force model, which was employed solely for purposes of extrapolation and interpolation. The evident similarity between these data and those in Figure 3, which represent single-exponential fits of numerical correlation functions computed for the Rouse-Zimm model, implies that that model may be substantially correct for DNA. Of special significance is the plateau behavior[73] of $D_{app}(K)$ at large K^2. Such behavior was reported by Caloin et al.[192] and has apparently also been observed for high molecular weight polystyrene in toluene.[141]

Based on analogy with the circular chain, for which an explicit result similar to Equation 28 could be obtained even in the presence of hydrodynamic interaction, and on computational results for linear chains, an algorithm was proposed for simple estimation of the parameters of the linear Rouse-Zimm model in the presence of hydrodynamic interaction. The steps are as follows.

1. Set $k_BT/f = D_{plat}$, where D_{plat} is the plateau value of $D_{app}(K)$ at large K^2.
2. Set $b^2 = 8/K_m^2$, where K_m^2 is the midpoint value of K^2 at which $D_{app}(K) = (D + D_{plat})/2$ is halfway between D and D_{plat}. The center-of-mass diffusion coefficient D is, of course, the limiting value of $D_{app}(K)$ at K = 0.
3. The number N + 1 of effective beads is found from the relation

$$(N+1)^{1/2} = \frac{F/(D_{plat}\cdot b) + \left\{[F/(D_{plat}\cdot b)]^2 + 4(D/D_{plat})\right\}^{1/2}}{2D/D_{plat}} \qquad (69)$$

where F is a quasi-constant tabulated by Lin and Schurr[133] for values of N + 1 from 5 to 30 and b values from 2000 to 4000 Å. At large values of N + 1, F is expected to become truly constant, as found for the circular chain. In any event, one or two iterations beginning with practically any guess for N + 1 produce satisfactory convergence.

Typical results for the Rouse-Zimm model parameters are given in Table 3 for both native and pH-denatured (pH 12.50) DNAs in the presence and absence of the Ca^{++}-sequestering agent EDTA. It is interesting that the effective number of beads in each case ranges from five to ten, as estimated for this DNA of 100 persistence lengths under the assumption that a minimum of 10 persistence lengths would be required for each bead-spring unit.[123] EDTA produces a large decrease in the length parameter b of native DNA, concomitant with an increase in N + 1, but has virtually no effect on the internal segment diffusion coefficient k_BT/f. The former observation implies that Ca^{++} acts to stiffen the chain locally, resulting in larger b and smaller N + 1. The absence of a comparable effect on k_BT/f is highly interesting and may indicate that segmental mobility is not governed exclusively by hydrodynamic friction, but may contain also a significant contribution from inter-segment interactions, or from mobilities of joints, or kinks, along the chain. Although the physical interpretation of these Rouse-Zimm model parameters is by no means clear, it is now apparent that the separate effects of chemical agents on static (b and N + 1) and dynamic (k_BT/f) manifestations of internal structure and motion can be distinguished.

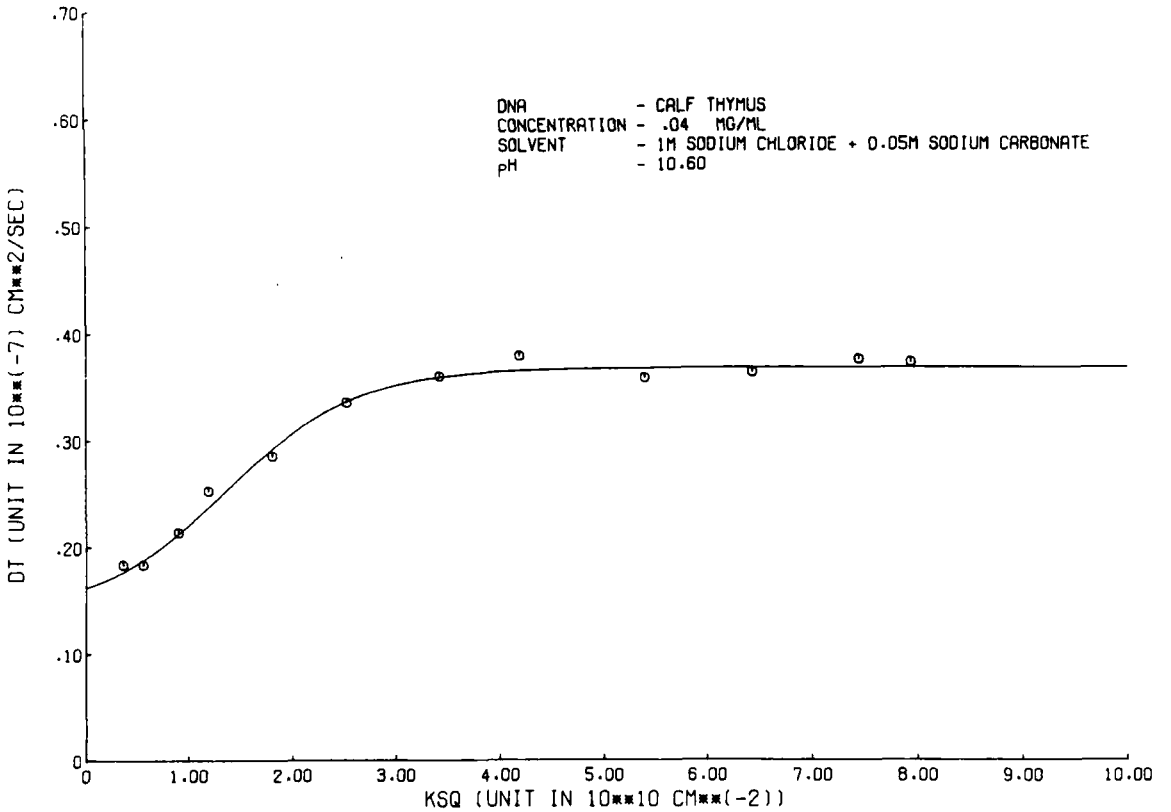

FIGURE 10. Apparent translational diffusion coefficient $DT \equiv D_{app}(K) = (2\tau_A K^2)^{-1}$ vs. $KSQ \equiv K^2$ for calf-thymus DNA ($M_r \cong 11 \times 10^6$). The DNA concentration is 0.04 g/l and solution conditions are 1.0 *M* NaCl + 0.05 *M* Na_2CO_3, pH 10.60, T = 22°.

TABLE 3

Rouse-Zimm Model Parameters for Calf-Thymus DNA at 22 to 23°C

pH	b (nm)	k_BT/f ($cm^2 s^{-1}$)	N + 1	g (dyn cm^{-1})	f (dyn cm^{-1} s)
Without EDTA					
10.30	260	4.2×10^{-8}	7.0	1.8×10^{-4}	9.69×10^{-7}
12.50	200	3.5×10^{-8}	5.2	3.0×10^{-4}	1.16×10^{-6}
With EDTA					
9.6	165	4.05×10^{-8}	9.5	4.6×10^{-4}	1.01×10^{-6}
12.50	161	5.0×10^{-8}	6.0	4.8×10^{-4}	8.14×10^{-7}

The data of Caloin et al.[192] show that increasing the ionic strength of NaCl from 0.01 *M* to 1.0 *M* produces only about a 10% decrease in k_BT/f, but a 50% decrease in b, which is rather similar to the effect of removing Ca^{++} by addition of EDTA.

Although the approaches adopted by Caloin et al.[192] and Lin and Schurr[133] should lead to equivalent results at large K^2 in the sense that $D + \tau_{int}/K^2$ should be equal to k_BT/f, this does not appear to be the case. The former values are nearly two times larger than the latter. The origin of this discrepancy is not yet known, but hopefully this dilemma will soon be resolved.

One may confidently expect a surge of activity in the analysis of internal dynamics of large polymers of all kinds by dynamic light scattering in the near future, especially now that the way has been opened for quantitative parametrization and modeling of the behavior of the data at large values of K^2b^2. Of course, at very large values of K^2b^2, one might anticipate the onset of still another unexplored dynamic regime. However, a recent short-wavelength inelastic neutron scattering study[288] of polytetrahydrofuran and its perdeutero analog also appears to conform to the $1/\tau \propto K^2$ result predicted by Equation 28 at large K^2b^2, suggesting that for many polymers the fluctuation wavelength restrictions imposed by the light source may confine investigations to the regime where Equation 28 remains applicable.

Newman et al.[188] have reported a very thorough study of both diffusion and sedimentation behavior of single-strand circular fd bacteriophage DNA, for which they report a molecular weight $M_w = 1.86 \pm 0.06 \times 10^6$ and a Stokes radius of 316 ± 6 Å. The dimensionless virial coefficients obtained for the sedimentation and diffusion constants, 6.7 ± 0.8 and 1.2 ± 0.4, respectively, are equal to the corresponding hard-sphere values of 6.55 in Equation 65 and 1.45, in the absence of solvent backflow, in Equation 67, respectively, within the experimental error. The value predicted by Mou and Chang[227] for k_D is even closer to the mean value. The dimensionless values were obtained using a molecular hard-sphere volume equal to that of the Stokes sphere. It was also noted that the thermodynamic dimensionless virial coefficient exhibited the appropriate hard-sphere value based on the same Stokes radius. It is not clear why solvent backflow apparently made no contribution.

Electrophoretic light-scattering studies of calf-thymus DNA from 0.001 to 0.1 *M* ionic strength have been reported by Hartford and Flygare.[290] At low ionic strength, the mobility was linear in the square root of the ionic strength, in accord with the Debye-Hückel theory for a constant surface charge density, and approached a constant value at high ionic strength, also in accord with conventional electrophoresis theory.[291] The static light-scattering study of Krasna[292] provides interesting information concerning the behavior of DNA at low salt concentrations, in particular pointing up the extremely weak scattering obtained from solutions at 10^{-4} to 10^{-5} *M* salt.

Nucleic Acids (tRNA)

A precise study of the diffusion coefficients of unfractionated *E. coli* tRNA and yeast phenylalanine tRNA as a function of both ionic strength and magnesium ion concentration was performed by Olson et al.[151] A major conformational change was observed at 0.1 *M* ionic strength in the presence of 10^{-3} *M* Mg^{++} ion, but was absent at 10^{-2} *M* Mg^{++} ion. A block and hinge model was proposed to account for this process. Further experiments on conformation changes associated

with aminoacylation of the tRNA have also recently been completed.[289]

In the studies of Olson et al.,[151] the variation of D_{app} with ionic strength and tRNA concentration was interpreted in terms of an equation that may be written for one to one electrolyte in the form

$$D_{app} = D_p \left[1 + \left(0.045\,\bar{v}_2 + \tfrac{1}{2}\frac{Z^2}{C_s} \right) C_p \right] \qquad (70)$$

where C_p and C_s are molar concentrations of tRNA and salt, respectively. This equation was derived from Equations 64 to 66 using Tanford's estimate[152] of the thermodynamic second virial coefficient. It was found for these tRNA solutions that the 0.045 $\bar{v}_2$ term was negligible compared to the charge term. Apart from a factor $(1 - D/D_p)$, the charge term in Equation 70 is identical to that in Equation 42 derived from linearized coupled mode theory. The effect of counterion dynamics, then, is to produce a change of at most a few percent in the diffusion virial coefficient compared to that derived from equilibrium forces alone. Olson et al. have confirmed the C_s^{-1} dependence of the diffusion virial coefficient in this system and have obtained a value of Z = 10 charges. In addition, evidence is presented for a weak association to form dimers in 10^{-2} *M* Mg^{++} with an equilibrium constant of approximately $K \cong 1 \pm 0.5 \times 10^3\ M^{-1}$ for unfractionated tRNA samples. If association only of like dimers occurs, this figure translates to about $K \cong 10^5\ M^{-1}$ for a pure tRNA.

Ovomucoid

The egg glycoprotein ovomucoid, which contains about 25% saccharides covalently bound to amino acids, was studied by McDonnell and Jamieson[293] as part of a general program to develop techniques for rapid determination of protein molecular weights. The molecular weight was estimated to be 31,400 from an empirical Flory-Mandelkern type relation between D, $[\eta]$, and molecular weight. The anomalously large value of its diffusion coefficient in 6 *M* Gdn·HCl was interpreted in terms of an unusually compact structure produced by chain branching.

Ovalbumin

The diffusion coefficient of a 3% ovalbumin solution in 0.5 *M* KCl was determined to be 7.1 ± 0.2×10^{-7} cm^2/sec in the early work of Dubin et al.[3]

Phycocyanin

A stable preparation of the fluorescent hexamer of phycocyanin was studied by dynamic light scattering as part of a hydrodynamic characterization also involving sedimentation and viscosity measurements.[212] From the values obtained, ($D_{20,w} = 4.73 \times 10^{-7}$ cm^2/sec, $S_{20,w}$ = 10.2 S, and $[\eta]$ = 3.89 ml/g), a molecular weight of 209,000 was deduced. The data were in agreement with a model in which spherical monomers of radius 22 Å were contiguously arranged with C_6 symmetry to form a hexagon 132 Å across. Although other geometries were also possible, substantially more compact geometries could be ruled out.

Polyacrylamide

Viscoelastic polyacrylamide gels[9,12] and partially hydrolyzed polyacrylamide[294] have both been studied by dynamic light-scattering techniques. The polarized scattered light from the gels gave surprisingly clean single-exponential relaxations with $1/\tau \propto K^2$, as would have been predicted by either the independent-segment mean-force model or the Rouse-Zimm model for macromolecules of visible dimensions. The depolarized light was too weak to measure.[9]

Tanaka et al.[9] have proposed a continuum viscoelastic model with an equation of motion for the displacement **u** of the gel network given by

$$\rho \frac{\partial^2 \mathbf{u}}{\partial t^2} = \mu \nabla^2 \mathbf{u} + (\beta + \tfrac{1}{3}\mu) \nabla (\nabla \cdot \mathbf{u}) - \zeta \frac{\partial \mathbf{u}}{\partial t} \qquad (71)$$

where ρ, μ, β and ζ are the network mass density, bulk modulus, shear modulus, and friction factor density for the fluid acting on the network. For the strongly overdamped, or nonpropagating, waves expected in these gels, the desired correlation function is given by[9]

$$M_V(K,t) = \text{const.} \frac{k_B T}{2\mu} \frac{1}{K^2} e^{-K^2 D_G t} \qquad (72)$$

where the effective diffusion coefficient for the gel is $D_G \equiv 2\mu/\zeta$. It was assumed[9] that Poisson's ratio was essentially zero, so that $\beta + (4/3)\mu = 2\mu$ for this gel. The scattered intensity, which is proportional to $M_V(K,0)$, gives μ, and the effective diffusion coefficient gives $2\mu/\zeta$, so that both constants, μ and ζ, can in principle be determined

from light-scattering measurements alone. In practice inhomogeneities in the gel diminish the reliability of intensity measurements. Tanaka et al.[9] measured both μ and ζ directly by mechanical means and verified that the dynamic light-scattering value of $D_G = 2\mu/\zeta$ was given accurately by the appropriate quotient.

The macroscopic parameters can be related to microscopic variables in the following way. The macroscopic friction density should be given by $\zeta = \nu f$, where ν is the number of polymer chains per unit volume in the gel and f is the friction factor of each chain. A chain is the section of polymer connecting two cross-links. Tanaka et al.[9] gave an expression for the elastic strain energy density associated with a constant-volume uniaxial deformation of a gel cylinder of length l, $\Delta A = \mu(3/2)\,(\Delta l/l)^2$. The corresponding expression for the elastic free-energy density of a perfect phantom network, $\Delta A = (k_B T/2)\,(1 - 2/\phi)\nu 3(\Delta l/l)^2$, where ϕ is the functionality of the cross-links, can be obtained from a recent formulation of Flory,[295] based on the distribution results of Eichinger[296] and Graessly.[297] Equating these macroscopic and microscopic expressions for the free energy gives $\mu = k_B T(1 - 2/\phi)\nu$. In terms of microscopic variables, then, there results

$$D_G = 2\mu/\zeta = (k_B T/f)2(1-2/\phi) \qquad (73)$$

which shows the dependence on cross-link functionality. Tanaka et al.[9] observed a temperature variation of D_G that was reasonably close to that predicted from Equation 73 with a friction factor (f) proportional to solvent viscosity.

Jamieson and Presley[294] have observed partially hydrolyzed polyacrylamide molecules in dilute solution. At very low ionic strength, where electric charge interactions were expected to be significant, two widely separated components were observed in the correlation function, the faster of which appeared to increase in prominence at very small angles. The amplitude of this rapid component was found to be almost completely suppressed in the presence of 0.5 *M* NaCl. These observations were interpreted in terms of anisotropic translational diffusion of highly extended charged rods (at low ionic strength) together with hindered rotational diffusion. High ionic strength conditions were believed to induce a random-coil conformation that exhibited essentially ordinary behavior. The weakness of this interpretation is that the diffusion coefficient corresponding to the fast component is a full order of magnitude larger than that of the high-salt random coil, which is not expected on hydrodynamic grounds alone. A substantial contribution from a rapid internal mode, or charge-induced enhancement of the diffusion coefficient, also seems likely to be involved.

Polypeptides (Poly-γ-benzyl-L-glutamate, Poly-L-proline, and Poly-L-lysine)

One of the earliest applications of autocorrelation analysis directly in the time domain was a study of diffusion and conformational changes of poly-γ-benzyl-L-glutamate (PBLG) in solvent mixtures ranging from pure 1,2-dichloroethane (DCE) to pure dichloroacetic acid (DCA).[162] For a polymer of molecular weight 3.35×10^5, the observed D (corrected to the viscosity of pure DCE) exhibited about a 30% increase in the course of the solvent-induced coil-to-helix transition.

Using a combination of static and dynamic light-scattering methods, Schleich and Yeh[298] demonstrated that polyproline II forms very large aggregates in aqueous solution at 1 to 2 mg/ml at 24°C. It was also found that Gdn·HCl, which does not affect the optical rotation, or helix structure, induces dissociation, as does 4 *M* $NaClO_4$, which does unfold the polyproline II helix. However, 4 *M* $CaCl_2$, which likewise unfolds polyproline II helix, induces further aggregation. The very long time scale of these changes was also noted. These studies clearly point out the weakness of relying entirely on a single structural tool, whether it be a short-range structure monitor such as optical rotatory power or a long-range structure monitor such as light scattering.

The diffusion dynamics of poly-L-lysine·HBr (PLL) in aqueous solution has been investigated as a function of molecular weight, pH, salt, and PLL concentration.[104,109,174,299] The power law coefficients for $D = K_d M^{-b}$ and $[\eta] = K_v M^a$ were determined to be $b = 0.6 \pm 0.03$ and $a = 0.80 \pm 0.11$ in 0.2 *M* NaBr at neutral pH, thus satisfying the relation $3b = a + 1$ expected for random coils.[174] A sharp rise in the diffusion coefficient between pH 9.5 and 10.5 during the onset of the helix coil transition was followed by an abrupt decrease at higher pH that could not be readily investigated because of profuse aggregation, even in solutions as dilute as 0.4 and 1.85 g/l for

molecular weights 200,000 and 35,000, respectively.[174] This aggregation, which was also observed in 10^{-2} *M* salt,[104] raises very serious doubts about the postulated existence of isolated single helices in aqueous solution. The rise in D during the onset of the transition was indicative of a more compact mixed-helix and random-coil structure, as also found in sedimentation and viscosity measurements.[300] Indeed, Ptitsyn and Skvortsov[300] have provided equations that allow one to determine the cooperativity parameter (σ) of the helix-coil transition from either the intrinsic viscosity or diffusion coefficient of the random-coil form and that of the intermediate mixed species corresponding to the minimum in the hydrodynamic radius; that is

$$(f_0)_m \equiv \frac{(R_G)^2_m}{(R_G)^2_{coil}} = \left(\frac{D_{coil}}{D_m}\right)^2 = \frac{3(1-\theta_m)}{(3-2\theta_m)\alpha_c^2} \quad (74)$$

$$\sqrt{\sigma} = \gamma^{-2}\frac{\theta_m^{1/2}(3-2\theta_m)}{(1-\theta_m)^{3/2}} \quad (75)$$

where θ_m is the fraction of peptides in the helix conformation at the minimum; α_c is the expansion factor for the random-coil form; and $\gamma = l_{coil}/l_{helix}$, where $l_{helix} \cong 2.0$ Å, is the contribution of each residue to the length of a helical region, and $l_{coil} = 6^{1/2} R_G/\alpha_c^2 \cdot h$ is the effective length in the random-coil form of each of the h residues in the chain. If θ_m is known from optical rotation data, then α_c can be calculated from Equation 74. Conversely, if α_c is known or assumed, then θ_m can be calculated. Using the PLL diffusion coefficients[174] ($D_{coil} = 1.38 \times 10^{-7}$ and $D_m = 1.78 \times 10^{-7}$ cm^2/sec) and assuming the value $\alpha_c^2 = 1.13$ determined by Ptitsyn and Skvortsov,[300] one finds $\theta_m = 0.66$ and $\sigma = 1.0 \times 10^{-3}$, which may be compared with the corresponding values $\theta_m = 0.35$ and $\sigma = 1.6 \times 10^{-3}$ determined from the viscosity at substantially higher salt concentrations.[300] Varying α_c^2 from 1.0 to 1.32 produces ±50% variations in σ. The mean number of residues per helical section is $1 + \sigma^{-1/2} \cong 33$ in this case. Because the helix-coil transition in PLL cannot be thermally induced, estimates of σ are available only from hydrodynamic methods such as these. Although possible manifestations of helix-coil kinetics in the correlation function were carefully sought, none were found. This is in agreement with acoustic absorption data that indicate a relaxation time of $\tau \cong 2 - 4 \times 10^{-8}$ sec, much too fast to have been observed with the apparatus employed.[174]

An unusual feature of the PLL data is the anomalously large value of $l_{coil} \cong 18$ Å, computed using the formula above. In contrast, McDonnell and Jamieson[293] report the value $l_{coil} = 9.7$ Å for a series of proteins denatured in 6 *M* Gdn·HCl and 0.1 *M* mercaptoethanol. Indeed, extrapolating the observed diffusion coefficient of Lee and Schurr[174] for PLL into the viscosity of the denaturing solvent used by McDonnell and Jamieson[293] gives a value far below that predicted by their universal curve for h = 955 amino acids. The PLL random coil in 0.2 *M* NaBr is evidently considerably more extended than are denatured proteins in 6 *M* Gdn·HCl. Whether this is due to steric or short-range charge effects is not yet known.

Of particular theoretical interest is the dependence of PLL diffusion on salt and polyion concentration. Solutions prepared in the absence of salt exhibited extremely weak scattering with no sign of a correlation function relaxing in the expected time range, but did manifest a small amplitude of extremely slow relaxation with $1/\tau \propto K^2$ and with an effective diffusion coefficient D_{app} in the range of 10^{-8} cm^2/sec.[104,299] Addition of NaOH, in what was called the annealing process, to raise the pH into the zone of the helix-coil transition, followed by addition of HBr to return the solution to neutral pH, converted the solution essentially completely from the extraordinary condition noted above to ordinary behavior. However, the solution could be returned to the extraordinary condition just by dialyzing against distilled water, showing that the primary effect of the annealing process was simply the addition of salt, which in fact was found to produce the same effect. The amount of salt present in the annealed solutions was actually about 10^{-2} *M*, rather than the 10^{-4} *M* erroneously reported.[104] In those solutions, D_{app} had nearly twice the value found in 0.2 *M* salt, and there was no significant rise in D_{app} associated with the onset of the coil-to-helix transition, showing that charge effects had the potential to effectively mask conformation changes.

Results of a more recent investigation[109] of the variation in D_{app} with salt concentration at each of two polyion concentrations are shown in Figure 11. Abrupt transitions from ordinary to extraordinary behavior were observed in each case,

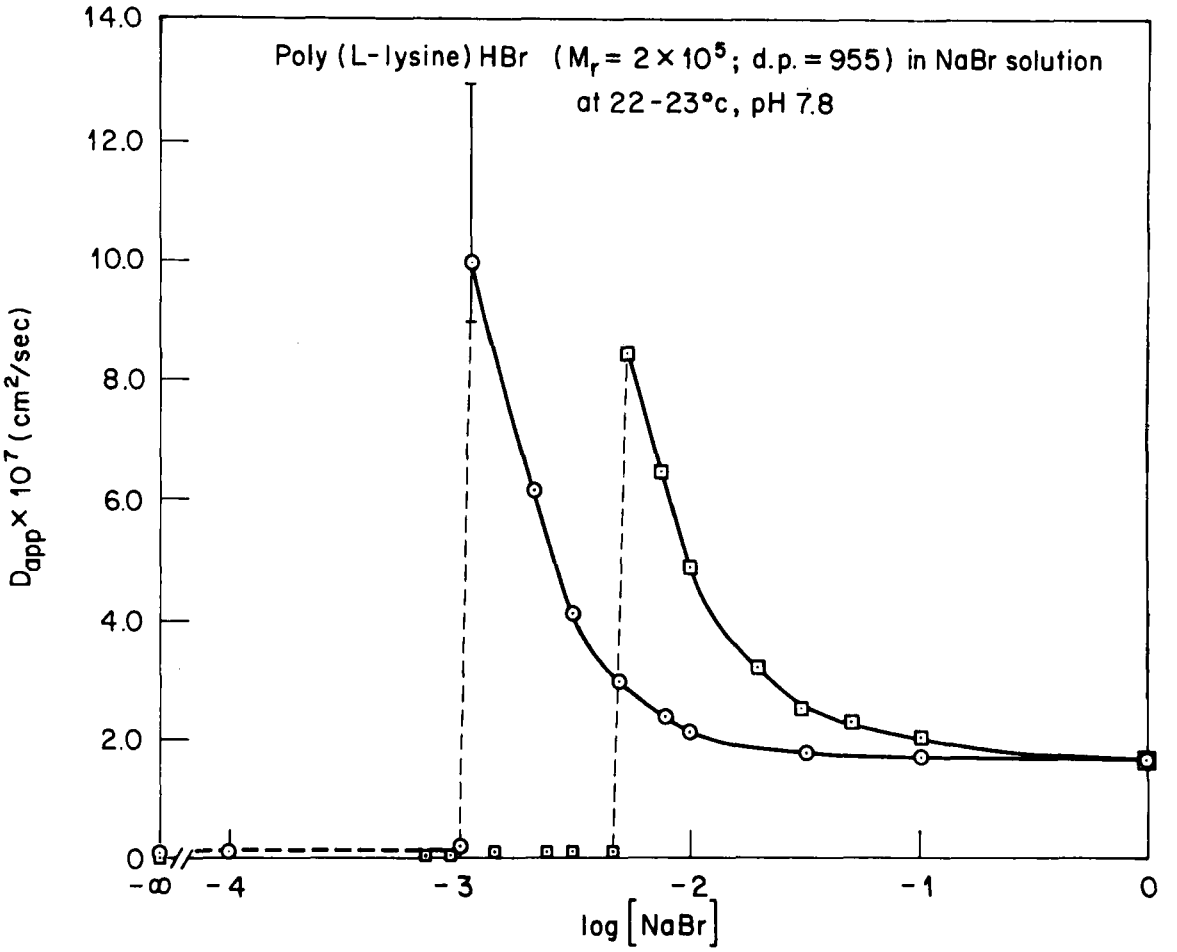

FIGURE 11. Apparent translational diffusion coefficient D_{app} vs. log[NaBr] for poly(L-lysine)·HBr (degree of polymerization 955). Poly(L-lysine) concentration is 3.0 g/l for the squares (⊡) and 1.0 g/l for the circles (⊙). The solution pH is 7.8, and T = 22 to 23°C. The error bar for the 10^{-3} *M* NaBr data is anomalously large and reflects an obviously nonexponential decay with both much faster and much slower components present in that correlation function. (From Lin, S.-C., Lee, W. I., and Schurr, J. M., *Biopolymers*, submitted. With permission.)

and the salt concentration at which the transition took place increased with increasing polyion concentration. At 6.5 g/l the transition occurred near 0.035 *M* NaBr. A several-fold increase in scattered intensity accompanied the extraordinary ⇌ ordinary transition. Moreover, at 10^{-3} *M* NaBr, where the transition occurred for 1 g/l PLL, a rapid relaxation that appeared to be independent of scattering angle was also observed. Two relaxation times of about 10 μsec and 60 to 75 μsec in $M_v(K,t)$ were believed to have been detected at all angles and were assigned to the kinetics of the ordinary ⇌ extraordinary transition process.[109] A transition between two solution phases with markedly different scattering powers is precisely the situation where kinetics are expected to be manifested in the scattered light, as suggested by Equation 34. In view of the comparatively small size of these polyions, the rather large change in scattering power at the transition necessarily implies a dominant contribution from intermolecular interference, which in turn implies a substantial change in the character of the equilibrium pair distribution function over a range of at least several thousand Ångströms.

It is not yet known whether the extraordinary low-salt phase exhibits true periodic long-range order, as observed for polystyrene latex spheres,[16,82] nor is it known what physical process is responsible for the very slow relaxations observed. In free-boundary diffusion studies of smaller PLL with h ≅ 50 and h ≅ 340 in the

absence of salt, Daniel and Alexandrowicz[154] observed enormous diffusion coefficients, (D_{app} = 55×10^{-7} and 50×10^{-7} cm^2/sec, respectively) independent of the polyion concentration. Even such rapid diffusion should have been readily detectable at scattering angles of 40° or less, provided that sufficient amplitude was available. However, according to Equation 35, an order of magnitude increase in D_{app} would have been accompanied by an order of magnitude decrease in G(K,0), or $\langle I_V^s \rangle$, rendering detection of any rapid diffusion essentially hopeless. The slow relaxation could conceivably represent the diffusion of grain boundaries in a mosaic array of ordered domains, as postulated to account for a similar slow component in the ordered phase of polystyrene latex spheres.[16]

Even in the ordinary phase some remarkable features were observed, including fivefold enhancements of D_{app} with decreasing salt concentration.[109] The linear dependence of D_{app} on polyion concentration predicted by Equation 42 is demonstrated in Figure 12. Proportionality of the slope $\partial D_{app}/\partial \bar{C}_p$ with reciprocal salt concentration $\bar{C}_s^{-1}$, also predicted by Equation 42, is indicated in Figure 13. Indeed, D_{app} was found to vary linearly with $\bar{C}_s^{-1}$ for both 1.0 and 3.0 g/l solutions. These linear graphical results enabled the empirical determination of a formula that fit all of the data down to $\bar{C}_s \cong 7.5 \times 10^{-3}$ *M* within ±5%; that is

$$D_{app} \cong 1.63 \times 10^{-7} - \frac{8.5 \times 10^{-10}}{\bar{C}_s} + (2.84 \times 10^{-4}) \frac{\bar{C}_p}{\bar{C}_s} \qquad (76)$$

This expression[109] resembles Equation 42 except for the middle term, which becomes comparable to the first term at $\bar{C}_s \cong 5 \times 10^{-3}$ *M*. In other words, values of D_{app} extrapolated to $\bar{C}_p = 0$ decrease precipitously below 0.02 *M* salt concentration to catastrophically small values, much lower than can be explained on hydrodynamic grounds alone, even with fully extended polypeptide chains. Indeed, the value of D_p computed from the formula of Broersma[208] for a 4000 Å × 12 Å diameter cylinder is 7.2×10^{-8} cm^2/sec, only slightly below the experimental value for 0.01 *M* NaBr in Figure 11. The picture of diffusion in the ordinary phase of PLL that has emerged[109] is one in which the friction of the individual polyions apparently grows to anomalously large values as the salt concentration declines, but in which the intermolecular repulsions also increase so strongly with increasing polyion concentration that the net effect is a substantial enhancement of diffusion for all but the very lowest polyion concentrations.

If the first and third terms in the empirical Equation 76 are identified with the first and second terms, respectively, in Equation 42, then an effective charge, Z = 59, can be calculated[109] for these PLL molecules, which actually bear a titration charge of 955. Then, the value $D_{app} = 59 \times 10^{-7}$ is computed using Equation 44 in the absence of salt, which is in suprisingly close agreement with those values measured by Daniel and Alexandrowicz[154] for smaller PLL molecules by free-boundary diffusion, as mentioned above. This agreement may be simply an interesting coincidence or it may indicate that the middle term in Equation 76 is absent in the extraordinary phase. Clearly, further work is required to fully understand the nature of these unusual and interesting phenomena.

An earlier investigation of PLL was that of Jamieson et al.[301] They detected a fast component with $\tau \cong 10$ μsec that is very likely related to the extraordinary-ordinary transition process, as noted by Lin et al.[109]

A dynamic light-scattering study of the electrically induced cholesteric to nematic phase transition in concentrated liquid crystalline poly-γ-benzyl-L-glutamate was reported by Duke and Dupre.[302]

Ribosomes

Chick embryo ribosomes have been studied by sedimentation and dynamic light-scattering techniques.[19] Decreases in both D and S by about 9%, when the ribosomes became bound to messenger RNA, indicated a change to a more compact structure with no loss in mass. This conformation change was not dependent on the presence of nascent polypeptide chains on the ribosome.

E. coli robosomes have also been studied by dynamic light-scattering methods.[17,18,181] Hocker et al. found that very large aggregates were formed with time under practically all KCl conditions studied at 4°C.[17] Nonetheless, they succeeded in obtaining the diffusion coefficient for the 70 S monomer and were able to demonstrate that high (≥ 0.1 *M*) KCl concentrations induced

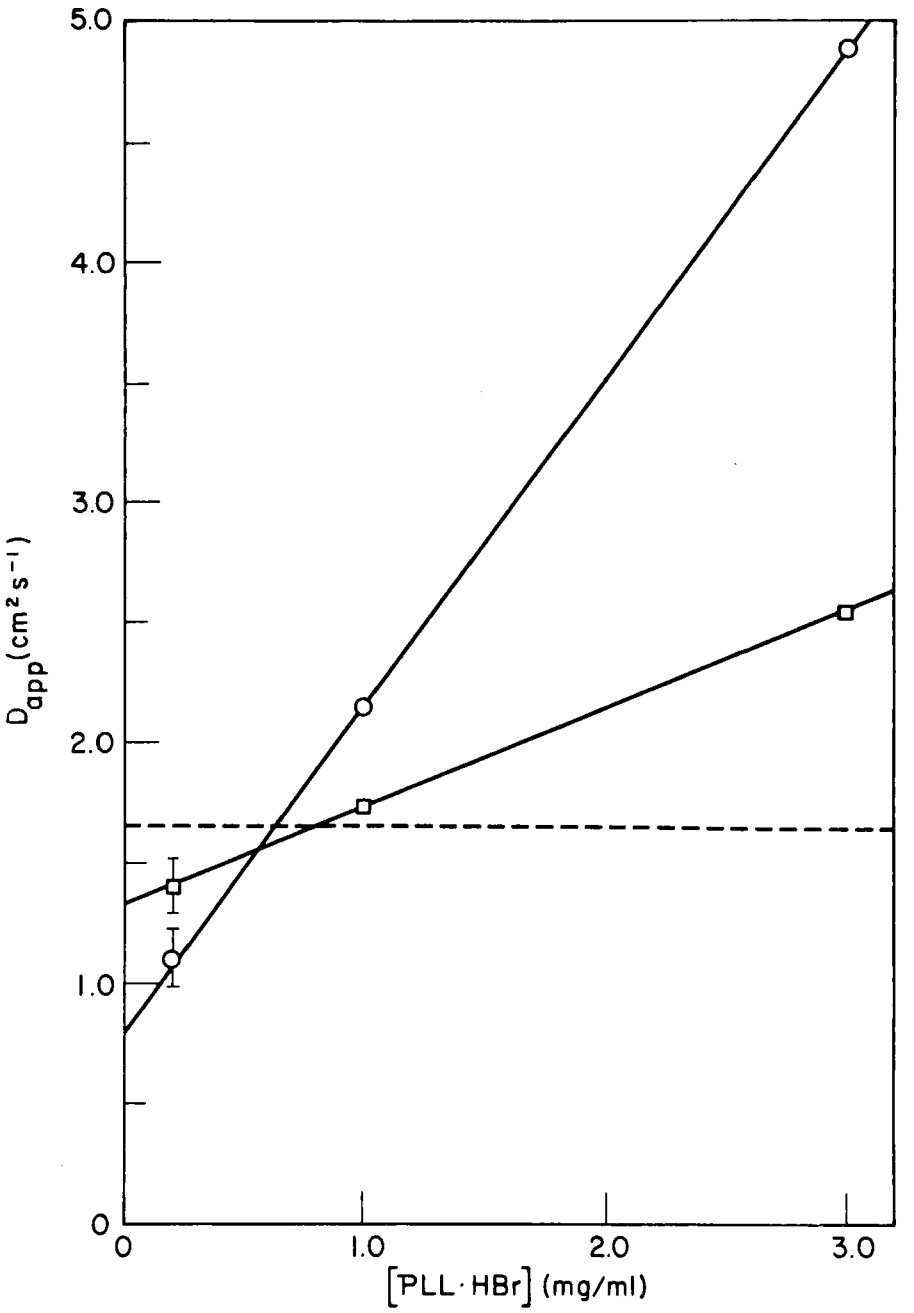

FIGURE 12. Apparent translational diffusion coefficient D_{app} vs. [PLL·HBr] for poly(L-lysine)·HBr (degree of polymerization 955). Salt concentration is 0.032 *M* NaBr for the squares (□) and 0.01 *M* NaBr for the circles (○). These solutions are pH 7.8, T = 22°C. (From Lin, S.-C., Lee, W. I., and Schurr, J. M., *Biopolymers*, submitted. With permission.)

dissociation of the 70 S ribosome to its subunits, whereas low ($\leqslant$ 0.005 *M*) KCl concentrations promoted self-association of ribosomes to form dimers. Using band sedimentation in a sucrose gradient in conjunction with dynamic light scattering, Koppel[181] was able to study the various species separately. For the 70 S, 50 S, and 30 S ribosomes, he obtained the respective molecular weights (M_w) 2.49 X 10^6, 1.55 X 10^6, and 0.87 X 10^6 and the respective diffusion coefficients ($D_{20,w}$) 1.71 X 10^{-7}, 1.90 X 10^{-7}, and 2.18 X 10^{-7} cm^2/sec. Gabler et al.[18] observed essentially

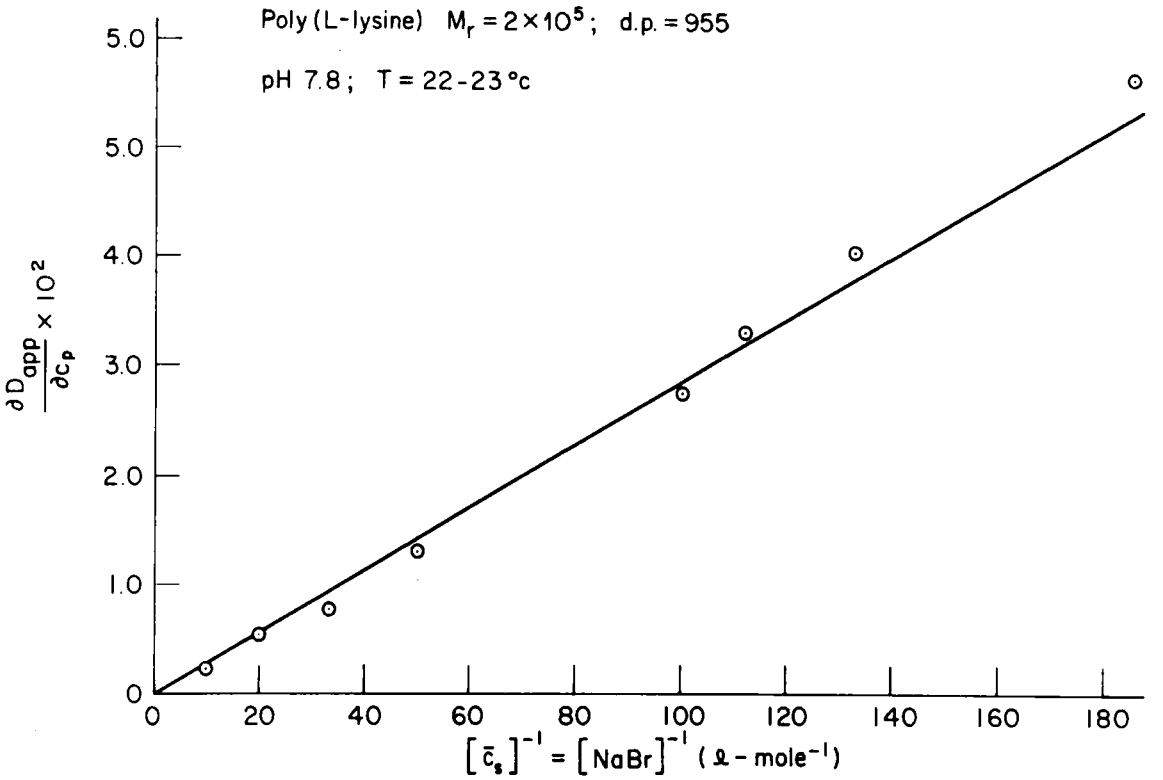

FIGURE 13. Slope $\partial D_{app}/\partial C_p$ vs. $[NaBr]^{-1}$ for poly(L-lysine)·HBr (degree of polymerization 955). The solution pH is 7.8, and T = 22 to 23°C. (From Lin, S.-C., Lee, W. I., and Schurr, J. M., *Biopolymers*, submitted. With permission.)

the same values of $D_{20,w}$. The hydrodynamic radii implied by these observations are 126 ± 2 Å, 113 ± 2 Å, and 98 ± 2 Å for 70 S, 50 S, and 30 S ribosomes, respectively. These values are substantially larger than the equivalent hydrodynamic radii computed for previously proposed ellipsoids.[18,181]

Three possible explanations have been considered: (1) a bound hydration layer extending some 13 to 18 Å into the solution; (2) much higher axial ratios than previously believed; (3) a surface with many deep clefts, giving radii of gyration much smaller than the hydrodynamic radii, which are affected only slightly by the introduction of clefts.[18,181] Other possibilities include partial unravelling and mRNA tails.

Gabler et al.[18] have found that the D-values obtained are preparation dependent. They also observed an apparent expansion of the 70 S ribosomes in the temperature range immediately below the point (near 30°C) where dissociation into subunits takes place. Indeed, calculations using best-fit prolate ellipsoid parameters indicate that subunits expand upon dissociation.[18] Kinetics of long-term changes following Mg^{++} and EDTA addition was also investigated.[18]

Polysaccharides

Translational diffusion coefficients of dextran were studied by Sellen,[303] who found that the data conformed to the empirical relation $D_{20} \cong 2.25 \times 10^{-4}\ M^{-0.45}$. Aggregation in Group C meningococcal polysaccharides has also been studied by dynamic light scattering.[304] Comparatively small values of D and large polydispersity index (i.e., K_2/K_1^2 in Equation 58) indicate the presence of very large aggregates that are, however, not revealed in the sedimentation molecular weights. These data imply that the aggregation is far more extensive than a simple monomer-dimer self-association. In view of the comparatively high concentrations employed, it is also possible that effects of solution congestion, such as induced anisotropic translational diffusion coupled to hindered rotation,[73,123] are making a significant contribution to the observed nonexponential character of the correlation functions.

Tamm-Horsfall Protein

The diffusion coefficient and molecular weight of the Tamm-Horsfall glycoprotein have been determined to be $D_{20,w} = 0.222 \pm 0.002 \times 10^{-7}$ cm^2/sec and $M_w = 14.2 \times 10^6 \pm 3$ to 4%, respectively.[305]

Tubulin

Gethner et al.[306,307] have brought dynamic light-scattering techniques to bear on the tubulin system, perhaps the most difficult problem undertaken to date. An ubiquitous large aggregate with $D \sim 0.5 - 0.6 \times 10^{-7}$ cm^2/sec was found at 4°C independent of whether or not the solution was centrifuged, indicating an equilibrium aggregation process. Raising the temperature to 36°C and recooling to 4°C resulted in the irreversible formation of a new large aggregate with $D \cong 0.74 \times 10^{-7}$ cm^2/sec. Intermediate aggregates were also observed, and a schematic diagram of the various aggregation equilibria in which the tubulin participates in the presence and absence of cholchicine was proposed.

Vesicles

In an elegant experiment, Norisuye et al.[22] isolated bovine photoreceptor membranes from retinal rod outer segments and suspended them in dilute sucrose solution, whereupon they underwent osmotic swelling to give a highly homogeneous suspension of spherical vesicles of 9,800 Å in diameter. In addition to dynamic light-scattering studies of the Stokes radius, static (or elastic) light scattering was employed to establish the narrowness of the distribution, to confirm the Stokes radius, and to verify that the light was scattered from spherical shells, rather than from solid spheres. The foundation is now in place for further studies of the effects of various chemical agents, osmotic pressure, and solution conditions on those membranes.

Lobster sarcoplasmic reticulum vesicles have been studied by Selser et al.[23,25] Both the modified (to incorporate a spherical shell structure factor) Z-average diffusion coefficient and relative dispersion about this value were measured.[23] The time course of the osmotic response of these vesicles, as manifested by changes in the diffusion coefficient, was also studied.[25] Agents employed to increase the osmotic pressure of the outside solution consisted of the nonelectrolytes ethylene glycol, glycerol, erythritol, glucose, and sucrose. Transient initial increases in D persisted in the steady state for erythritol, glucose, and sucrose, but relaxed back essentially to zero for ethylene glycol and glycerol, indicating that the membrane was permeable to these latter smaller molecules but not to the former. On this basis, the pore radii of the membrane were estimated to be 3.1 to 3.5 Å. The variation of the steady-state diffusion coefficient with the external water activity in sucrose and erythritol solutions demonstrated that these vesicles responded faithfully to changes in water activity between 1.00 and 0.98. However, at water activities below 0.98, the vesicle size appeared to remain constant and independent of activity, suggesting that the membrane had been compressed to a rigid limiting area as the radius was decreased by one third, at which point the area was four ninths of its original value in isotonic solution.

Phosphatidyl choline vesicles formed by sonication of aqueous suspensions of the lipid have been studied by dynamic light scattering.[308-310] Substantial polydispersity, including a small amount of very large aggregates, was noted by Chen et al.[308] and by Goll and Stock[310] who modeled the distribution using a linear spline. More recently, Chen et al.[309] have obtained monodisperse vesicle suspensions using Sepharose chromatography. Although stable for a few days, the vesicles were found to aggregate in time. Valinomycin appeared to inhibit vesicle aggregation. Typical diameters of monomeric vesicles ranged from 200 to 500 Å.

Viruses (Tobacco Mosaic Virus)

Translational and rotational motions of tobacco mosaic virus (TMV) have been investigated by dynamic light-scattering techniques on numerous occasions.[3,27-33] Values of the diffusion coefficients obtained in these studies, as well as results obtained by transient electric birefringence (TEB), electric dichroism (ED), and electric field induced light scattering (ELS), are presented in Table 4. The translational diffusion coefficients are in reasonable agreement with each other except for the value of Cummins et al.,[27] which is unaccountably low.

From the minimum concentrations listed, it is apparent that transient electric birefringence is by far the most sensitive technique for studying rotational diffusion and presumably provides the most reliable numbers. The recent value of

TABLE 4

Translational and Rotational Diffusion Coefficients of Tobacco Mosaic Virus

Investigators	Method	$D_{20} \times 10^8$ (cm²/sec)[a]	$D_{R,20}$ (sec^{-1})[a]	c(g/l)	Solvent
Dubin et al.[3]	DLS (pol)	3.5 ± 0.02		0.1	10^{-2} *M* PO_4, pH 7.2
Cummins et al.[27]	DLS (pol)	2.80 ± 0.06	320 ± 18	0.1	10^{-3} *M* PO_4, pH 7.5
Wada et al.[29]	DLS (pol)	3.20	360	≥0.4	10^{-3} *M* PO_4, pH 7.5
Fujime[31]	DLS (pol)	3.41 ± 0.01	390 ± 40	0.5	0.25 *M* Ac, pH 6
			360 ± 20	3.0	0.025 *M* Ac, pH 6
Schaefer et al.[30]	DLS (pol)	3.41 ± 0.01	368	0.2–0.4	10^{-3} *M* EDTA, pH 7.5
King et al.[33]	DLS (pol)	3.4 ± 0.01	355 ± 25	0.175	10^{-3} *M* PO_4, pH 7.5
	DLS (depol)		345 ± 35	0.175	10^{-3} *M* PO_4, pH 7.5
Wada et al.[28]	DLS (depol)		350± 20	1.0	0.1 *M* PO_4, pH 7.5
Schurr and Schmitz[32]	DLS (depol)		317	0.05	distilled H_2O, pH 6
			304	0.05	distilled H_2O, pH 9.1
O'Konski and Haltner[313]	TEB		291 ± 12	0.0022–0.5	10^{-3} *M* PO_4, pH 7.0
Newman and Swinney[311]	TEB		318 ± 3	0.0048–0.48	10^{-3} *M* PO_4, pH 7.5
Jennings and Jerrard[314]	ELS		328	3	Not given
Allen and Van Holde[312]	ED		298	0.08–0.4	≤ 10^{-4} *M* tris-HCl or glycine-NaOH, pH 5.0–9.2

[a]Values corrected to 20,w conditions, except for data of Wada et al.[28]

Newman and Swinney[311] is certainly the most precise and, probably, also the most reliable, unless repeated pulsing in the course of signal-averaging caused some degradation of their sample. Values of the rotational diffusion coefficient obtained by either polarized or depolarized light scattering are significantly larger than those obtained by electro-optic methods, except for the values of Schurr and Schmitz[32] and Cummins et al.[27] In view of the anomalously low value obtained for the corresponding translational diffusion coefficient, the data (and/or sample) of Cummins et al. must be viewed with suspicion. The data of Schurr and Schmitz[32] differ from the others in that their TMV were suspended in distilled water, rather than a buffer of finite ionic strength. Whether differences in D_R are due to solution conditions, to differences in preparations, or to other causes is not known. Allen and Van Holde[312] found that end-to-end dimers, stable near pH 6, dissociated almost completely to monomers upon raising the pH to 8.2 to 9. The samples of O'Konski and Haltner[313] and Schurr and Schmitz[32] exhibited no significant pH dependence of the extent of dimer formation over the same range.

The reliability of the D_R values obtained by dynamic light-scattering methods is not actually so high that the electro-optic values are seriously challenged. Of the investigations using polarized scattered light, only the careful analysis of Schaefer et al.[30] took into account the anisotropy of translational diffusion and its coupling to the orientational part of the correlational function. It was found that a reasonable sign for the anisotropy could be obtained only if an excessively large rotational diffusion coefficient could be assumed. The substantial concentration dependence of D_T observed by King et al.[33] indicates that intermolecular forces, which are expected to be strongly orientation dependent, make a rather substantial contribution to D_T for concentrations above 0.1 g/l. Such orientation-dependent intermolecular forces could well produce unforeseen complications in the analysis of the polarized light data. Analysis of TMV data in terms of the simple Equation 22 above is not sufficient in any case, as noted by Schaefer et al.[30] Thus, D_R values obtained from the polarized scattered light should not be taken too seriously. The zero-angle depolarized scattering experiment, first demonstrated by Wada et al.,[28] leads, in principle, to simpler data analysis, based on Equation 49 with $K^2 = 0$, but is, in practice, a more difficult experiment in the sense that it is much more easily perturbed by defects in the optical elements, vibrations, and fluctuations in both laser polarization and beam direction. The photocurrent spectrum of Wada et al.[28] was obtained at very high concentration (1 g/l), is rather noisy and does not present a well-defined high-frequency baseline. King et al.[33] present no correlation functions, but do explicitly mention experimental difficulties in studying concentrations below 0.175 g/l. The comparatively noise-free correlation functions obtained at lower concentration (0.05 g/l) by Schurr and Schmitz[32] suffer somewhat from the contamination of their samples with significant amounts of end-to-end dimer. Thus, despite the plethora of reported values of D_R, the numbers are simply not as firm as one would like. The value $D_R = 318 \pm 3\ sec^{-1}$ can be employed with the formula of Broersma[209] and a diameter of 150 Å to determine a length of 2925 ± 10 Å, in close agreement with values determined from electron microscopy.[311]

Two principal advantages of light-scattering techniques over electro-optic methods are that no external perturbation of the system, with the inevitable risk of sample degradation, is required and that bending or flexing motions can be observed, if they occur with significant amplitude. A careful search for such rapid bending motions of TMV was carried out, but none were observed.[32] By setting an upper limit of 30° of arc for the root-mean-squared amplitude of bending that could have escaped detection, corresponding to about 7% of the total relaxing amplitude, a lower limit for the Young's modulus of TMV, regarded as a solid rod, could be obtained, $E \geq 2.5 \times 10^7$ dyn/cm^2. TMV is evidently at least as stiff as automobile tire rubber and may well be much stiffer.

Hartford and Flygare[290] have reported light-scattering electrophoretic mobilities of TMV. As for DNA, the mobility was found to be a linear function of ionic strength at low salt and to approach a more nearly constant value at high salt. The values obtained were in agreement with classic moving boundary measurements.

Viruses (T4, T5, T7, λ, R17, QB, PM2, Bushy Stunt Virus, and Vesicular Stomatitis Virus)

Translational diffusion coefficients and mol-

TABLE 5

Experimental Data for Selected Viruses

Virus	$D_{20,w} \times 10^{8}$ [a] (cm^2/sec)	mol $wt_{virus} \times 10^6$	mol $wt_{DNA} \times 10^6$	Ref.
T4	2.95 ± 0.03	192.5 ± 6.6	105.7 ± 3.8	34
T5	3.97 ± 0.04	109.2 ± 4.0	67.3 ± 3.1	34
T7	6.03 ± 0.06	50.4 ± 1.8	25.8 ± 1.0	34
	6.44 ± 0.07	50.9 ± 1.7		36
λ	4.97 ± 0.05			34
R17	15.34 ± 0.15	4.02 ± 0.17		36
Qβ	14.23 ± 0.14	4.55 ± 0.16		36
PM2	6.50 ± 0.07	47.9 ± 1.7		36
BSV[b]	12.46 ± 0.13	8.81 ± 0.17		36
SVS(IND)[c]	2.68 ± 0.10	355 ± 45		35
SVS(NJ)[d]	2.69 ± 0.10	351 ± 45		35
SVST-l[e]	2.97 ± 0.18	252 ± 35		35
SVST-s[f]	3.46 ± 0.14	163 ± 25		35

[a]Diffusion coefficients corrected to 20,w conditions.
[b]Tomato bushy stunt virus.
[c]Indiana serotype vesicular stomatitus virus.
[d]New Jersey serotype vesicular stomatitus virus.
[e]The long defective T-particle (deletion mutant) of SVS(NJ).
[f]The short defective T-particle (deletion mutant) of SVS(NJ).

ecular weights have been determined for a number of viruses,[34-36,167] and the results are given in Table 5. The reader is referred to the original works for solvent conditions, details of the bioassays, and values of the size and shape parameters. Agreement of the size parameters with those determined by other methods, such as X-ray diffraction and electron microscopy, was generally very good, with no need to invoke more than a few Ångströms of bound water at the surface in any case. On the other hand, the computed solvations based on the difference between the partial molecular volume and the hydrodynamic volume were enormous (~1 cm^3 H_2O/g dry virus) and implied that a great deal of interstitial space between the viral subunits, or deep fenestrations of the outer surface, was available for occupation by the solvent.[36] About 52 to 65% of the hydrodynamic volume was occupied by solvent, depending on the virus.

In a novel application of light-scattering methods, Benbasat and Bloomfield[40] have studied the kinetics of attachment of tails to T4D phage heads to form tail-fiberless particles. Kinetics of this reaction was also followed by infectivity assays. After the diffusion coefficients of the predominant scatterers, namely heads and tail-fiberless particles, were determined separately, the correlation function for any mixture could be resolved into the amplitudes of its two main scattering components. Thus, the relative amplitudes could be followed as a function of time over the course of this reaction, which was sufficiently slow because of the tremendous dilutions employed. A bimolecular rate constant at 22°C of 1.02×10^7 M^{-1} sec^{-1} was determined for the association of tails and heads. Infectivity assays at 30°C gave an apparent bimolecular rate constant of 1.28×10^7 M^{-1} sec^{-1}. Under the assumption of diffusion-controlled reaction, adjustment of both rates to 20°C gave 0.97×10^7 and 0.98×10^7 M^{-1} sec^{-1} for the light-scattering and infectivity rate constants, respectively. These results were interpreted in terms of a diffusion controlled reaction with a severe orientational constraint. Employing Equation 3 of recent work by Schurr and Schmitz,[315] a value of $\theta_0 \cong 11°$ can be estimated for the half-cone constraint angle.

The electrophoretic mobilities and diffusion coefficients of whole T4D bacteriophage bearing six tail fibers and its corresponding tail-fiberless particles have been determined by Lim et al.[183] using combined band electrophoresis and dynamic light-scattering techniques. From these data, it was estimated that each tail fiber contributed about 193 positive charges to the phage particle. This

TABLE 6

Experimental Data for RNA Tumor Viruses

Virus	$D_{20,w} \times 10^{8}$ [a] (cm^2/sec)	mol wt × 10^6	d_h(nm)[b]	d_{EM}(nm)[c]
AMV in tris or PO_4 buffer	3.11 ± 0.07	390	138 ± 4	134–143
AMV in buffered sucrose	3.19 ± 0.09		144 ± 3	
MuLV in tris or PO_4 buffer	2.96 ± 0.12	400	145 ± 7	147
MuLV in buffered sucrose	2.78 ± 0.12		154 ± 3	
MuMTV	2.99 ± 0.12	317 ± 32	144 ± 6	147 ± 3
RSV	2.91 ± 0.13	417 ± 42	147 ± 7	139 ± 3
FeLV	2.55 ± 0.09	550 ± 55	168 ± 6	161 ± 5

[a]Diffusion coefficients corrected to 20,w conditions.
[b]Hydrodynamic (or Stokes) diameter.
[c]Electron microscopy diameter.

value was compared with a tail-fiber charge of 327 computed from the amino acid composition.

Viruses (RNA Tumor Viruses)

Translational diffusion coefficients and molecular weights of avian myeloblastosis virus (AMV), murine leukemia virus (MuLV), murine mammary tumor virus (MuMTV), Rous sarcoma virus (RSV), and feline leukemia virus (FeLV) have been determined by dynamic light-scattering and sedimentation methods with the results given in Table 6. Data for AMV and MuLV were reported by Salmeen et al. in Reference 83, and those for MuMTV, RSV, and FeLV were reported in Reference 37. The Stokes hydrodynamic diameters D_h are given, as well as the light-scattering intensity-weighted average values determined from electron micrographs, D_{EL}. The agreement is very good indeed. Again, a comparison of hydrodynamic and partial molecular volumes showed that a very large fraction of the hydrodynamic volume, 57 to 71%, depending on the virus, was occupied by solvent.[37,83]

A novel aspect of the work of Salmeen et al.[83] was their technique of diluting samples into the region where number fluctuations became comparable to those from interference scattering in order to determine the concentrations of virus particles. They estimated the precision of that technique, based on Equation 51, to be ±30%.

Light-scattering electrophoretic mobilities of AMV, MuLV, FeLV, and MuMTV were determined by Rimai et al.[38] At high pH, the mobilities of these viruses were nearly the same, indicating that their surface charge densities were comparable. At low pH, substantial differences in mobilities developed. In the 0.005 *M* ionic strength solutions employed, the Debye screening length was very much smaller than the dimensions of these enormous viruses.[37] Thus, the electrophoretic mobilities were expected to depend not on size or shape, but only upon the surface charge densities.[291] These results have established a firm basis for the subsequent analysis of mixtures containing such viruses by light-scattering electrophoresis techniques.

EFFECTS OF LONG-RANGE IONIC FORCES

Several interesting and dramatic effects have been noted in studies of highly charged macromolecules, as mentioned at various points in the preceding discussion, and it is perhaps worthwhile to summarize them together.

The formation of periodic arrays exhibiting macroscopic long-range order and melting transitions is now well established for large polystyrene latex spheres charged with adsorbed detergent under very low-salt conditions.[16,82] Whether the low-salt extraordinary phase of poly-L-lysine[104,109,299] is also such an ordered phase is still an open question. The linear chain nature of such polymers may also admit the possibility of

mesophases with various degrees of spatial and orientational order. The vanishing scattered intensity from solutions of DNA at 10^{-4} to 10^{-5} *M* ionic strength, as reported by Krasna,[292] is very likely an indication of similar behavior in DNA solutions. The transition to the extraordinary phase has been observed to occur at salt concentrations as high as 0.035 *M* NaBr for only a 6 g/l poly-L-lysine solution.[109] It will be expecially interesting to see whether the transition can be induced at salt concentrations in the physiological range with higher concentrations of polyions. Determinations of both the tracer diffusion coefficient and rotational diffusion coefficient in the extraordinary phase will be of paramount importance in understanding the dynamics of these systems. It should be mentioned that over 20 years ago Kirkwood and Mazur[316] predicted the onset of long-range order in solutions of polyions of sufficiently great charge and concentration at sufficiently low ionic strength.

There have been numerous indications of a dramatic rise in the friction factors of isolated polyions as the salt concentration declined below about 0.03 *M*. In addition to the poly-L-lysine discussed previously,[109] similar increases in friction factor at low salt have been observed for tRNA.[151] Moreover, Schaefer and Berne[317] found that the values of $G(\mathbf{K},0)$ and $D_{app}(\mathbf{K})$ observed for charged, spherical R17 virus at low salt could not be reconciled with Equation 35 unless D_0 was substantially less than the corresponding Stokes-Einstein value found at high salt. The D_{app} observed for BSA fell increasingly further below the values predicted by Equations 40 and 41 with decreasing salt concentration, as noted in Table 1. The latter two observations suggest that even for spherical polyions the friction factors may be markedly enhanced at low ionic strength. Further evidence for a marked rise in the friction factors of charged polyelectrolytes is found in the work of Killmann and Preusser,[318, 319] who observed as much as fivefold increases in friction factors of their charged poly(*N*-vinylpyrrolidone)/Blancophore BA complexes as the salt was decreased from 1.0 to 0.01 *M*. As in the case of poly-L-lysine, such an increase in friction factor appears to be substantially greater than one would predict on hydrodynamic grounds alone, even assuming complete extension of the polyion at 0.01 *M*. This fact together with the apparent observation of similar effects for spherical polyions suggests that these dramatic increases in friction factor may be primarily due to polyion/small-ion interactions, rather than to changes in polyion shape. Finally, it is cautioned that these remarks are in part speculative and that further work will be required to unequivocally establish the validity of this hypothesis.

Despite the dramatic rise in friction factors of these polyelectrolytes at low salt, their apparent diffusion coefficients rise so steeply with increasing polyion concentration that net enhancements by three- to fivefold, or more, of D_{app} are commonplace,[103,109,154,233,239] even at polyion concentrations as low as a few tenths of one percent. Such enhancements of D_{app} with an increasing concentration of mutually repulsive macromolecules are in accord with results of recent general theoretical treatments for two-component solutions[105,144,299] at sufficiently small K values.

As a final point, it is noted that Equation 42 apparently correctly predicts not only the linear variation of D_{app} with $\bar{C}_p$, but also the proportionality of the slope $\partial D_{app}/\partial \bar{C}_p$ with reciprocal salt concentration.[109,150,154] Moreover, there is some suggestion that the corresponding Equation 44 may apply equally well in the absence of salt.[109,150] In view of the remarkable phenomena cited above, the apparent success of the simple linearized model from which these equations were derived must also be regarded as somewhat surprising. A deeper understanding must await future developments.

ACKNOWLEDGMENTS

Thanks are due to virtually all of my colleagues in the field of dynamic light scattering for making available both reprints and preprints of their current work and for bringing to my attention pertinent work of others in the field.

Dynamic light scattering research in my own laboratory has been supported by Grants GP-25551 and PCM 75-23631 from the National Science Foundation.

REFERENCES

1. Ford, N. C. and Benedek, G. B., Observation of the spectrum of light scattered from a pure fluid near its critical point, *Phys. Rev. Lett.*, 15, 649, 1965.
2. Cummins, H. Z., Knable, N., and Yeh, Y., Observation of diffusion broadening of Rayleigh scattered light, *Phys. Rev. Lett.*, 12, 150, 1964.
3. Dubin, S. B., Lunacek, J. H., and Benedek, G. B., Observation of the spectrum of light scattered by solutions of macromolecules, *Proc. Natl. Acad. Sci. U.S.A.*, 57, 165, 1967.
4. Foord, R., Jakeman, E., Oliver, C. J., Pike, E. R., Blagrove, R. J., Wood, E., and Peacocke, A. R., Determination of diffusion coefficients of haemocyanin at low concentration by intensity fluctuation spectroscopy of scattered laser light, *Nature*, 227, 242, 1970.
5. Lin, S. H. C., Dewan, R. K., Bloomfield, V. A., and Morr, C. V., Inelastic light scattering study of the size distribution of bovine milk casein micelles, *Biochemistry*, 10, 4788, 1971.
6. Lin, S. H. C., Leong, S. L., Dewan, R. K., Bloomfield, V. A., and Morr, C. V., Effect of calcium ion on the structure of native bovine casein micelles, *Biochemistry*, 11, 1818, 1972.
7. Dewan, R. K., Chudgar, A., Mead, R. J., Jr., Bloomfield, V. A., and Morr, C. V., Molecular weight and size distribution of bovine milk casein micelles, *Biochim. Biophys. Acta*, 342, 313, 1974.
8. Mazer, N. A., Benedek, G. B., and Carey, M. C., An investigation of the micellar phase of sodium dodecyl sulfate in aqueous sodium chloride using quasielastic light scattering spectroscopy, *J. Phys. Chem.*, 80, 1075, 1976.
9. Tanaka, T., Hocker, L. O., and Benedek, G. B., Spectrum of light scattered from a viscoelastic gel, *J. Chem. Phys.*, 59, 5151, 1973.
10. Geissler, E. and Hecht, A. M., Rayleigh light scattering from concentrated solutions of polystyrene in hexane, *J. Chem. Phys.*, 65, 103, 1976.
11. King, T. A., Knox, A., and McAdam, J. D. G., Polymer dynamics in solutions and gels from Rayleigh light-scattered line widths, *J. Polym. Sci. Polym. Symp.*, 44, 195, 1974.
12. Wun, K. L. and Carlson, F. D., Harmonically bound particle model for quasi-elastic light scattering by gels, *Macromolecules*, 8, 190, 1975.
13. McAdam, J. D. G., King, T. A., and Knox, A., Molecular motion in polymer networks and concentrated solutions from photon correlation spectroscopy, *Chem. Phys. Lett.*, 26, 64, 1974.
14. Munch, J. P., Candau, S., Duplessix, R., Picot, C., Herz, S., and Benoit, H., Spectrum of light scattered from viscoelastic gels, *J. Polym. Sci. Polym. Phys. Ed.*, 14, 1097, 1976.
15. Jamieson, A. M., Simic-Glavaski, B., Tansey, K., and Walton, A. G., Studies of elastin coacervation by quasielastic light scattering, *Discuss. Faraday Soc.*, in press.
16. Schaefer, D. W. and Ackerson, B. J., Melting of colloidal crystals, *Phys. Rev. Lett.*, 35, 1448, 1976.
17. Hocker, L., Krupp, J., Benedek, G. B., and Vournakis, J., Observations of self-aggregation and dissociation of *E. coli* ribosomes by optical mixing spectroscopy, *Biopolymers*, 12, 1677, 1973.
18. Gabler, R., Westhead, E. W., and Ford, N. C., Studies of ribosomal diffusion coefficients using laser light scattering spectroscopy, *Biophys. J.*, 14, 528, 1974.
19. Vournakis, J. and Rich, A., Size changes in eukaryotic ribosomes, *Proc. Natl. Acad. Sci. U.S.A.*, 68, 3021, 1971.
20. Fujime, S., Maruyama, M., and Asakura, S., Flexural rigidity of bacterial flagella studied by quasielastic scattering of laser light, *J. Mol. Biol.*, 68, 347, 1972.
21. Fujime, S., Maruyama, M., and Asakura, S., Spectral distribution of light quasielastically scattered from straight and curved rods, *Macromolecules*, 5, 813, 1972.
22. Norisuye, T., Hoffman, W. F., and Yu, H., Intact photoreceptor membrane from bovine rod outer segment: size and shape in bleached state, *Biochemistry*, 15, 5678, 1976.
23. Selser, J. C., Yeh, Y., and Baskin, R. J., A light scattering characterization of membrane vesicles, *Biophys. J.*, 16, 337, 1976.
24. Selser, J. C. and Yeh, Y., A light scattering method of measuring membrane vesicle number-averaged size and size dispersion, *Biophys. J.*, 16, 847, 1976.
25. Selser, J. C., Yeh, Y., and Baskin, R. J., A light-scattering measurement of membrane vesicle permeability, *Biophys. J.*, submitted.
26. Dubin, S. B., Quasielastic Light Scattering from Macromolecules, Ph.D. thesis, Massachusetts Institute of Technology, Cambridge, Mass., 1970.
27. Cummins, H. Z., Carlson, F. D., Herbert, T. J., and Woods, G., Translational and rotational diffusion coefficients of tobacco mosaic virus from Rayleigh linewidths, *Biophys. J.*, 9, 518, 1969.
28. Wada, A., Suda, N., Tsuda, T., and Soda, K., Rotatory-diffusion broadening of Rayleigh lines scattered from optically anisotropic macromolecules in solution, *J. Chem. Phys.*, 50, 31, 1969.
29. Wada, A., Ford, N. C., and Karascz, F. E., Rotational diffusion of tobacco mosaic virus, *J. Chem. Phys.*, 55, 1798, 1971.
30. Schaefer, D. W., Benedek, G. B ., Schofield, P., and Bradford, E., Spectrum of light scattered quasielastically from tobacco mosaic virus, *J. Chem. Phys.*, 55, 3884, 1971.
31. Fujime, S., Quasi-elastic light scattering from solutions of macromolecules. I. Doppler broadening of light scattered from solutions of tobacco mosaic virus particles, *J. Phys. Soc. Jpn.*, 29, 416, 1970.

32. Schurr, J. M. and Schmitz, K. D., Rotational relaxation of macromolecules determined by dynamic light scattering. I. Tobacco mosaic virus, *Biopolymers*, 12, 1021, 1973.
33. King, T. A., Knox, A., and McAdam, J. D. G., Translational and rotational diffusion of tobacco mosaic virus from polarized and depolarized light scattering, *Biopolymers*, 12, 1917, 1973.
34. Dubin, S. B., Benedek, G. B., Bancroft, F. C., and Freifelder, D., Molecular weights of coliphages and coliphage DNA. II. Measurements of diffusion coefficients using optical mixing spectroscopy and measurement of sedimentation coefficients, *J. Mol. Biol.*, 54, 547, 1971.
35. Hartford, S. L., Lesnaw, J. A., Flygare, W. H., McLeod, R., and Reichman, M. E., Physical properties of New Jersey serotype of vesicular stomatitis virus and its defective particles, *Proc. Natl. Acad. Sci. U.S.A.*, 72, 1202, 1975.
36. Camerini-Otero, R. D., Pusey, P. N., Koppel, D. E., Schaefer, D. W., and Franklin, R. M., Intensity fluctuation spectroscopy of laser light scattered by solutions of spherical viruses: R17, Qβ, BSV, PM2 and T7. II. Diffusion coefficients, molecular weights, solvation, and particle dimensions, *Biochemistry*, 13, 960, 1974.
37. Salmeen, I., Rimai, L., Luftig, R. B., Liebes, L., Retzel, E., Rich, M., and McCormick, J. J., Hydrodynamic diameters of murine mammary, Rous sarcoma, and feline leukemia RNA tumor viruses: studies by laser beat frequency light-scattering spectroscopy and electron microscopy, *J. Virol.*, 17, 584, 1976.
38. Rimai, L., Salmeen, I., Hart, D., Liebes, L., and Rich, M. A., Electrophoretic mobilities of RNA tumor viruses. Studies by Doppler-shifted light scattering spectroscopy, *Biochemistry*, 14, 4621, 1975.
39. Pike, E. R., The accuracy of diffusion-constant measurements by digital autocorrelation of photon-counting fluctuations, *J. Phys. (Paris) Suppl.*, 33-Cl, 177, 1972.
40. Benbasat, J. A. and Bloomfield, V. A., Joining of bacteriophage T4D heads and tails: A kinetic study by inelastic light scattering, *J. Mol. Biol.*, 95, 335, 1975.
41. Nossal, R., Chen, S. H., and Lai, C. C., Use of laser light scattering for quantitative determinations of bacterial motility, *Opt. Commun.*, 1, 35, 1971.
42. DuBois, M., Jouannet, P., Berge, P., and David, G., Spermatazoa motility in human cervical mucous, *Nature*, 252, 711, 1975.
43. Nossal, R. and Chen, S. H., Effects of chemoattractants on the motility of *E. coli*, *Nature (London) New Biol.*, 244, 254, 1973.
44. Nossal, R. and Chen, S. H., Light scattering from motile microorganisms, *J. Phys. (Paris) Suppl.*, 33 Cl, 171, 1972.
45. Schaefer, D. W., Banks, G., and Alpert, S. S., Intensity fluctuation spectroscopy of motile microorganisms, *Nature*, 248, 162, 1974.
46. Banks, G., Schaefer, D. W., and Alpert, S. S., Light-scattering study of the temperature dependence of *E. coli* motility, *Biophys. J.*, 15, 253, 1975.
47. Schaefer, D. W. and Berne, B. J., Number fluctuation spectroscopy of motile microorganisms, *Biophys. J.*, 15, 785, 1975.
48. Lee, W. I. and Verdugo, P., Laser light scattering spectroscopy: a new application in the study of ciliary activity, *Biophys. J.*, 16, 1115, 1976.
49. Bonner, R. F. and Carlson, F. D., Structural dynamics of frog muscle during isometric contraction, *J. Gen. Physiol.*, 65, 633, 1975.
50. Carlson, F. D., Structural fluctuations in steady-state of muscular contraction, *Biophys. J.*, 15, 633, 1975.
51. Fujime, S., Optical diffraction and scattering studies of muscle fibers, in press.
52. Newton, S. A., Ford, N. C., Jr., Langley, K. H., and Sattelle, D. B., Laser light scattering analysis of protoplasmic streaming in the slime mold *Physarum polycephalum*, *Biochim. Biophys. Acta*, submitted.
53. Langley, K. H., Piddington, R. W., Ross, D., and Sattelle, D. B., Photon correlation analysis of cytoplasmic streaming, *Biochim. Biophys. Acta*, 444, 893, 1976.
54. Mustacich, R. V. and Ware, B. R., Observation of protoplasmic streaming by laser light scattering, *Phys. Rev. Lett.*, 33, 617, 1974.
55. Pike, E. R., The theory of light scattering, in *Photon Correlation and Light Beating Spectroscopy*, Cummins, H. Z. and Pike, E. R., Eds., Plenum Press, New York, 1974, 3.
56. Cummins, H. Z., Applications of light beating spectroscopy to biology, in *Photon Correlation and Light Beating Spectroscopy*, Cummins, H. Z. and Pike, E. R., Eds., Plenum Press, New York, 1974, 285.
57. Pusey, P. N., Macromolecular diffusion, in *Photon Correlation and Light Beating Spectroscopy*, Cummins, H. Z. and Pike, E. R., Eds., Plenum Press, New York, 1974, 387.
58. Schaefer, D. W., Applications of photon statistics and photon correlation, in *Laser Applications to Optics and Spectroscopy*, Jacobs, S. F., Scully, M. O., Sargent, M., III, and Scott, J. F., Eds., Addison-Wesley, Reading, Mass., 1975, 197.
59. Ware, B. R., Electrophoretic light scattering, *Adv. Colloid Interface Sci.*, 4, 1, 1974.
60. Flygare, W. H., Hartford, S. L., and Ware, B. R., Electrophoretic light scattering, in *Molecular Electro-optics*, O'Konski, C. T., Ed., Marcel Dekker, New York, chap. 6.
61. Shepherd, I. W., Inelastic laser light scattering from synthetic and biological polymers, *Rep. Prog. Phys.*, 8, 565, 1975.
62. Pusey, P. N. and Vaughan, J. M., Light scattering and intensity fluctuation spectroscopy, in *Dielectric and Related Molecular Processes*, Vol. 2, Davies, M., Ed., The Chemical Society, London, 1975, 48.

63. Berne, B. J. and Pecora, R., Laser light scattering from liquids, *Annu. Rev. Phys. Chem.*, 25, 233, 1974.
64. Chen, S. H. and Holz, M., Medical application of photon correlation spectroscopy, *Med. Res. Eng.*, in press.
65. Chen, S. H. and Nurmikko, A. V., Photon correlation spectroscopy in biology, in *Spectroscopy in Biology and Chemistry – Neutrons, Lasers, and X-rays*, Chen, S. H. and Yip, S., Eds., Academic Press, London, 1975, 377.
66. Pecora, R., Quasi-elastic light scattering from macromolecules, *Annu. Rev. Biophys. Bioeng.*, 1, 259, 1972.
67. Dubin, S. B., Measurement of translational and rotational diffusion coefficients by laser light scattering, in *Methods in Enzymology, Enzyme Structure II*, Vol. 26C, Hirs, C. H. W. and Timasheff, S. N., Eds., Academic Press, New York, 1972, chap. 7.
68. Fujime, S., Quasi-elastic scattering of laser light: a new tool for the dynamic study of biological macromolecules, *Adv. Biophys.*, 3, 1, 1972.
69. Pusey, P. N., Measurement of diffusion coefficients of polydisperse solutes by intensity fluctuation spectroscopy, in *Industrial Polymers: Characterization by Molecular Weight*, Green, J. H. S. and Dietz, R., Eds., Transcripta Books, London, 1973, 26.
70. Ford, N. C., Jr., Gabler, R., and Karascz, F. E., Self-beat spectroscopy and molecular weight, *Adv. Chem. Ser.*, 125, 25, 1973.
71. Ford, N. C., Jr., Biochemical applications of laser Rayleigh scattering, *Chem. Scr.*, 2, 193, 1972.
72. Jamieson, A. M. and Maret, A. M., Quasielastic laser light scattering, *Chem. Soc. Rev.*, 2, 325, 1973.
73. Schurr, J. M., Relaxation of rotational and internal modes of macromolecules determined by dynamic light scattering, *Q. Rev. Biophys.*, 9, 109, 1976; presented in lecture at Symposium on Macromolecular Dynamics, 5th Int. Biophysics Congr., Copenhagen, August 1975.
74. Berne, B. J. and Pecora, R., *Dynamic Light Scattering*, Interscience, New York, 1974.
75. Chu, B., *Laser Light Scattering*, Academic Press, New York, 1974.
76. Jakeman, E., Pusey, P. N., and Vaughan, J. M., Intensity fluctuation spectroscopy using a conventional light source, *Opt. Commun.*, 17, 305, 1976.
77. Jones, C. R. and Johnson, C. S., Photon correlation spectroscopy using a jet stream dye laser, *J. Chem. Phys.*, 65, 2020, 1976.
78. Raman, C. V., *Lectures on Physical Optics, Part I*, Indian Academy of Sciences, Bangalore, 1959, 160.
79. Mathews, J. and Walker, R. L., *Mathematical Methods of Physics*, W. A. Benjamin, New York, 1965, 108.
80. Tartaglia, P. and Chen, S. H., Intensity correlation of light scattered from hydrodynamic fluctuations, *J. Chem. Phys.*, 58, 4389, 1973.
81. Cummins, H. Z. and Swinney, H. L., Light beating spectroscopy, in *Progress in Optics*, Vol. 8, Wolf, E., Ed., North-Holland, Amsterdam, 1970, 135.
82. Williams, R. and Crandall, R. S., The structure of crystallized suspensions of polystyrene spheres, *Phys. Lett. A*, 48, 224, 1974.
83. Salmeen, I., Rimai, L., Liebes, L., Rich, M. A., and McCormick, J. J., Hydrodynamic diameters of RNA tumor viruses. Studies by laser beat frequency light scattering spectroscopy of Avian myeloblastosis and Rauscher murine leukemia viruses, *Biochemistry*, 14, 134, 1975.
84. Yeh, Y. and Cummins, H. Z., Localized fluid flow measurements with an He-Ne laser spectrometer, *Appl. Phys. Lett.*, 4, 176, 1964.
85. Ware, B. R. and Flygare, W. H., The simultaneous measurement of the electrophoretic mobility and diffusion coefficient in bovine serum albumin solutions by light scattering, *Chem. Phys. Lett.*, 12, 81, 1971.
86. Uzgiris, E. E., Laser Doppler spectrometer for study of electrokinetic phenomena, *Rev. Sci. Instrum.*, 45, 74, 1974.
87. Blum, L. and Salsburg, Z. W., Light scattering from a chemically reactive fluid. I. Spectral distribution, *J. Chem. Phys.*, 48, 2292, 1968.
88. Berne, B. J., Deutch, J. M., Hynes, J. T., and Frisch, H. L., Light scattering from chemically reactive mixtures, *J. Phys. Chem.*, 49, 2864, 1968.
89. Schurr, J. M., Theory of quasielastic light scattering from chemically reactive ionic solutions, *J. Chem. Phys.*, 73, 2820, 1969.
90. Blum, L. and Salsburg, Z. W., Light scattering from chemically reactive fluids. II. Case with diffusion, *J. Chem. Phys.*, 50, 1654, 1969.
91. Blum, L., Light scattering from reactive fluids. III. Intensity calculation, *J. Chem. Phys.*, 48, 5024, 1969.
92. Berne, B. J. and Pecora, R., Light scattering as a probe of fast-reaction kinetics: the depolarized spectrum of scattered light from a chemically reacting medium, *J. Chem. Phys.*, 50, 783, 1969.
93. Weinberg, M. and Kapral, R., Light scattering from chemically reacting fluids: coupled chemical reactions, *J. Chem. Phys.*, 53, 4409, 1970.
94. Knirk, D. L. and Salsburg, Z. W., Light scattering from chemically reactive fluids. IV. Intensity calculations for the Eulerian fluid with one reaction, *J. Chem. Phys.*, 54, 1251, 1971.
95. Bloomfield, V. A. and Benbasat, J. A., Inelastic light scattering studies of macromolecular reaction kinetics. I. The reactions $A \rightleftharpoons B$ and $2A \rightleftharpoons A_2$, *Macromolecules*, 4, 609, 1971.
95a. Marshall, A. G. and Pecora, R., Depolarized scattering from a helix-coil system, *J. Chem. Phys.*, 55, 1245, 1971.
96. Benbasat, J. A. and Bloomfield, V. A., Inelastic light scattering study of macromolecular reaction kinetics. II. The reaction $A + B \rightleftharpoons C$, *Macromolecules*, 6, 593, 1973.

97. Fujime, S., Spectrum of light quasielastically scattered from coupled reaction systems of macromolecules, *Macromolecules*, 6, 361, 1973; corrections in *Macromolecules*, 7, 148, 1973.
98. McQueen, D. H. and Hermans, J. J., Determination of the translational diffusivity of detergent micelles from the spectrum of scattered light, *J. Colloid Interface Sci.*, 39, 389, 1972.
99. Berne, B. J. and Giniger, R., Electrophoretic light scattering as a probe of reaction kinetics, *Biopolymers*, 12, 1161, 1973.
100. Lekkerker, H. N. W. and Laidlaw, W. G., The effect of a chemical reaction on the damping of the hydrodynamic modes and the spectrum of scattered light, *Phys. Chem. Liq.*, 3, 225, 1972.
101. Lekkerker, H. N. W. and Laidlaw, W. G., Spectral analysis of the light scattered from a chemically relaxing fluid binary mixture, *Phys. Rev. A*, 9, 346, 1974.
102. Stephen, M. J., Spectrum of light scattered from charged macromolecules in solution, *J. Chem. Phys.*, 55, 3878, 1971.
103. Doherty, P. and Benedek, G. B., The effect of electric charge on diffusion of macromolecules, *J. Chem. Phys.*, 61, 5426, 1974.
104. Lee, W. I. and Schurr, J. M., Laser light-scattering studies of Poly-L-lysine HBr in aqueous solutions, *J. Polym. Sci. Polym. Phys. Ed.*, 13, 873, 1975.
105. Phillies, G. D. J., Effects of intermacromolecular interactions on diffusion. I. Two-component solutions, *J. Chem. Phys.*, 60, 976, 1974.
106. Phillies, G. D. J., Effects of intermacromolecular interactions on diffusion. II. Three-component solutions, *J. Chem. Phys.*, 60, 983, 1974.
107. Phillies, G. D. J., Effects of intermacromolecular interactions on diffusion. III. Electrophoresis in 3-component solutions, *J. Chem. Phys.*, 59, 2613, 1973.
108. Phillies, G. D. J., Contribution of slow charge fluctuations to light scattering from a monodisperse solution of scattered light, *Macromolecules*, 9, 447, 1976.
109. Lin, S.-C., Lee, W. I., and Schurr, J. M., Brownian motion of highly charged Poly (L-lysine). Effects of salt and polyion concentration, *Biopolymers*, submitted.
110. Pecora, R., Doppler shifts in light scattering. II. Flexible polymer molecules, *J. Chem. Phys.*, 43, 1562, 1965.
111. Pecora, R., Spectral distribution of light scattered from flexible-coil macromolecules, *J. Chem. Phys.*, 49, 1032, 1968.
112. DuBois-Violette, E. and deGennes, P.-G., Quasi-elastic light scattering by dilute ideal polymer solutions. II. Effects of hydrodynamic interactions, *Physics*, 3, 181, 1967.
113. deGennes, P.-G., Quasi-elastic scattering of neutrons by dilute polymer solutions. I. Free-draining limit, *Physics*, 3, 37, 1967.
114. Saito, N. and Ito, S., Rayleigh linewidth of the light scattered from flexible polymers in solution, *J. Phys. Soc. Jpn.*, 25, 1446, 1968.
115. Silbey, R. and Deutch, J. M., Quasielastic light scattering from large macromolecules, *J. Chem. Phys.*, 57, 5010, 1972.
116. Ono, K. and Okano, K., Spectral distribution of the light scattered from dilute solutions of optically anisotropic flexible macromolecules (forward scattering), *Jpn. J. Appl. Phys.*, 9, 1356, 1970.
117. Fujime, S., Quasi-elastic light scattering from solutions of macromolecules. III. Detectability of internal modes of motion, *J. Phys. Soc. Jpn.*, 31, 1805, 1971.
118. Fujime, S. and Maruyama, M., Spectrum of light quasi-elastically scattered from linear macromolecules, *Macromolecules*, 6, 237, 1973.
119. Pusey, P. N., The dynamics of interacting Brownian particles, *J. Phys. A Math Nucl. Gen.*, 8, 1433, 1975.
120. Ackerson, B. J., Correlations for interacting Brownian particles, *J. Chem. Phys.*, 64, 242, 1976.
121. Pecora, R., Doppler shifts in light scattering from pure liquids and polymer solutions, *J. Chem. Phys.*, 40, 1604, 1964.
122. Pecora, R., Spectral distribution of light scattered from monodisperse rigid rods, *J. Chem. Phys.*, 48, 4126, 1968.
123. Lee, W. I., Schmitz, K. S., Lin, S.-C., and Schurr, J. M., Dynamic light scattering studies of DNA. I. The coupling of internal modes with anisotropic translational diffusion in congested solutions, *Biopolymers*, 16, 583, 1977.
124. Maeda, H. and Saito, N., Spectral distribution of the light scattered from rod-like macromolecules in solution, *J. Phys. Soc. Jpn.*, 27, 984, 1969.
125. Schmidt, R. L., Observation of the internal motion in N1-DNA, *Biopolymers*, 12, 1427, 1973.
126. Schmitz, K. S. and Schurr, J. M., Rotational relaxation of macromolecules determined by dynamic light scattering. II. Temperature dependence for DNA, *Biopolymers*, 12, 1543, 1973.
127. Schmitz, K. S. and Pecora, R., Quasi-elastic light scattering by calf-thymus DNA and λDNA, *Biopolymers*, 14, 521, 1975.
128. Schmidt, R. L., Boyle, J. A., and Mayo, J. A., Intensity fluctuation spectroscopy of Deoxyribonucleic Acid (DNA). I. Temperature profile of bacteriophage N1-DNA, *Biopolymers*, 16, 317, 1977.
129. Schmidt, R. L., Whitehorn, M. A., and Mayo, J. A., Intensity fluctuation spectroscopy of Deoxyribonucleic Acid (DNA). II. Temperature profile of bacteriophage φ29-DNA, *Biopolymers*, 16, 327, 1977.
130. Maeda, T. and Fujime, S., Quasi-elastic light scattering from muscle F-actin, in press.

131. Zimm, B. H., Dynamics of polymer molecules in dilute solution: viscoelasticity, flow birefringence, and dielectric loss, *J. Chem. Phys.*, 24, 269, 1956.
132. Schurr, J. M., Relaxation times manifested by the Rouse-Zimm model in dynamic light scattering experiments, *Biopolymers*, 16, 461, 1977.
133. Lin, S.-C. and Schurr, J. M., Dynamic light scattering studies of internal motions in DNA. I. Applicability of the Rouse-Zimm model, *Biopolymers*, in press.
134. Wang, M. C. and Uhlenbeck, G. E., On the theory of Brownian motion II, *Rev. Mod. Phys.*, 15, 323, 1945.
135. Uhlenbeck, G. E. and Ornstein, L. S., On the theory of Brownian motion, *Phys. Rev.*, 36, 823, 1930.
136. Ferry, J. D., *Viscoelastic Properties of Polymers*, John Wiley & Sons, New York, 1961.
137. Jolly, D. and Eisenberg, H., Photon correlation spectroscopy, total intensity light scattering with laser radiation, and hydrodynamic studies of a well-fractionated DNA sample, *Biopolymers*, 15, 61, 1975.
138. Perico, A., Piaggio, P., and Cuniberti, C., Dynamics of chain molecules. II. Spectral distribution of the light scattered from flexible macromolecules, *J. Chem. Phys.*, 62, 2690, 1975.
139. Saleh, B. E. and Hendrix, J., The correlation function profile of light scattered from polydisperse large random coil macromolecules in dilute solutions, *Chem. Phys.*, 12, 25, 1976.
140. Lee, W. I. and Schurr, J. M., Intensity autocorrelation function for a flexible polymer, *Chem. Phys. Lett.*, 23, 603, 1973.
141. Hendrix, J., Saleh, B., Gnaedig, K., and DeMaeyer, L., Measurement of the intramolecular fluctuations of random coil polymers by photon correlation spectroscopy, *Polymer*, 18, 10, 1977.
141a. Bloomfield, V. A., Polymer normal mode analysis by inelastic light scattering, *Macromolecules*, 7, 846, 1974.
141b. Schmitz, K. S., Quasi-elastic light-scattering by flexible polymers in the presence of a sinusoidal driving field: internal relaxation modes, *Chem. Phys. Lett.*, 42, 137, 1976.
141c. Schurr, J. M. and Schmitz, K. S., unpublished calculations.
142. Harris, R. A. and Hearst, J. E., On polymer dynamics, *J. Chem. Phys.*, 44, 2595, 1966.
143. Carlson, F. D. and Fraser, A. B., Dynamics of F-actin and F-actin complexes, *J. Mol. Biol.*, 89, 273, 1974.
143a. Carlson, F. D., Letter to the editor, *J. Mol. Biol.*, 95, 139, 1975.
144. Allison, S. A. and Schurr, J. M., unpublished theory.
145. Uzgiris, E. E. and Golibersuch, D. C., Excess scattered-light intensity fluctuations from hemoglobin, *Phys. Rev. Lett.*, 32, 37, 1974.
146. Haas, D. D., Mustacich, R. V., Smith, B. A., and Ware, B. R., Angular dependence of light-scattering linewidths from hemoglobin solutions, *Biochem. Biophys. Res. Commun.*, 59, 174, 1974.
147. Bauer, D. R., Hudson, B., and Pecora, R., Resonance enhanced depolarized Rayleigh scattering from diphenylpolyenes, *J. Chem. Phys.*, 63, 588, 1975.
148. Onsager, L. and Fuoss, R., Irreversible processes in electrolytes. Diffusion, conductance, and viscous flow in arbitrary mixtures of strong electrolytes, *J. Phys. Chem.*, 36, 2689, 1932.
149. Schurr, J. M., Dielectric dispersion of linear polyelectrolytes, *Biopolymers*, 10, 1371, 1971.
149a. Oosawa, F., Field fluctuation in ionic solutions and its biological significance, *J. Theor. Biol.*, 39, 373, 1973.
150. Alexandrowicz, Z. and Daniel, E., Sedimentation and diffusion of polyelectrolytes. I. Theoretical description, *Biopolymers*, 1, 447, 1963.
151. Olson, T., Fournier, M. J., Langley, K. H., and Ford, N. C., Detection of a major conformational change in transfer Ribonucleic Acid by laser light scattering, *J. Mol. Biol.*, 102, 193, 1976.
152. Tanford, C., *Physical Chemistry of Macromolecules*, John Wiley & Sons, New York, 1961, chap. 5.
153. Kedem, O. and Katchalski, A., Diffusion of polyelectrolytes in salt-free solutions, *J. Polym. Sci.*, 15, 321, 1955.
154. Daniel, E. and Alexandrowicz, Z., Sedimentation and diffusion of polyelectrolytes. II. Experimental studies with poly-L-lysine hydrochlorides, *Biopolymers*, 1, 473, 1963.
155. Ermak, D. L. and Yeh, Y., Equilibrium electrostatic effects on the behavior of polyions in solution: polyion – mobile ion interaction, *Chem. Phys. Lett.*, 24, 243, 1974.
156. Ermak, D. L., A computer simulation of charged particles in solution. I. Technique and equilibrium properties, *J. Chem. Phys.*, 62, 4189, 1975.
157. Ermak, D. L., A computer simulation of charged particles in solution. II. Polyion diffusion coefficient, *J. Chem. Phys.*, 62, 4197, 1975.
158. Varoqui, R. and Schmitt, A., Limiting sedimentation and diffusion coefficients of polyelectrolytes. The charge effect, *Biopolymers*, 11, 1119, 1972.
159. Pecora, R., Spectrum of light scattered from optically anisotropic macromolecules, *J. Chem. Phys.*, 49, 1032, 1968.
160. Favro, L. D., Theory of rotational Brownian motion of a free rigid body, *Phys. Rev.*, 119, 53, 1960.
161. Bauer, D. R., Alms, G. R., Brauman, J. I., and Pecora, R., Depolarized Rayleigh scattering and ^{13}C NMR studies of anisotropic molecular reorientation of aromatic compounds in solution, *J. Chem. Phys.*, 61, 2255, 1974.
162. Ford, N. C., Lee, W., and Karascz, F. E., Light scattering by Poly-α-amino acid solutions, *J. Chem. Phys.*, 50, 3098, 1969.
163. Jakeman, E. and Pike, E. R., Spectrum of clipped photon-counting fluctuations of Gaussian light, *J. Phys. A Math. Nucl. Gen.*, 2, 411, 1969.

164. Koppel, D. E., Analysis of Gaussian light by clipped-count autocorrelation: the effect of finite sampling times and incomplete spatial coherence, *J. Appl. Phys.*, 42, 3216, 1971.
165. Tartaglia, P. and Chen, S. H., The spatial coherence factor in light scattering from a system of independent particles, *Opt. Commun.*, 7, 379, 1973.
166. Chen, S. H., Veldkamp, W. B., and Lai, C. C., Simple digital clipped correlator for photon correlation spectroscopy, *Rev. Sci. Instrum.*, 46, 1356, 1975.
167. Pusey, P. N., Koppel, D. E., Schaefer, D. W., Camerini-Otero, R. D., and Koenig, S. H., Intensity fluctuation spectroscopy of laser light scattered by solutions of spherical viruses: R17, Qβ, BSV, PM2, and T7. I. Light scattering technique, *Biochemistry*, 13, 952, 1974.
168. Mandel, L., Correlation properties of light scattered from fluids, *Phys. Rev.*, 181, 75, 1969.
169. Asch, R. and Ford, N. C., Jr., Design of an ideal digital correlation computer, *Rev. Sci. Instrum.*, 44, 506, 1973.
170. Ford, N. C., personal communication, 1977.
171. Tartaglia, P., Postol, T. A., and Chen, S. H., Correlation of scaled photon-counting fluctuation. Comment, *J. Phys. A Math Nucl. Gen.*, 6, L35, 1973.
172. Jakeman, E., Oliver, C. J., Pike, E. R., and Pusey, P. N., Correlation of scaled photon-counting fluctuations, *J. Phys. A Math. Nucl. Gen.*, 5, L93, 1972.
173. Hallett, F. R., Gray, A. L., Rybakowski, A., Hunt, J. L., and Stevens, J. R., Photon correlation spectroscopy using a PDP-9 computer, *Can. J. Phys.*, 50, 2368, 1972.
174. Lee, W. I. and Schurr, J. M., Dynamic light scattering studies of poly-L-lysine HBr in the presence of added salt, *Biopolymers*, 13, 903, 1974; erratum, *Biopolymers*, 13, 1513, 1974.
175. King, T. A. and Lee, W. I., Spectral analysis by analogue time correlation of light scattered from macromolecule solutions, *J. Phys. E*, 5, 1091, 1972.
176. Soda, K., Nishio, I., and Wada, A., Analysis of noises in photocurrent time-correlation spectroscopy of scattered light, *J. Appl. Phys.*, 47, 729, 1976.
177. Jones, R., Oliver, C. J., and Pike, E. R., Experimental and theoretical comparison of photon-counting and current measurements of light intensity, *Appl. Opt.*, 10, 1673, 1971.
178. Cannell, D. S. and Dubin, S. B., Differential light scattering technique for the study of conformational changes in macromolecules, *Rev. Sci. Instrum.*, 46, 706, 1975.
179. Dubin, S. B. and Cannell, D. S., The effect of succinate on the translational diffusion coefficient of aspartate transcarbamylase, *Biochemistry*, 14, 192, 1975.
180. Alon, Y. and Hochberg, A., Improving light beating experiments by dust discrimination, *Rev. Sci. Instrum.*, 46, 388, 1975.
181. Koppel, D. E., Study of *E. coli* ribosomes by intensity fluctuation spectroscopy of scattered laser light, *Biochemistry*, 13, 2712, 1974.
182. Loewenstein, M. A. and Birnboim, M. H., A method for measuring sedimentation and diffusion of macromolecules in capillary tubes by total intensity and quasi-elastic light-scattering techniques, *Biopolymers*, 14, 419, 1975.
183. Lim, T. K., Baran, G. J., and Bloomfield, V. A., Measurement of diffusion coefficient and electrophoretic mobility with a quasi-elastic light-scattering band electrophoresis apparatus, *Biopolymers*, 16, 1473, 1977.
184. Josefowicz, J. and Hallett, F. R., Homodyne electrophoretic light scattering of polystyrene spheres by laser cross-beam intensity correlation, *Appl. Opt.*, 14, 740, 1975.
185. Bauer, D. R., Opella, S. J., Nelson, D. J., and Pecora, R., Depolarized light-scattering and carbon nuclear resonance measurements of the isotropic rotational correlation time of muscle calcium binding protein, *J. Am. Chem. Soc.*, 97, 2580, 1975.
186. Isenberg, I., Dyson, R. D., and Hanson, R., Analysis of fluorescence decay data by the method of moments, *Biophys. J.*, 13, 1090, 1973.
187. McAdam, J. G. and King, T. A., Polymer dynamics in solution from Rayleigh line profile spectroscopy, *Chem. Phys.*, 6, 109, 1974.
188. Newman, J., Swinney, H. L., Berkowitz, S., and Day, L. A., Hydrodynamic properties and molecular weight of fd bacteriophage DNA, *Biochemistry*, 13, 4382, 1974.
189. Chen, F. C., Yeh, A., and Chu, B., Dynamics of calf thymus DNA by single-clipped photon correlation, *J. Chem. Phys.*, 66, 1290, 1976.
190. Brown, J. C., Pusey, P. N., and Dietz, R., Photon correlation study of polydisperse samples of polystyrene in cyclohexane, *J. Chem. Phys.*, 62, 1136, 1975.
191. Chen, F. C., Chrzesczyk, A., and Chu, B., Quasielastic laser light scattering of phosphatidylcholine vesicles, *J. Chem. Phys.*, 64, 3403, 1976.
192. Caloin, M., Wilhelm, B., and Daune, M., Quasi-elastic light scattering: effect of ionic strength upon the internal dynamics of DNA, *Biopolymers*, in press.
193. Provencher, S. W., A fourier method for the analysis of exponential decay curves, *Biophys. J.*, 16, 27, 1976.
194. Provencher, S. W., An eigenfunction expansion method for the analysis of exponential decay curves, *J. Chem. Phys.*, 64, 2772, 1976.
195. Lee, S. P. and Chu, B., Least-squares integration method in intensity fluctuation spectroscopy of macromolecular solutions with bimodal distributions, *Appl. Phys. Lett.*, 24, 261, 1974.

196. Bargeron, C. B., Analysis of intensity correlation spectra of mixtures of polystyrene latex spheres: a comparison of direct least squares fitting with the method of cumulants, *J. Chem. Phys.*, 60, 2516, 1974.
197. Koppel, D. E., Analysis of macromolecular dispersity in intensity correlation spectroscopy: the method of cumulants, *J. Chem. Phys.*, 57, 4814, 1972.
198. Bargeron, C. B., Measurement of a continuous distribution of spherical particles by intensity fluctuation spectroscopy. Analysis by cumulants, *J. Chem. Phys.*, 61, 2134, 1974.
199. Brown, J. C., Pusey, P. N., and Dietz, R., Photon-correlation study of polydisperse samples of polystyrene in cyclohexane, *J. Chem. Phys.*, 62, 1136, 1975.
200. Aragon, S. R. and Pecora, R., Theory of dynamic light scattering from polydisperse systems, *J. Chem. Phys.*, 64, 2395, 1976.
201. Huang, W.-N., Vrancken, E., and Frederick, J. E., Comparison of effects of polydispersity on the Rayleigh line width as determined by homodyning and heterodyning spectrometry, *Macromolecules*, 6, 58, 1973.
202. Benbasat, J. A. and Bloomfield, V. A., Spectrum of light scattering from polydisperse polymer solutions, *J. Polym. Sci.*, 10, 2475, 1972.
203. Raczek, J. and Meyerhoff, G., Streufunktionen polymolekularer Substanzen bei der inelastischen Lichtstreuung, *Makromol. Chem.*, 177, 1199, 1976.
204. Brehm, G. A. and Bloomfield, V. A., Analysis of polydispersity in polymer solutions by inelastic laser light scattering, *Macromolecules*, 8, 663, 1975.
205. Benoit, H., Freund, L., and Spach, G., Dilute solutions of polypeptides: light scattering and hydrodynamics, in *Poly-α-Amino Acids: Protein Models for Conformational Studies*, Fasman, G., Ed., Marcel Dekker, New York, 1967, 105.
206. Koenig, S. H., Brownian motion of an ellipsoid. A correction to Perrin's results, *Biopolymers*, 14, 2421, 1975.
207. Wright, A. K. and Baxter, J. E., A numerical inversion of the Perrin equations for rotational and translational diffusion constants by iterative techniques, *Biophys. J.*, 16, 931, 1976.
208. Broersma, S., Viscous force constant for a closed cylinder, *J. Chem. Phys.*, 32, 1632, 1960.
209. Broersma, S., Rotational diffusion of a cylindrical particle, *J. Chem. Phys.*, 32, 1626, 1960.
210. Kirkwood, J. G., The general theory of irreversible processes in solutions of macromolecules, *J. Polym. Sci.*, 12, 1, 1954.
211. Paul, E. and Mazo, R. M., Hydrodynamic properties of a plane-polygonal polymer, according to Kirkwood-Riseman theory, *J. Chem. Phys.*, 51, 1102, 1969.
212. Kato, M., Lee, W. I., Eichinger, B. E., and Schurr, J. M., Molecular weight and shape of the phycocyanin hexamer, *Biopolymers*, 13, 2293, 1974.
213. Teller, D. S., Swanson, E., and de Haen, C., A rigorous calculation of transport properties of rotational ellipsoids and proteins using the Kirkwood-Riseman theory, *Fed. Proc. Fed. Am. Exp. Biol.*, 36(Abstr. 2092), 668, 1977.
214. Rotne, J. and Prager, S., Variational treatment of hydrodynamic interaction in polymers, *J. Chem. Phys.*, 50, 4831, 1969.
215. Yamakawa, H., Transport properties of polymer chains in dilute solution: hydrodynamic interaction, *J. Chem. Phys.*, 53, 436, 1970.
216. Garcia de la Torre, J. and Bloomfield, V. A., Hydrodynamic properties of macromolecular complexes, *Biopolymers*, submitted.
217. Schmitz, K. S., The role of hydrodynamic shielding in macromolecular complexes, *Biopolymers*, submitted.
218. Hu, C. M. and Zwanzig, R., Rotational friction coefficients for spheroids with the slipping boundary condition, *J. Chem. Phys.*, 60, 4354, 1974.
219. Kirkwood, J. G. and Riseman, J., The intrinsic viscosities and diffusion constants of flexible macromolecules in solution, *J. Chem. Phys.*, 16, 565, 1948.
220. Flory, P. J., *Principles of Polymer Chemistry*, Cornell University Press, Ithaca, N.Y., 1953, chap. 14.
221. Felderhof, B. U. and Deutch, J. M., Frictional properties of dilute polymer solutions. I. Rotational friction coefficient, *J. Chem. Phys.*, 62, 2391, 1975.
222. McCammon, J. A., Deutch, J. M., and Bloomfield, V. A., Low values of the Scheraga-Mandelkern β parameters for proteins. An explanation based on porous sphere hydrodynamics, *Biopolymers*, 14, 2479, 1975.
223. Batchelor, G. K., Sedimentation in a dilute dispersion of spheres, *J. Fluid Mech.*, 52, 245, 1972.
224. Altenberger, A. R. and Deutch, J. M., Light scattering from dilute macromolecular solutions, *J. Chem. Phys.*, 59, 894, 1973.
225. Anderson, J. L. and Reed, C. C., Diffusion of spherical macromolecules at finite concentration, *J. Chem. Phys.*, 64, 3240, 1976.
226. Phillies, G. D. J., Diffusion of spherical macromolecules at finite concentration, *J. Chem. Phys.*, 65, 4334, 1976.
227. Mou, C. Y. and Chang, E. L., Concentration dependence of diffusion of interacting spherical Brownian particles, *Mol. Phys.*, submitted.
228. Phillies, G. D. J., Benedek, G. B., and Mazer, N. A., Diffusion in protein solutions at high concentrations: a study by quasielastic light scattering spectroscopy, *J. Chem. Phys.*, 65, 1883, 1976.
229. Buldt, G., Interpretation of quasi-elastic light scattering measurements from moderately concentrated solutions, *Eur. Polym. J.*, 12, 239, 1976.

230. Freed, K., Concentration dependence of the translational friction coefficient for polymer solutions, *J. Chem. Phys.*, 65, 4103, 1976.
231. Altenberger, A. R., Generalized diffusion processes and light scattered from a moderately concentrated solution of spherical particles, *Chem. Phys.*, 15, 269, 1976.
232. Efremov, F., Periodic colloid structures, in *Surface and Colloid Science*, Vol. 8, Matijevic, E., Ed., Interscience, New York, 1975, 85.
233. Brown, J. C., Pusey, N., Goodwin, J. W., and Ottewill, R. H., Light scattering study of dynamic and time-averaged correlations in dispersions of charged particles, *J. Phys. A Math. Nucl. Gen.*, 8, 664, 1975.
234. Pusey, P. N., personal communication, 1977.
235. Ahmed, A. I., Feeney, R. E., Osuga, D. T., and Yeh, Y., Antifreeze glycoproteins from Antarctic fish, *J. Biol. Chem.*, 250, 3344, 1975.
236. Ahmed, A. I., Yeh, Y., Osuga, D. T., and Feeney, R. E., Antifreeze glycoproteins from Antarctic fish, *J. Biol. Chem.*, 251, 3033, 1976.
237. Ware, B. R. and Flygare, W. H., Light scattering in mixtures of BSA, BSA dimers, and fibrinogen under the influence of electric fields, *J. Colloid Interface Sci.*, 39, 670, 1972.
238. Sellen, D. B., Rayleigh scattering linewidth measurements on some globular protein solutions, *Polymer*, 14, 359, 1973.
239. Raj, T. and Flygare, W. H., Diffusion studies of bovine serum albumin by quasielastic light scattering, *Biochemistry*, 13, 3336, 1974.
240. Palmer, G. and Fritz, O. G., A homodyne light-beating spectroscopy study of human fibrinogen, in press.
241. Birnboim, M. H. and Lederer, K., Diffusion coefficient of bovine fibrinogen as measured by quasi-elastic light scattering, *Polym. Rep.*, 13, 203, 1972.
242. Mohan, R., Steiner, R., and Kaufman, R., Laser doppler spectroscopy as applied to electrophoresis in protein solutions, *Anal. Biochem.*, 70, 506, 1976.
243. Uzgiris, E. E., A laser Doppler assay for the antigen-antibody reaction, *J. Immunol. Methods*, 10, 85, 1976.
244. Shaw, B. R. and Schmitz, K. S., Quasielastic light scattering by biopolymers. Conformation of chromatin multimers, *Biochem. Biophys. Res. Commun.*, 73, 224, 1976.
245. Wun, K. L. and Prins, W., Histone-induced conformational changes in DNA as probed by quasi-elastic light scattering, *Biopolymers*, 14, 111, 1975.
246. Ramsay-Shaw, B. and Schmitz, K. S., Reanalysis of histone-induced conformational changes in DNA determined by quasielastic light scattering, *Biopolymers*, 15, 2313, 1976.
247. French, M. J., Angus, J. C., and Walton, A. G., A study of collagen and gelatin solutions by optical self-beat spectroscopy, *Biochim. Biophys. Acta*, 251, 320, 1971.
248. Obrink, B., Non-aggregated tropocollagen at physiological pH and ionic strength, *Eur. J. Biochem.*, 25, 563, 1972.
249. Fletcher, G. C., Dynamic light scattering from collagen solutions. I. Translational diffusion coefficient and aggregation effects, *Biopolymers*, 15, 2201, 1976.
250. Privalov, P. L., Serdyuk, I. N., and Tiktopulo, E. I., Thermal conformational transformations of tropocollagen. II. Viscometric and light scattering studies, *Biopolymers*, 10, 1777, 1971.
251. Schurr, J. M. and McLaren, A. D., Kinetics of trypsin hydrolysis and the structure of both free-solution and gel-state gelatin. Enzyme reactions in structurally restricted systems, VII, *Enzymologia*, 29, 315, 1965.
252. Jamieson, A. M., Lee, T.-Y., and Schafer, I. A., Structural studies of human placental dermatan sulfate during development using optical mixing spectroscopy, *Biopolymers*, 13, 2133, 1974.
253. Jamieson, A. M., Downs, C. E., and Walton, A. G., Studies of elastin coacervation by quasielastic light scattering, *Biochim. Biophys. Acta*, 271, 34, 1972.
254. Dubin, S. B., Clark, N. A., and Benedek, G. B., Measurement of the rotational diffusion coefficient of lysozyme by depolarized light scattering: configuration of lysozyme in solution, *J. Chem. Phys.*, 54, 5158, 1971.
255. Steinrauf, L. K., Preliminary X-ray data for some new crystalline forms of β-lactoglobulin and hen egg-white lysozyme, *Acta Crystallogr.*, 12, 77, 1959.
256. Dubin, S. B., Feher, G. B., and Benedek, G. B., Study of the chemical denaturation of lysozyme by optical mixing spectroscopy, *Biochemistry*, 12, 714, 1973.
257. Gabler, R., Ford, N. C., Jr., and Westhead, E. W., Conformational changes of glyceraldehyde-3-phosphate dehydrogenase observed using laser light scattering spectroscopy, *Biophys. J.*, 15, 747, 1975.
258. Cohen, R. J., Jedziniak, J. A., and Benedek, G. B., Study of the aggregation and allosteric control of bovine glutamate dehydrogenase by means of quasi-elastic light scattering spectroscopy, *Proc. R. Soc. London Sci. Ser. A*, 345, 73, 1975.
259. Cohen, R. J. and Benedek, G. B., The functional relation between polymerization and catalytic activity of beef liver glutamate dehydrogenase. I. Theory, *J. Mol. Biol.*, 108, 151, 1976.
260. Cohen, R. J., Jedziniak, J. A., and Benedek, G. B., The functional relation between polymerization and catalytic activity of beef liver glutamate dehydrogenase. II. Experiment, *J. Mol. Biol.*, 108, 179, 1976.
261. Julien, M. and Thusius, D., Mechanism of bovine liver glutamate dehydrogenase self-assembly, *J. Mol. Biol.*, 101, 397, 1976.
262. Raj, T. and Flygare, W., Translational diffusion coefficient of α-chymotrypsinogen A by laser light scattering spectroscopy, *Biopolymers*, 16, 545, 1977.

263. Rimai, L., Hickmott, J. T., Cole, T., and Carew, E. B., Quasi-elastic light scattering by diffusional fluctuations in RNase solutions, *Biophys. J.*, 10, 20, 1970.
264. Wilson, W. W., Luzzana, M. R., Penniston, J. T., and Johnson, C. S., Jr., Pregelation aggregation of sickle cell hemoglobin, *Proc. Natl. Acad. Sci. U.S.A.*, 71, 1260, 1974.
265. Chen, F. C., Yeh, A., and Chu, B., Diffusion coefficients of histone (lysine-rich) by quasielastic light scattering, *J. Chem. Phys.*, 65, 4508, 1976.
266. Chu, B., Yeh, A., Chen, F. C., and Weiner, B., Self-association of β-lactoglobulin A in acid solution. I. Translational diffusion coefficients, *Biopolymers*, 14, 93, 1975.
267. Dewan, R. K., Chudgar, A., Bloomfield, V. A., and Morr, C. V., Size distribution and solvation of casein micelles in bovine milk containing α_{s1}-casein A, *J. Dairy Sci.*, 57, 394, 1974.
268. Dewan, R. K. and Bloomfield, V. A., Molecular weight of bovine milk casein micelles from diffusion and viscosity measurements, *J. Dairy Sci.*, 56, 66, 1973.
269. Morr, C. V., Lin, S. H. C., Dewan, R. K., and Bloomfield, V. A., Molecular weights of fractionated bovine milk casein micelles from analytical ultracentrifugation and diffusion measurements, *J. Dairy Sci.*, 56, 415, 1973.
270. Holzbach, R. T., Oh, S. Y., McDonnell, M. E., and Jamieson, A. M., Quasielastic laser spectrometry studies of pure bile salt and bile salt-mixed lipid micellar systems, in *Proc. Intl. Symposium on Micellization, Solubilization and Microemulsion*, Mittal, K. L., Ed., Plenum Press, New York, 1976, in press.
270a. Cooper, V. G., Yedgar, S., and Barenholz, Y., Diffusion coefficients of mixed micelles of Triton® X-100 and sphingomyelin and of sonicated sphingomyelin liposomes, measured by autocorrelation spectroscopy of Rayleigh scattered light, *Biochim. Biophys. Acta*, 363, 86, 1974.
271. Holtzman, J. L., Erickson, R. R., Dewan, R. K., and Bloomfield, V. A., Inelastic laser light scattering and particle size of detergent-treated microsomes, *Biochem. Biophys. Res. Commun.*, 52, 15, 1973.
272. Fujime, S. and Ishiwata, S., Dynamic study of F-actin by quasielastic scattering of laser light, *J. Mol. Biol.*, 62, 251, 1971.
273. Fujime, S., Quasi-elastic light scattering from solutions of macromolecules. II. Doppler broadening of light scattered from solutions of semi-flexible polymers, F-actin, *J. Phys. Soc. Jpn.*, 29, 751, 1970.
274. Fujime, S., Ishiwata, S., and Maeda, T., F-actin-heavy meromyosin complex studied by optical homodyne and heterodyne methods, *Biochim. Biophys. Acta*, 283, 351, 1972.
275. Fujime, S. and Ishiwata, S., A dynamic study of F-actin-heavy meromyosin solutions by quasi-elastic light scattering, *J. Phys. Soc. Jpn.*, 29, 1651, 1970.
276. Ishiwata, S. and Fujime, S., A dynamic study of F-actin-tropomyosin solution by quasi-elastic light scattering, *J. Phys. Soc. Jpn.*, 30, 302, 1970.
277. Ishiwata, S., and Fujime, S., Effect of Ca^{++} on the F-actin-tropomyosin-troponin complex studied by quasi-elastic light scattering, *J. Phys. Soc. Jpn.*, 30, 303, 1970.
278. Maeda, T., Ishiwata, S., and Fujime, S., Light-beating study of the effect of β-actinin on the interaction between F-actin and heavy meromyosin, *Biochim. Biophys. Acta*, 336, 445, 1974.
279. Ishiwata, S. and Fujime, S., Effect of calcium ions on the flexibility of reconstituted thin filaments of muscle studied by quasielastic scattering of laser light, *J. Mol. Biol.*, 68, 511, 1972.
280. Maeda, T. and Fujime, S., Quasielastic light scattering from muscle F-actin, 1977, in press.
281. Fraser, A. B., Eisenberg, E., Kielly, W. W., and Carlson, F. D., The interaction of heavy meromyosin and subfragment 1 with actin. Physical measurements in the presence of adenosine triphosphate, *Biochemistry*, 14, 2207, 1975.
282. Herbert, T. J. and Carlson, F. D., Spectroscopic study of the self-association of myosin, *Biopolymers*, 10, 2231, 1971.
283. Ding, D.-W., Rill, R., and Van Holde, K. E., The dichroism of DNA in electric fields, *Biopolymers*, 11, 2109, 1972.
284. Callis, P. R. and Davidson, N., Hydrodynamic relaxation times of DNA from decay of flow dichroism measurements, *Biopolymers*, 8, 379, 1969.
285. Han, C. C.-C., and Yu, H., Intra-molecular chain dynamics by forward depolarized scattering, *J. Chem. Phys.*, 61, 2650, 1974.
286. Pritchard, A. E. and Eichinger, B. E., Helix-coil transitions of compositionally heterogeneous DNA, *Biopolymers*, 14, 1357, 1975.
287. Buldt, G., Mean relaxation times in quasi-elastic light scattering, *Macromolecules*, 9, 606, 1976.
288. Allen, G., Ghosh, R., Higgins, J. S., Cotton, J. P., Farnoux, B., Jannink, G., and Weill, G., Observation of the neutron quasi-elastic broadening by polymers in solution, *Chem. Phys. Lett.*, 38, 577, 1976.
289. Potts, R., Fournier, M. J., and Ford, N. C., Jr., Effect of aminoacylation on the conformation of yeast phenylalanine tRNA, 1977, in press.
290. Hartford, S. L. and Flygare, W. H., Electrophoretic light scattering on calf-thymus deoxyribonucleic acid and tobacco mosaic virus, *Macromolecules*, 8, 80, 1975.
291. Rice, S. A. and Nagasawa, M., *Polyelectrolyte Solutions*, Academic Press, London, 1961, 187.
292. Krasna, A. I., Changes in the light-scattering properties of DNA on denaturation, *J. Colloid Interface Sci.*, 39, 632, 1972.
293. McDonnell, M. E. and Jamieson, A. M., Rapid characterization of protein molecular weights and hydrodynamic structures by quasielastic laser-light scattering, *Biopolymers*, 15, 1283, 1976.

294. Jamieson, A. M. and Presley, C. T., Anistropic translational diffusion in dilute aqueous solutions of partially hydrolyzed polyacrylamide by quasielastic light scattering, *Macromolecules*, 6, 358, 1973.
295. Flory, P. J., Statistical thermodynamics of random networks, *Proc. R. Soc. London Sci. Series A*, 351, 351, 1976.
296. Eichinger, B. E., Elasticity theory. I. Distribution functions for perfect phantom networks, *Macromolecules*, 5, 496, 1972.
297. Graessly, W. W., Elasticity and chain dimensions in Gaussian networks, *Macromolecules*, 8, 865, 1975.
298. Schleich, T. and Yeh, Y., The solution behavior of poly-L-proline. I. Light scattering studies in water and concentrated aqueous neutral salt solutions, *Biopolymers*, 12, 993, 1973.
299. Lee, W. I. and Schurr, J. M., Effect of long-range hydrodynamic and direct intermacromolecular forces on translational diffusion, *Chem. Phys. Lett.*, 78, 71, 1976.
300. Ptitsyn, O. B. and Skvortsov, A. M., Theory of helix-coil transitions in biopolymers. V. Method for determining the cooperativeness of the helix-coil transition in polypeptide chains from change in the size of the macromolecules in the region of transition, *Biofizika*, 10, 909, 1965; *Biophysics*, 10, 1007, 1965.
301. Jamieson, A. M., Mack, L., and Walton, A. G., Quasielastic light scattering investigation of the isothermal "helix to extended coil" transition of poly-L-lysine HBr, *Biopolymers*, 11, 2267, 1972.
302. Duke, R. W. and DuPré, D. W., Examination of the electrotropic cholesteric to nematic phase transition of liquid crystal poly(γ-benzyl-L-glutamate) by laser light-beating spectroscopy, *Macromolecules*, 7, 374, 1974.
303. Sellen, D. B., Light scattering Rayleigh linewidth measurements on some dextran solutions, *Polymer*, 16, 561, 1975.
304. Chen, F. C., Tcharnuter, W., Schmidt, W., Chu, B., and Liu, T. Y., Measurement of diffusion coefficients of meningococcal polysaccharide by optical mixing spectroscopy. I. A preliminary characterization of the aggregation of group C polysaccharide, *Biopolymers*, 13, 2281, 1974.
305. Oliver, C. J., Pike, E. R., Cleave, A. J., and Peacocke, A. R., Determination of the diffusion coefficient and molecular weight of Tamm-Horsfall glycoprotein by intensity fluctuation spectroscopy, *Biopolymers*, 10, 1731, 1971.
306. Gethner, J. S., Flynn, G. W., Berne, B. J., and Gaskin, F., The characterization of heterogeneous solutions using laser light scattering: a study of the tubulin system, *Biochemistry*, submitted.
307. Gethner, J. S., Glynn, G. W., Berne, B. J., and Gaskin, F., The equilibrium components of tubulin preparations, *Biochemistry*, submitted.
308. Chen, F. C., Chrzeszcyk, A., and Chu, B., Quasi-elastic laser light scattering of phosphatidylcholine vesicles, *J. Chem. Phys.*, 8, 3403, 1976.
309. Chen, F. C., Tu, S. I., and Chu, B., Characterization of phosphatidylcholine vesicles by quasielastic laser light scattering, in *Proc. Int. Conf. on Colloids and Surfaces*, Academic Press, New York.
310. Goll, J. and Stock, G., Determination by photon correlation spectroscopy of particle size distributions in lipid vesicle suspensions, *Biophys. J.*, submitted.
311. Newman, J. and Swinney, H. L., Length and dipole moment of TMV by laser signal-averaging transient electric birefringence, *Biopolymers*, 15, 301, 1976.
312. Allen, F. S. and Van Holde, K. E., Dichroism of TMV in pulsed electric fields, *Biopolymers*, 10, 865, 1971.
313. O'Konski, C. T. and Haltner, A. J., Characterization of the monomer and dimer of tobacco mosaic virus by transient electric birefringence, *J. Am. Chem. Soc.*, 78, 3604, 1956.
314. Jennings, B. R. and Jerrard, H. G., Light-scattering study of tobacco mosaic virus solutions when subjected to electric fields, *J. Chem. Phys.*, 44, 1291, 1966.
315. Schurr, J. M. and Schmitz, K. S., Orientation constraints and rotational diffusion in biomolecular solution kinetics. A simplification, *J. Phys. Chem.*, 80, 1934, 1976.
316. Kirkwood, J. G. and Mazur, J., The radial distribution functions of electrically charged macromolecules in solution, *J. Polymer Sci.*, 9, 519, 1952.
317. Schaefer, D. W. and Berne, B. J., Dynamics of charged macromolecules in solution, *Phys. Rev. Lett.*, 32, 1110, 1974.
318. Killmann, E. and Preusser, F., Über Grösse und Ladung des Polyelektrolytsystems Poly-N-vinylpyrrolidon/Blankophor BA. I. Qualitative Beschreibung und Deutung der Sedimentationskoeffizienten in Abhängigkeit von der Ladungsdichte und der Fremdsalzkonzentration, *Angew. Makromol. Chem.*, 37, 187, 1974.
319. Killmann, E. and Preusser, F., Über Grösse und Ladung des Polyelektrolytsystems Poly-N-vinylpyrrolidon/Blankophor BA. II. Die Änderung des Reibungskoeffizienten mit der Ladungsdichte und der Salzkonzentration, *Angew. Makromol. Chem.*, 37, 199, 1974.